FACULTY OF SCIENCE
UNIVERSITY OF COPENHAGEN

FUTURE AIR POLLUTION LEVELS IN THE NORTHERN HEMISPHERE

Sensitivity to climate change and projected emissions

PhD Thesis, 2011

Gitte Brandt Hedegaard

AARHUS UNIVERSITY

DMI

Data sheet

Title:	Future air pollution levels in the northern hemisphere. Sensitivity to climate change and projected emissions
Subtitle:	PhD Thesis
Author:	Gitte Brandt Hedegaard
Institute:	Niels Bohr Institute, University of Copenhagen, Department of Environmental Science, Aarhus University and Danish Climate Centre, Danish Meteorological Institute
Publisher:	Aarhus University - Denmark
URL:	http://www.dmu.au.dk
Year of publication:	2011
PhD supervisors:	Aksel Walløe Hansen, Jens Hesselbjerg Christensen & Jørgen Brandt
Please cite as:	Hedegaard, G.B. 2011. Future air pollution levels in the northern hemisphere. Sensitivity to climate change and projected emissions. PhD thesis. Institute of Environmental Science, Aarhus University, Denmark, .

Abstract:	Climate change impacts the atmospheric composition of the atmosphere, since the concentration of chemical species in the atmosphere depends on different meteorological parameters and hence is sensitive to changes in the climate. A model framework has been setup where the Danish Eulerian Hemispheric Model (DEHM) has been driven on past, present and future meteorology projected by the Atmosphere-Ocean Climate model ECHAM5/MPI-OM. Several simulations have been carried out with the DEHM model forced with different combinations of meteorology and emission scenario data in order to investigate the impact of climate change and emission change on future air pollution levels. Ozone, black carbon, total nitrogen, total sulphate and PM2.5 have been thoroughly investigated. The signal from the changes in anthropogenic emissions dominates for most species. However, opposing effects from impact of climate change and emission change are found for some species implying a so called "climate penalty"; to reach a certain reduction level further actions needs to be taken into account in air pollution regulation in order to counteract the impact of climate change

Keywords:	Climate change, Emissions, Future air pollution levels, Interactions
Front page photo:	The picture in front page is taken the October 1st, 2011 the warmest day ever registered in October in Denmark (26.7°C), high air pollution levels were registered as well. Photo taken in Greve Landsby by Gitte Brandt Hedegaard
ISBN:	978-87-92825-07-0
Number of pages:	145
Supplementary notes:	The thesis was, together with six peer reviewed papers, defended and at the H.C. Ørsted Institute, University of Copenhagen, Denmark November 25th 2011 and the PhD degree was awarded.

Future air pollution levels in the Northern Hemisphere

- Sensitivity to climate change and projected emissions

PHD Thesis

Gitte Brandt Hedegaard

Internal supervisor	Aksel Walløe Hansen, Niels Bohr Institute, University of Copenhagen
External supervisor	Jørgen Brandt, Department of Environmental Science, Aarhus University
External supervisor	Jens Hesselbjerg Christensen, Danish Climate Centre, Danish Meteorological Institute

Niels Bohr Institute

The PhD School of Science
Faculty of Science
University of Copenhagen
Denmark

October 2011

Preface

The research for this PhD thesis, entitled "Future air pollution levels in the Northern Hemisphere - Sensitivity to climate change and projected emissions", has mainly been carried out at Department of Environmental Science, Aarhus University (formerly known as: National Environmental Research Institute, Department of Atmospheric Environment) under the supervision of Dr. Jørgen Brandt. About 1/3 of the work has been conducted in the Danish Climate Centre, Danish Meteorological Institute under the supervision of Dr. Jens Hesselbjerg Christensen. The main internal supervisor of the project is Associated Professor Aksel Walløe Hansen, Niels Bohr Institute, University of Copenhagen.

The PhD project was carried out from April 2007 to October 2011 and was funded partly by the Faculty of Science, University of Copenhagen (1/3), the COGCI (Copenhagen Global Change Initiative) PhD school, University of Copenhagen (1/3), Danish Meteorological Institute, Danish Climate Centre (1/6) and finally partly by the Department of Environmental Science, Aarhus University (former known as: Department of Atmospheric Environment, National Environmental Research Institute (NERI)) (1/6).

The PhD project has contributed to both national and international projects (ENSCLIM and Copenhagen Climate), networks (ACCENT and HTAP) and research centres (BNI, AMAP, CEEH).

The thesis can be read as an independent report. Moreover 5 peer review scientific papers and 1 scientific book contribution is included in appendix B and supports the work in the thesis. A short description of these papers and their relevance with respect to this thesis can be found in the Introduction. The included papers are:

Paper I:
Hedegaard, G. B., J. Brandt, J. H. Christensen, L. M. Frohn, C. Geels and M. Stendel; Impacts of climate change on air pollution levels in the Northern Hemisphere with special focus on Europe and the Arctic, Atmospheric Chemistry and Physics, 8, 3337-3367, 2008.

Paper II:
Hedegaard, G. B.; Natural Sources, in: Air pollution - from a local to a global perspective, Polyteknisk Forlag, Eds.: Jes Fenger and Jens Christian Tjell., 163-174, 2008.

Paper III:
Skjøth, C. A., Geels, C., Hvidberg, M., Hertel, O., Brandt, J., Frohn, L. M., Hansen, K. M., Hedegaard, G. B., Christensen, J. H., Moseholm, L.; An inventory of tree species in Europe-An essential data input for air pollution modelling, Ecological Modelling, 217, 3-4, 292-304, 2008.

Paper IV:
Brandt, J., Silver, J. D., Frohn, L. M., Geels, C., Gross, A., Hansen, A. B., Hansen, K. M., Hedegaard, G. B., Skjøth, C. A., Villadsen, H., Zare, A. and Christensen, J. H.; An integrated model study for Europe and North America using the Danish Eulerian Hemispheric Model with focus on intercontinental transport of air pollution, submitted to Atmospheric Environment (Special issue), May 2011. (2011a).

Paper V:
Brandt, J., Silver, D., Frohn, L. M., Christensen, J. H., Andersen, M. S., Geels, C., Gross, A., Hansen, K. M., Hansen, A. B., Hedegaard, G. B, and C. A. Skjøth; Assessment of Health-Cost Externalities of Air Pollution at the National Level using the EVA Model System, in preparation (draft), (2011b).

Paper VI:
Geels, C., Hansen, K. M., Christensen, J. H, Skjøth, C. A., Ellerman, T., Hedegaard, G. B, Hertel, O., Frohn, L. M., Gross, A., Hansen, A. B., Brandt, J.; Projected change in atmospheric nitrogen deposition to the Baltic Sea towards 2020, Atmospheric Chemistry and Physics Discussions, 11, 21533-21567, 2011.

Summary

Climate change impacts the atmospheric composition of the atmosphere, since the concentration of chemical species in the atmosphere depends on different meteorological parameters and hence is sensitive to changes in the climate. Furthermore past, present and future anthropogenic emissions of air pollutants alter the chemical composition of the atmosphere. In this thesis the sensitivity of ozone and its related precursors are investigated together with black carbon, and other particles with respect to the individual impacts from climate change and changes in future anthropogenic emissions.

A model framework has been setup based on the Danish Eulerian Hemispheric Model (DEHM), which is an Eulerian Atmospheric Chemistry Transport Model (ACTM). The DEHM model has been driven on past, present and future meteorology projected by the Atmosphere-Ocean Climate model ECHAM5/MPI-OM. The applied climate simulation covers 340 year and has been forced with the SRES A1B emission scenario in the future.

Within the climate change-air quality research community it is common to do time-slice experiments. In this thesis attention is paid on the precautions and pre-analysis of the climate data that need to be carried out before using the data for impacts studies. Specifically, four time-slices have been chosen (1890s, 1990s, 2090s and 2190s) to represent the differences between the three centuries. Empirical Orthogonal Function (EOF) analysis and other statistical tools have been used in order to verify the use of time-slices for simulations with the ACTM. It is concluded that it is scientifically sound to use the specific four time-slices. The chance of choosing an abnormal decade from the climate simulation with respect to the internal variability is only 4 out 34 within a 10 % significance level.

Several simulations have been carried out with the DEHM model forced with different combinations of meteorology and emission scenario data. The emission inventories used are the EMEP, EDGAR and GEIA databases and the newly developed RCP4.5 emission scenario. The impact of climate change on the future surface ozone concentration has thoroughly been evaluated with respect to the different sinks and sources of surface level ozone. It was found that the changes in future ozone concentrations due to climate changes lead to a general decrease in the remote and semi-remote areas. In urban

areas the ozone concentration will increase due to increased production from increased biogenic emissions of VOCs.

The largest changes in surface level ozone are found to happen in the current century. However, the tendencies found will continue into the 22nd century. The fate of ozone is in general driven by two competing effects; ozone destruction due to increased water vapour in the clean areas and ozone production in the more polluted areas. The impact from climate change implies a promoting effect on production on biogenic isoprene which in the presence of NO_x results in increase in the ozone concentration.

The addition of changes in the anthropogenic emissions prescribed by the RCP4.5 emission scenario, result in a different picture. The signal from the changes in anthropogenic emissions dominates for most species in most areas. However, opposing effects from impact of climate change and emission change are found for some species implying a so called "climate penalty"; to reach a certain reduction level further actions needs to be taken into account in air pollution regulation in order to counteract the impact of climate change.

Dansk Sammenfatning

Klimaændringer har indflydelse på den kemiske sammensætning i atmosfæren, da koncentrationen af de kemiske stoffer i atmosfæren afhænger af forskellige meteorologiske parametre og derfor er følsomme overfor klimaændringer. Endvidere kan den fortidige, nutidige og fremtidige menneskelige udledning af luftforurenende stoffer ændre atmosfærens sammensætning. I denne afhandling bliver følsomheden af ozon og de ozon-dannende stoffer, samt sod og andre partikler undersøgt med hensyn til effekten af klimaændringer og effekten af ændringer i de fremtidige menneskeskabte emissioner.

Et model system er blevet etableret, baseret på den Danske Eulerske Hemisfæriske Model (DEHM), som er en Eulersk atmosfære kemisk transport model (ACTM). DEHM modellen er kørt på fortidig, nutidig og fremtidig meteorologi beregnet med atmosfære-ocean klimamodellen ECHAM5/MPI-OM. Klimasimuleringen som er blevet anvendt er 340 år lang og er blevet forceret med SRES A1B emissions scenariet.

I forskning inden for klimaændringer og luftforurening er det almindeligt at lave klimaeksperimenter baseret på relativ korte tidsperioder. I denne afhandling er der sat fokus på de forholdsregler og pre-analyser, som man bør foretage før man bruger klimadata i effektstudier. Specifikt er der valgt fire tidsperioder (1890'erne, 1990'erne, 2090'erne og 2190'erne) som skal repræsentere forskellen over tre 100-års perioder. Empirisk Ortogonal Funktions (EOF) analyse og andre statistiske metoder er blevet brugt til at verificere brugen af kortere tidsperioder i ACTM kørsler. Konklusionen er, at det er videnskabelig forsvarligt at bruge de fire valgte tidsperioder. Risikoen for at vælge en unormal dekade ud af den fulde 340-år lange klimasimuleringen er 4 ud af 34 under et 10% signifikans niveau.

Adskillige simuleringer er blevet kørt hvor DEHM modellen er blevet forceret med forskellige kombinationer af meteorologi og emissions scenarier. Emissionsopgørelserne som er brugt til simuleringerne er baseret på EMEP, EDGAR, GEIA emissions databaserne og det nyudviklede RCP4.5 emissionsscenarie. Effekten fra klimaændringer på de fremtidige ozon koncentrationer er blevet grundigt testet med hensyn til de forskellige ozon dræn og kilder. Ændringen, som skyldes klimaændringer, i de fremtidige ozon koncentrations niveauer

resulterer i et fald i koncentrationerne i de rene områder og en stigning i de tætbefolkede mere forurenede områder.

Det viste sig i de fremtidige ozon koncentrationer at ændringerne på grund af klimaændringer førte til en general stigning i de ikke-forurenede områder. I byområderne vil ozon koncentrationerne derimod stige på grund af en øget produktion fra øget naturlige emissioner af VOC'er.

Den største ændring i overflade ozon koncentrationen blev fundet i dette århundrede, men tendensen ville fortsætte ind i det næste 22. århundrede. Ozon fordelingen er generelt drevet af to konkurrerende effekter; ozon nedbrydning på grund af øget vand damp i de rene områder og ozon produktion pga. øget VOC niveauer og øget vanddamp i de forurenede områder. Klimaændringer fremmer de naturlige VOC emissioner (isoprene) og øger dermed ozon produktionen i områder hvor der er relativt høje NO_x niveauer.

Medtages effekten fra ændrede menneskeskabte emissioner i dette tilfælde baseret på RCP4.5 scenariet, ses et andet billede. Signalet fra ændrede emissioner dominerer for de fleste stoffer i de meste af model domænet. Dog er signalet fra klimaændringer i nogle tilfælde modsatrettet signalet fra emissions ændringer. Denne dæmpende effekt af emissions reduktioner er blevet betegnet som "Klimastraffen". Det vil sige for at opnå et bestemt koncentrations niveau er man nødt til at reducere yderligere og medregne denne tillægsreduktion i luftforureningsregulativerne i fremtiden for at kompensere for effekten fra klimaændringer.

Abbreviations

ACCENT - Atmospheric Composition Change: the European Network
AOGCM - Atmophere-Ocean General Circulation Model
AQ-CC - Air Quality - Climate Change
AQMEII - Air Quality Modelling Evaluation International Initiative
AVOC - Anthropogenic Volatile Organic Compounds
BC - Black Carbon
BVOC - Biogenic Volatile Organic Compounds
CEEH - Centre for Energy Environment and Health
CMIP3/5 - coupled Model Inter-comparison Project Phase 3/5
CTM - Chemical Transport Model
COGCI - Copenhagen Global Climate Initiative
COP15 - The 15th United Nations Framework Convention on Climate Change
DEHM - Danish Eulerian Hemispheric Model
ECHAM - Combined word based on "ECMWF" and MPI-"Hamburg"
EDGAR - Emission Database for Global Atmospheric Research
EMEP - European Monitoring and Evaluation Programme
ENSCLIM - Robustness of predictions of climate change impact on dispersion and effects of airborne pollutants in Northern Europe
EOF - Empirical Orthogonal Function
EVA - Economic Valuation of Air pollution
GEIA - Global Emissions Inventory Activity
gph - geopotential height
HTAP - Hemispheric Task-force on Air Pollution
hPa - hecto Pascal
IDL - Interactive Data Language
IPCC - Intergovernmental Panel on Climate Change
MPI - Max Planck Institute MPI-OM - Max Planck Institute - Ocean Model
MSLP - Mean Sea Level Pressure
NAO - North Atlantic Oscillation
NEC - National Emission Ceilings directive
NMVOC - Non-Methane Volatile Organic Carbon
PM2.5 - Particulate matter with diameter $< 2.5\mu m$
PM10 - Particulate matter with diameter $< 10\mu m$

PNA - Pacific-North American Oscillation
PC - Principal Component
PCA - Principal Component Analysis
ppbV - parts per billion Volume
PCMDI - Program for Climate Model Diagnosis and Intercomparison
RCP - Representative Concentration Pathways
SNAP - Selected Nomenclature for Sources of Air Pollution
SRES - Special Report on Emission Scenarios (IPCC)
VOC - Volatile Organic Compounds
WMO - World Meteorological Organisation

Contents

1 Introduction

Since industrialization the concentration of greenhouse gases in the atmosphere has increased. The greenhouse gases affect our climate, which has been undergoing a continuous change into what we experience today. Continued anthropogenic emissions of CO_2 will lead to further warming and at some point the natural carbon sinks of the earth will be filled up which will accelerate the warming of the climate system. The natural CO_2 sinks can only take up a certain amount of emitted CO_2 and the remaining $CO_2(\sim 20\%)$ will stay in the atmosphere for at least a millennium [Monastersky, 2009]. Additionally the large heat capacity of the oceans are delaying the warming effect of the already emitted greenhouse gases. This means that when we stop emitting CO_2 the atmosphere will continue to warm due to energy stored in the oceans.

In the 4th assessment report from IPCC published in 2007 it is stated that: "Warming of the climate system is today an indisputable fact and it is very likely that most of the warming has an origin in the anthropogenic interference with the environment" [Pachauri & Reisinger, 2007].

Since the atmospheric chemistry is highly dependent on temperature, humidity and solar radiation the observed warming will inherently affect the chemical composition of the atmosphere. The climate system of the earth is very complex and intertwined. A general temperature increase will lead to changes of other meteorological parameters such as for example precipitation, pressure patterns, humidity and cloud cover. Common to these parameters is that they influence the air pollution levels and distribution via physical and chemical processes.

The effect of changes in meteorology on air pollution levels implies that even though we today decide to keep the anthropogenic emissions of air pollutants constant, the air pollution levels will change anyway. Since air pollution can have tremendous effect on human health, agriculture, the terrestrial and marine eco-systems etc., it is important to try to predict the future air pollution levels in order to develop and implement air pollution legislation that hopefully will minimize the negative consequences of human interference with the environment. Evaluations and developments of new emission reduction strategies should include the additional effect from

climate change and therefore sensitivity studies with respect to impacts of climate change and anthropogenic emission are a necessity.

In the current study the Danish Eulerian Hemispheric Model (DEHM) [Christensen, 1997; Frohn et al., 2001, 2002a,b; Brandt et al., 2011] has been driven on meteorology of the past, present and future projected by the ECHAM5/MPI-OM Atmosphere-Ocean General Circulation Model [Roeckner et al., 2003, 2006; May, 2008] forced with IPCC SRES A1B emission scenario [Nakicenovic et al., 2000]. Several DEHM simulations have been carried out with different combinations of meteorology (past/pressent/future) and different emission scenarios in order to study the sensitivity of different air pollutants due to climate change and changes in anthropogenic emission. More specifically ozone and the related photochemical species have been investigated thoroughly throughout three centuries with respect to the impacts of climate change. Further, the competitive effects of climate change and changes in anthropogenic emissions have been evaluated in the 21st century with focus on ozone, black carbon, nitrogen, sulfuric compounds and PM2.5 in general. The thesis consists of three parts:

First the changes in surface ozone concentrations over three centuries due to climate change alone are studied. Ozone is in the low level atmosphere a toxic gas, that through respiratory and cardiovascular diseases can lead to premature death of human beings. Furthermore ozone is a climate gas due to its radiative properties. It is harmful to plants in high concentrations and can diminish the crop yield substantially. In this study the ozone concentration has been investigated throughout out the past, the present and the future century. The focus has been on the photochemistry which is affected by a changing climate. The main scientific questions of this part of the thesis have been:

> *- How will the surface ozone concentration and related chemistry change in a changing climate during the 21st century?*
>
> *- How did the surface ozone concentration change during the 20th century according to the model and will the projected change in the 21st century continue with the same force throughout the 22nd?*
>
> *- What chemical and physical processes are the main drivers in the model for the changes projected?*

The next part of the thesis concentrate on the 21st century and projected changes in the anthropogenic emissions are included. The focus has been on both ozone and particulate matter. The main scientific questions of this research were:

- Is the signal from climate change on future air pollution levels significant relative to the signal from changes in the anthropogenic emissions?

- Are the two signals opposing or amplifying each other?

- Are there any secondary effects of the two signals operating simultaneously in the atmosphere that needs to be accounted for in future air pollution legislation?

Finally the third part deals with a more general topic with respect to impact studies. Often, and it is also the case in this thesis, impact modellers have to do time-sliced experiments, which simply implies that changes over e.g. a century is simulated by subtracting two time-slices from the beginning and the end of the century. The lengths of these time-slices depends on the availability of data, computer and storage capacity and the complexity of the impact model. In this third part of the thesis the climate simulation used for the impact studies has been analysed to verify the following:

- Is it scientifically sound to use ten-year time-slices from a CTM driven on Climate to describe the effect of climate change on air pollution?

- Specifically do the four chosen time-slices 1890s, 1990s, 2090s and 2190s reasonably represent the full data set (1860-2200) with respect to inter-annual to decadal variability in atmospheric circulation.

- How long should the time-slices be in the climate simulation used in this thesis in order to separate out errors due to inter-annual and decadal variability in the data set?

Furthermore the thesis includes 5 scientific papers and one scientific book contribution (Appendix B) based on research carried out during this PhD. The first paper "Modelling the impacts of climate change on air pollution levels in the Northern Hemisphere" (app. B1) is based on the beginning of the work with Climate Change - Air Quality (CC-AQ) interactions in the Department of Environmental Science, Aarhus University (formerly known as Department of Atmospheric Environment, National Environmental Research Institute). The DEHM-ECHAM model setup is in this paper evaluated over Europe against observations and projections from a similar but different model setup. In the paper it is concluded that DEHM model driven in climate mode with meteorological input from ECHAM performs well with respect to the annual mean values and seasonal variation based on

monthly mean values of several chemical species (e.g. the ozone concentration). Moreover the paper includes an investigation of the air pollution levels in the 21st century projected by the DEHM-ECHAM model setup.

The second contribution included in the appendix (app. B2) is a contribution written for a university level educational book on air pollution. As the title "Natural Sources, in: Air pollution - from a local to a global perspective" indicates, the chapter is about the biogenic sources that contribute to air pollution. It is relevant with respect to the thesis, since most natural sources are especially sensitive to changes in the meteorological parameters. In Particular the book contribution includes a section on Volatile Organic Compounds (VOCs) including isoprene, which has a central role in the climate experiments carried out in this thesis.

The third paper "An inventory of tree species in Europe - An essential data input for air pollution modelling" (app. B3) documents a tree species inventory we developed in our department. It is originally developed for pollen modelling but can also be used for other purposes e.g. to optimize emissions biogenic VOCs. In general it is difficult to obtain correct descriptions of even the current tree populations in Europe (and worse in less developed countries) since counting procedures and the categorizations of tree species is different for every country. Furthermore the data varies in quality, is spatially unevenly distributed and needs to be sorted, filtered and gridded before it is ready to use as model input to e.g. atmospheric models. The inventory provides a full gridded data set ready for use as input data.

The fourth paper "An integrated model study for Europe and North America using the Danish Eulerian Hemispheric Model with focus on intercontinental transport" (app. B4) is a paper submitted for a special issue of the AQMEII model inter-comparison project. The paper contains a thoroughly up to date description of the DEHM model used in this thesis. Moreover the paper describes the inter-continental transport of pollutants. In the DEHM model we have an option to use a tagging method, which in this paper has been used to evaluate the contributions of air pollutants between Europe and North America. The tagging method is described in this and in paper V.

The fifth paper "Assessment of Health-Cost Externalities of Air Pollution at the National Level using the EVA Model System" (app. B5) is still under preparation and will be submitted in a shorter version soon. It evaluates the Economic Valuation of Air pollution (EVA) model system that has been developed in the Centre for Energy, Environment and Health (CEEH) financed by The Danish Strategic Research Program on Sustainable Energy under contract no 2104-06-0027. The EVA model system is an integrated model system based on the impact-pathway chain and can be used to assess the health-related economic externalities of air pollution. In particular, the EVA system can be used to estimate the external costs resulting from specific emission sources, countries or SNAP categories. In this paper, the EVA

system is applied over Europe and special attention is paid to Denmark and the international shipping traffic.

The sixth and final included paper (app. B6) "Projected change in atmospheric nitrogen deposition to the Baltic Sea towards 2020" deals with the change in future nitrogen deposition to the Baltic sea area. Like paper IV and paper V the tagging method is applied in order to study future emission legislation. Particularly the implication of the new National Emission Ceilings directive (NEC-II), currently under negotiation in the EU, is evaluated with respect to the present and future contributions from the countries surrounding the Baltic sea. The paper concludes, that for some countries, the projected decrease in N deposition arising from the implementation of the NEC-II directive, will be a considerable part of the reductions agreed on in the provisional reduction targets of the Baltic Sea Action Plan. In relation to the research focus of this thesis, the current paper solely aims at predicting the changes due to emission reduction and neglects the effects from climate change. The next step would be to include the impacts of climate change. Since this paper evaluates a particular legislation (NEC-II) until year 2020, the results are difficult to compare directly with the rest of the results in this thesis. However the research described in the paper is highly relevant in general with respect to the issue of climate change, emission change and future air pollution levels and their mutual interactions.

This thesis begins with a chapter (2) on state of the art within climate change - air pollution interactions, followed by chapter (3) describing the emission inventories and scenarios used. Next, the chemical transport model (DEHM) is described in chapter 4 followed by a chapter (5) about the climate model, the simulations and the the meteorological output of the climate model.

The results of the first research topic "Impacts of climate change on ozone chemistry over three centuries" are outlined in chapter 6 together with a thorough evaluation of the ozone related chemistry included in the model. Chapter 7 deals with the second research topic "The relative importance of the signal from climate change and the signal from emission change". Finally the subject of time-slices is treated in chapter 8. First the topic is introduced, secondly methods for evaluating the variability of time-slices is described. In chapter 9 the results are outlined.

In general the results are discussed briefly as they are presented and in chapter 10, the results of all three research topics are summarised and discussed jointly. The final conclusions are stated in chapter 11 together with a future outlook.

2 The state of the art in Climate Change - Air Quality modelling

Since about a decade ago a new branch of air quality modelling has developed within the international atmospheric chemistry transport modelling community. The observed climate change within the last century and an establishment of the anthropogenic origin of these changes by the publishing of the fourth IPCC Assessment Report in 2007 (IPCC, 2007) have initiated an urge to understand, how these changes in the global climate system affect future air quality.

The distribution and lifetimes of air pollutants depend strongly on many meteorological parameters. It is therefore very likely that the fate of the air pollutants will be altered under changed climate conditions even though the anthropogenic emissions are stagnated to levels of today. Both regional [Hogrefe et al., 2004; Langner et al., 2005; Meleux et al., 2007; Tagaris et al., 2007; Dawson et al., 2008; Katragkou et al., 2010; Andersson & Engardt, 2010], hemispheric [Hedegaard et al., 2008], and global [Johnson et al., 2001; Brasseur et al., 2005; Liao et al., 2007; Murazaki & Hess, 2006; Stevenson et al., 2005; Wu et al., 2008a; Racherla & Adams, 2008] chemistry transport models have been used to quantify the changes in air pollution levels due to climate change, and today more and more research groups all over the world develop coupled (in most cases one-way coupling) climate/air-quality-models in order to answer the growing amount of questions from policy makers.

There is a general belief that the size of the signal from climate change on air pollution levels and distributions is large enough to necessarily be accounted for when future emission legislation are developed (e.g. Hogrefe et al. [2004]; Langner et al. [2005]; Andersson & Engardt [2010]). Wu et al. [2008b] defines "climate penalty" as the need for stronger emission controls in order to achieve a given air quality standard. As an example Wu et al. [2008b] concludes from their results that air quality control needed to reduce the NO_x levels 40% under current climate conditions will match a reduction

of 50% under 2050 climate conditions. This 25% larger reduction by the authors defined as the "climate penalty" add to the fact that policy makers must take into account the effects from climate change when making new air quality control strategies.

In the following section (2.1) the evolution of the CC-AQ model community through the last decade including some methods and conclusions are included. For a more detailed review and comparison of some of the results see Carmichael & Dentener [2007]; Jacob & Winner [2009]; Hjorth & Raes [2009] and specifically for the United States see [Weaver et al., 2009]. Further section 2.1.1 introduces the field of on-line coupled models.

2.1 Evolution the of CC-AQ modelling community

Historically, one of the first studies published, with one-way coupling of climate model to a full chemistry transport model with an advanced chemistry scheme, was carried out by Johnson et al. [2001]. They used the three-dimensional Lagrangian tropospheric chemistry model STOCHEM [Collins et al., 1997, 1999] driven projected climate data from the Hadley Centre Atmophere-Ocean General Circulation Model (AOGCM) forced with the SRES A2 emission scenario [Nakicenovic et al., 2000] for the period 1990-2100 and showed that the impacts of climate change leads to a decrease in the net production of tropospheric ozone combined with a smaller increase of stratospheric input ozone at the top of the model domain. However, the vertical resolution in the model of the upper stratosphere was relatively low. The extended up to 100 hPa and were only represented by nine layers in the vertical and had a horisontal resolution of $5.0^\circ \times 5.0^\circ$. Furthermore Johnson et al. [2001] did not include the feedback from natural emissions, which together with the relatively low model resolution makes the results very preliminary. In 2004 Hogrefe et al. [2004] used a regional model centred over the eastern United States and showed that the effect from a changed climate may contribute to the air pollution levels in the future equal to the effects from changed emissions.

From 2005 and forth more and more research groups began to study the effects on climate change on air pollution levels and the model setups became more refined. Today, approximately half a decade later, a small climate change - air pollution community has developed within the chemistry transport modelling community.

In 2005 Langner et al. published results including climate change-air pollution interaction from a regional study. They studied the tropospheric surface ozone over Europe, using the regional Multiscale Atmospheric Transport and Chemistry Model (MATCH) forced with climate data from the regional Rossby centre Atmospheric Climate model(RCA) version 1. Langner et al.

[2005] found a general increase in surface ozone over southern and central Europe and a general decrease over northern Europe. They stated that, if the climate scenario used in the simulations is representative for the future climate, the increase in surface ozone in the future is comparable to the expected reductions resulting from emission reduction protocols in force by the time published.

Meleux et al. [2007] did similar experiments, which confirm the results found by [Langner et al., 2005]. [Meleux et al., 2007] used the CHIMERE chemistry-transport model forced with climate predictions from the Regional Climate Model (RegCM). They also found a substantial increase in the daily peak ozone during the European summer periods which might pose a more serious threat to human health, agriculture and natural ecosystems in the future. Meleux et al. [2007] also conclude that the summer of 2003 very well could be a good example of future threats from air pollution and climate change on human, agriculture and nature.

Murazaki & Hess [2006] were the first to publish results from a global simulation with one-way coupling of a climate model and a chemical transport model projecting the effects of climate change on air pollution levels throughout the 21st century. They used the global Model of OZone and Related Chemical Tracers, version 2 (MOZART-2) forced with future meteorology from the National Center for Atmospheric Research (NCAR) climate system model(CSM 1.0). Murazaki & Hess [2006] fixed both the anthropogenic and the biogenic emissions at a 1997 level in order to separate out the effects from climate change on air pollution. In general they found that background ozone will decrease in the future in contrast to the locally produced ozone. Contrary, the ozone levels over the densely populated areas (high NO_x levels) will increase significantly since the predicted decrease in background ozone is far smaller than an expected increase in locally produced ozone[1].

In 2008 Hedegaard et al. [2008] published similar results as Murazaki & Hess [2006] but the simulation included variable biogenic emissions. The level of Biogenic Volatile Organic Compounds (BVOCs) increases significantly due to their temperature dependency and the temperature evolution during the 21st century. Besides ozone, Hedegaard et al. [2008] also examined the consequence of climate change on some particles. As an example they found that the sulphate levels over the already polluted areas would increase significantly due to an enhanced chemical production.

At the same time several regional studies over the United states were published [Wu et al., 2008a,b; Pye et al., 2009; Tagaris et al., 2007, 2008; Liao et al., 2007, 2010]. These studies are al focused on different parts of the United States, Canada and Mexico. Most of them concentrate on the impacts of

[1] Stevenson et al. [2005] who carried out similar simulation with a global model but only for the period 1990-2020.

climate change alone and a few also evaluates the impacts of changes in the anthropogenic emissions. Details of some of these studies will be discussed later in this thesis.

Latest Katragkou et al. [2010]; Andersson & Engardt [2010] and Lam et al. [2011] have published results of ozone over Europe and ozone particles over the United States due to impacts of climate change. Andersson & Engardt [2010] used the Swedish MATCH model to investigate importance of biogenic emissions and dry deposition for the future ozone concentration. They found that the dynamical inclusion of biogenic emissions are together with a meteorology dependent parameterisations of the dry deposition to vegetation is extremely important when estimating the future ozone concentrations in Europe. They did some sensitivity studies where they change the dry deposition to vegetation in a way such that it could vary according the meteorological conditions based on the fact that the ozone uptake from vegetation depends on the climate conditions they are exposed to. Andersson & Engardt [2010] concludes that the dry deposition by plant uptake in Spain accounts for 80% of the increase in the projected ozone concentration.

Katragkou et al. [2010] also did a sensitivity study of the impact from changes in different meteorological boundary conditions in a study of ozone over Europe. It is well known that when using a regional Chemical Transport Model (CTM), the chemical boundary conditions chosen have an impact on the final output. Katragkou et al. [2010] used a model setup where the CAMx reginal CTM were driven on meteorology from the regional climate model RegCM3. They changed the meteorological boundary conditions between the ERA40 reanalysis and a climate projection by ECHAM5 and found that the external meteorological forcings are just as important as the chemical boundary conditions. This problem is minimized in global model setups since the boundary conditions is reduced to the top of the domain. Nevertheless, Tang et al. [2007] have found the top boundary conditions can be quit important too. According to their results the top boundary conditions have strong effects on the atmosphere above 4 km.

Most recently Lam et al. [2011] have published a paper focussing on the impacts from biogenic emissions under a combination of different climate conditions and anthropogenic emissions on future ozone and particulate matters distribution over the United States. Further, both the global GEOS-Chem model and the regional CMAQ model have been used in order to investigate the effects of down-scaling. Lam et al. [2011] concludes that for Particulate matter with a diameter $<2.5\ \mu m$ the impact from climate change have insignificant effects compared to impacts from changes in anthropogenic emissions. On the contrary the climate change has a small effect on the future ozone concentration especially in the Northeast of US where the impacts from changes in biogenic emissions were stronger.

2.1.1 Online models

All the models mentioned above are offline model setups. Only a very few groups have made simple online couplings of Climate GCM-CTM models (e.g. Forkel & Knoche [2006]; Liao et al. [2009]; Unger et al. [2009]). The advantages from online coupling is the model ability to account for the radiative feedbacks from short-lived greenhouse gases like ozone and methane as well as aerosols between the large scale climate system and the small scale chemical regimes. However, online coupled climate-chemistry models demand very high scientific understanding of the individual feedbacks and physical processes and set high demands to the computational resources. The differences in the results of online and offline coupled models varies a lot depending on the complexities of the given models [Zhang, 2008].

Within online models, two conventional frameworks exist, - unified online coupling and separate online coupling. The first integrates an air quality model into a meteorological model and the second consists of two separated systems (meteorology model/air quality model), that exchange information at every time step. These types of coupling are with respect to climate change mostly used for regional climate/air quality modelling [Zhang, 2008].

On a global scale the online coupling is more focusing on earth system models, which is a large model system including atmosphere, ocean, biosphere, cryosphere and chemistry models. However, earth system models are still in their premature stages with respect to the inclusion of chemistry and biosphere. The large uncertainties in accurately describing the climate-aerosol-chemistry-cloud-radiation feedback processes and the large temporal and spatial demands in order to predict effects of climate change, justifies using the offline method.

Recently Raes et al. [2010] published a study where they propose a generalised method to include atmospheric chemistry into the theory of climate feedbacks. They suggest a method based on a the well known sensitivities (λ) and radiative forcings (RF) which they couples by a coupling describing the effects from climate on the atmospheric chemistry and coupling factor oppositely directed describing the effects from atmospheric chemistry on the climate system. Through considerations of the thermodynamic equations, planetary energy balance, the Eulerian equation of motion and some perturbation analysis, they end up with a simple fraction describing the "gain" for each individual chemical component. This gain is fraction between the change in the concentration of a given component due to a forcing in the fully coupled climate-chemistry system divided by the change in the uncoupled system. The result is a parameter (gain) that gives insight into the importance of climate as a feedback within the atmospheric chemistry system [Raes et al., 2010].

Further they apply their developed theory and finds for aerosols, that for

the individual aerosols the global atmospheric burden can be up to 30% higher compared to results where only emissions from a "fixed" climate is included. The gain for ozone is 1.15 in the Northern hemisphere and 0.80 over the remote oceans which means that the we can expect the future ozone burden to be 15% higher (20% lower) compared to the results with fixed climate. However, the author states that this really preliminary results since the model they use do not include all possible processes that can result in feedbacks and there are not accounted for the direct and indirect effects of sea salt and dust nor the long term effect from perturbation of the methane [Raes et al., 2010]. However, such a system is highly parameterized and does not provide new understanding of the underlying processes. Moreover, there is a high risk that the parameterizations of the gain is very uncertain and maybe even wrong ,since it does not include the physical and chemical processes.

3 Emission Scenarios

The thesis is build on a model setup, which uses several types of emissions scenarios. In the following sections, the emissions used in this thesis are described together with a short overview of the scientific processes behind the scenarios. The SRES A1B emission scenario (sec. 3.1), the newly developed RCP scenarios (sec. 3.2.2) are described and together with the EMEP, GEIA and EDGAR (sec. 3.3) emission inventories.

In order to project the future atmospheric composition, the future anthropogenic emission has to be known. Obviously, such emission inventories do not exist since they depend on a large amount of unknown parameters, like e.g. population growth, economic development, technological evolution and politics. Therefore anthropogenic emission scenarios have been developed based on future projection concerning politics, demography, technology, socio-economy etc. These scenarios are the first assumption atmospheric or climate system modellers have to accept in order to project the future conditions of the atmosphere.

3.1 SRES A1B Scenario

In 1992 the first IPCC emission scenarios (IS92) were created. These were in 1998 replaced by the IPCC SRES emission scenarios, which are a set of different storylines of how demography, economy, technology etc. can develop in the future and the resulting emission up to year 2100 are prescribed. Based on these emissions, climate modellers made climate projections for the 21st century. Having the climate projection and the original emissions, integrated assessment modellers carried out impact, adaptation and vulnerability studies. A huge problem with this approach has been that the whole process has been ten year under way and the original socio-economic aspects that the storylines are built on were outdated at the time the impact community started using the scenarios [Moss et al., 2010]. An example of this is the prediction of the sulphur emissions. The sulphur emission reductions initiated during the 1980s and early 1990s can already be seen in observations from late the 1990s and the beginning of the 2000s. These reductions

are not included in the scenarios made before 1997.

The SRES (Special Report on Emission Scenarios) emission scenarios consist of four storylines A1, B1, A2 and B2. These are denoted families and each family includes several scenarios [Nakicenovic et al., 2000]. For example the A1 family includes the A1F1 which represents a fossil fuel intensive future, A1T is based green technologies and dominated by non-fossil fuel energy and finally there are A1B scenario which has been used in the in to forced the climate simulation that this thesis work builds upon Nakicenovic et al. [2000].

The A1B is an in-between balanced scenario. The A1B scenario assumes a future world with very rapid economic growth and a rapid introduction of new and more efficient technologies balanced between both fossil - and non-fossil intensive energy sources. The population growth peaks in about 2050 and declines hereafter [Nakicenovic et al., 2000].

3.2 RCP Scenarios

The Representative Concentration Pathways (RCP) consist of four sets of emissions; RCP2.6, RCP4.5, RCP6 and RCP8 that lead to four predetermined radiative forcing levels (2.6 W/m^2 ,4.5 W/m^2,6 W/m^2, 8.5 W/m^2). In the following, the process leading to these new scenarios is briefly described together with a brief overview of the four scenarios. In the thesis the RCP4.5 scenario are used and details is summarized in subsection 3.2.2.

3.2.1 The parallel process

In the acronym Representative Concentration Pathways (RCP), "Representative" means there are many different scenarios which have similar radiative forcings and emissions characteristics and still reach the same target [Moss et al., 2008, 2010]. "Pathways" refers to the time before reaching the target and it indicates that the evolution towards the target does not have to follow a certain trajectory [Moss et al., 2008, 2010]. For example overshooting can be a possibility or a period of rapid increase in the radiative forcing levels followed by a decline could be another path towards a predetermined radiative forcing level. And furthermore these concentration levels or trajectories can also be reached by different combinations of new technologies, demographic and economic evolutions etc. In contrast to a more straight forward development process of the SRES scenarios, the method just described is called the "new parallel process" [Moss et al., 2008].

The main purpose of the parallel process is to speed up whole process in order two get scenario data which by the time it is ready for use still is based on state-of-the-art models Moss et al. [2008] and [Moss et al., 2010]. First

some forcing levels are determined and a set of emissions leading to each of these forcing levels are constructed. In the next step climate modellers and socio-economist work in parallel in determine the future climate and the socio-economic worlds that lead to these predetermined forcing levels. The outcome of the second step is climate projections and specific emissions where the different pollutants are divided into sectors ready to use as input to impact, vulnerability, and adaptation research. In contrast to the research published in the 4th report from IPCC, the climate models used for assessment research will not be outdated even before the assessment research are published.

The whole RCP process is believed to facilitate new research questions on how broad the socio-economic conditions can be in order to reach a specific forcing level in time. This is both with respect to the ultimate level pathway over time and spatial patterns. Subsequently with this research of the different ways to match a specific RCP, it is expected that new reference scenarios will be developed, in order to study uncertainties or e.g. alternative demographic, socioeconomic, land use and technology scenarios [Moss et al., 2008, 2010].

The outcome of the above described process is the four scenarios RCP2.6 (RCP3.0-PD), RCP4.5, RCP6 RCP8, which leads to a radiative forcing of 2.6 W/m^2, 4.5 W/m^2, 6 W/m^2, 8.5 W/m^2 by the end of this century (2100). RCP2.6 or RCP3-PD (peak and decline) is the scenario resulting in the lowest forcing. It attains a forcing level of 3 W/m^2 before year 2100 and decline to about 2.6 W/m^2 by the end of the century. The two middle scenarios RCP4.5 and RCP6 both stabilize at their predetermined level without any overshooting before year 2100. RCP8 rises throughout the whole century and passes a radiative forcing level 8.5 W/m^2 by the end of the century, which corresponds to a CO_2 equivalence concentration level of 1370 W/m^2.

3.2.2 RCP 4.5

In the current study the RCP4.5 [Smith & Wigley, 2006; Clarke et al., 2007; Wise et al., 2009] is chosen. This means a RCP that stabilizes at radiative forcing of 4.5 W/m^2 after year 2100. At the time the first simulation of this study was carried out RCP2.8, RCP4.5 and RCP8.5 were the only scenarios available in the RCP database (www.iiasa.ac.at/web-apps/tnt/RcpDb) and the RCP4.5 was chosen, since it was in the middle range of these three scenarios and was most similar to the old SRES A1B scenario with respect to radiative forcing which the ECHAM5 simulation used in this thesis has been forced with. A radiative forcing of 4.5 W/m^2 corresponds to a 650 ppm CO_2-equivalent level after year 2100.

The emission data in the IIASA RCP data base (www.iiasa.ac.at/web-apps/tnt/RcpDb) are global and have a resolution of $0.5^\circ \times 0.5^\circ$. One data

set is provided for each decade, which in this case means for the period 1990-1999 the 2000 emissions have been used for every year and for the 2090-2099 decade the data of year 2100 has been used every year.

The data base contains emission data of the common climate gases (CO2, CH4, N2O, CFCs etc.) and the air pollutants; Black Carbon (BC), Sulfur, (SO_2), carbon monoxide (CO), NO_x (NO), Volatile Organic Compounds (VOCs) and ammonia (NH_3). In the chemical transport model DEHM the short term emissions of these compounds have been estimated by forcing of monthly, weekly and diurnal cycles upon the annual value.

To put the RCP4.5 scenario in perspective, it can be mentioned that EU decided on a two-degree target after the COP15 meeting in Copenhagen in 2009 and in the last IPCC report it was concluded that: "In order to have a 50% chance of keeping the global mean temperature rise below 2°C relative to pre-industrial levels, atmospheric GHG concentrations must stabilise below 450ppm CO2 equivalence" [Pachauri & Reisinger, 2007]. And further "Stabilisation below 400ppm will increase the probability to roughly 66% to 90%" [Pachauri & Reisinger, 2007]. RCP4.5 stabilizes at 650 CO_2-eq after year 2100 whereas the RCP2.6 peaks at 3.0 W/m2 corresponding to a CO_2-equivalence level of 490 W/m2.

3.3 GEIA, EMEP and EDGAR

For the first part of this thesis (chapter 6) the emissions of the primary pollutants in DEHM are based on data from the Global Emissions Inventory Activity (GEIA) [Graedel et al., 1993], the Emission Database for Global Atmospheric Research (EDGAR2000 Fast track) [Olivier et al., 1996; Olivier & Berdowski, 2001] both with global coverage, and the EMEP emissions [Vestreng, 2001; Mareckova et al., 2008] covering Europe. The GEIA database includes natural emissions of NOx from soil and lightning and Black Carbon, which mainly originate from biomass burning. Further, emissions from retrospective wildfires are included based on Schultz et al. (2008).

The emissions divided into ten different SNAP categories (Selected Nomenclatur for Air Pollution), and are distributed with height above the surface following patterns depending on the appointed SNAP categories. With respect to the temporally distribution, the emission inventories provides annual mean values and these have been forced with monthly, weekly and daily cycles.

All the emission described are above have been only been used in the first study where for the anthropogenic emissions have been kept constant at a 2000 level to isolate the impacts from climate change on ozone and the related photochemistry. On the contrary the emissions of biogenic VOCs

are calculated interactively in the model and have not been free to vary in accordance with the forcings from climate change.

3.3.1 Biogenic isoprene emissions

The natural emissions of VOCs are calculated dynamically in the model according to the IGAC-GEIA biogenic emission model (International Global Atmospheric Chemistry - Global Emission Inventory Activity) [Guenther et al., 1995]. The IGAC-GEIA biogenic emission model describes the emissions of isoprene and these are e.g. sensitive to temperature changes. Other naturally emitted VOCs like for example terpenes are not yet included in the model, however experiments with the Model of Emissions of Gases and Aerosols from Nature (MEGAN) emission model [Guenther et al., 2006] are currently being analysed and will most likely be implemented in the DEHM model soon. Some of the preliminary results will be discussed in chapter 10

4 The DEHM Model Framework

DEHM (Danish Eulerian Hemispheric Model) is an Eulerian Atmospheric Chemistry Transport Model (ACTM) with a two-way nesting capability to obtain higher resolution over limited areas [Christensen, 1997; Frohn et al., 2002a,b; Frohn, 2004; Brandt et al., 2011]. The chemistry scheme in DEHM is originally based on a chemical scheme by Strand & Hov [1994] which has been extended with a detailed description of the ammonia (NH_3) chemistry through the inclusion of NH_3 and related species: ammonium nitrate (NH_4NO_3), ammonium bisulphate (NH_4HSO_4), ammonium sulphate ($(NH_4)_2SO_4$) and particulate nitrate (NO_3^-) formed from nitric acid (HNO_3). Furthermore, reactions concerning the wet-phase production of particulate sulphate have been included. Several of the original photolysis rates as well as rates for inorganic and organic chemistry have been updated with rates from the chemical scheme applied in the EMEP model [Simpson et al., 2003]. The current model version includes 58 photo-chemical compounds (including NO_x, SO_x, VOC, NH_x, CO, etc.) and 9 species representing primarily emitted particulate matter ($PM_{2.5}$, PM_{10}, TSP, sea-salt $< 2.5\,\mu$m, sea-salt $> 2.5\,\mu$m, fresh black carbon, aged black carbon and organic carbon). DEHM includes 122 chemical reactions.

The continuity equation is setup for each chemical component followed by application of a simple non-symmetric splitting procedure according to [McRae et al., 1982]. For further details see [Frohn et al., 2002b; Brandt et al., 2011]. Physically the model is based on full 3-D advection-diffusion equation which is driven on meteorological data from a general circulation model (weather or climate prediction model). The advection is solved numerically using an Accurate Space Derivatives scheme with non-periodic boundary conditions for the horizontal advection [Dabdub & Seinfeld, 1994] and a finite elements scheme for the vertical advection [Pepper et al., 1979]. Temporal, advection is solved using a Taylor series expansions method to third order. The diffusion is solved using the finite elements scheme to discritize in space and the Θ-method to discritize in time [Lambert, 1991]. Finally wet and dry depositions are parameterized similar to the EMEP model

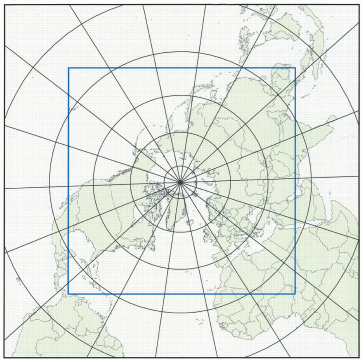

Figure 4.1: The model domain covering a little more than the Northern Hemisphere. In this thesis only the largest domain have been used, though DEHM has several other possibilities (see blue box for the small mother domain and furthermore nests with higher resolution (not shown) can be applied over Europe, northern Europe and Denmark)

[Simpson et al., 2003; Emberson et al., 2000], except for the dry deposition of species on water surfaces where the deposition depends on the solubility of the chemical specie and the wind speed [Asman et al., 1994; Hertel et al., 1995; Frohn, 2004]).For further details on the numerics, physics and chemistry of the model see Christensen [1997]; Frohn et al. [2002a,b]; Frohn [2004]; Brandt et al. [2011] and references therein.

In this thesis, only the mother domain has been used. It covers slightly more than the Northern Hemisphere and has a horizontal grid resolution of 150 km $\times$ 150 km using a polar stereographic projection true at 60°N (see figure 4.1). In the vertical there are 20 unevenly distributed layers and these are defined in a terrain following σ-level coordinate system. The top layer of the model is situated at 100 hPa.

When simulating impacts of climate change on air pollution levels, the chemical boundary conditions can be important for interpreting the results. The boundary conditions depend on the wind direction. Free boundary conditions are used for areas where mass is transported out of the domain and elsewhere the boundary conditions are set to an annual average background value. E.g. for ozone, the initial and boundary conditions are based on ozonesonde measurements, interpolated to global monthly 3D values with a resolution of $4° \times 5°$ (Logan, 1999). The same boundary conditions have been used for all simulations and since we focus on differences, the effect from boundaries can be eliminated from the interpretation of the results.

The DEHM model has been validated against observation from Europe over a ten-year period [Geels et al., 2005] and have recently been evaluated against 20 years of observations over Europe (Hansen et al. [2011] in preparation). Further the model has participated in several model intercomparison projects and is evaluated to perform well compared to other models (see e.g. Van Loon et al. [2007]; Vautard et al. [2006, 2009]; Cuvelier et al. [2007]).

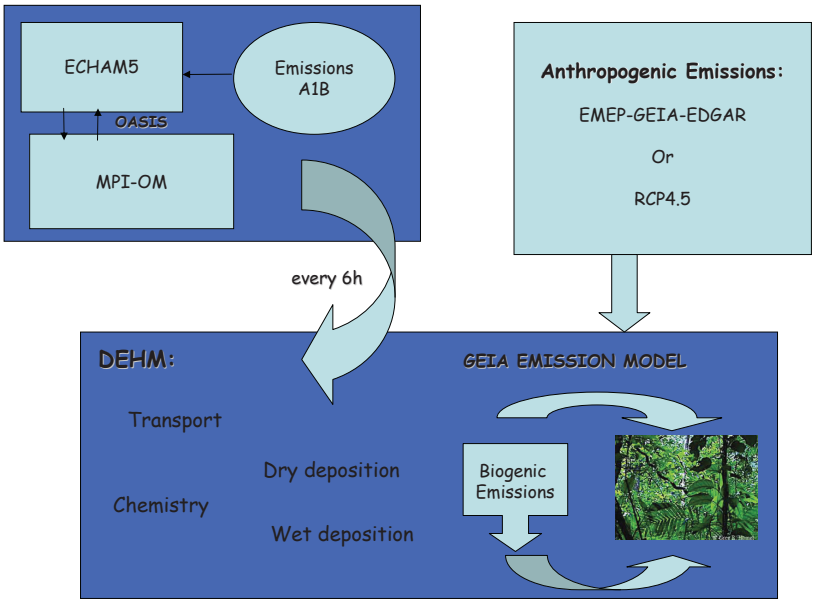

Figure 4.2: The DEHM model is driven on six-hourly meteorological input projected by the ECHAM5/OM-MPI atmosphere-ocean model forced with SRES A1B emission scenario. Further DEHM emission input from either from a combination of the EMEP, GEIA and EDGAR databases or from the RCP4.5 emission scenario. The biogenic emissions of isoprene depend on the meteorological conditions and is calculated inter-actively in the DEHM model according to the GEIA emission model

4.1 Overall model setup

In all the experiments included in this thesis the ECHAM5/OM-MPI Atmosphere-ocean General Circulation Model forced with the SRES A1B emission scenario has been used to drive the Chemical Transport Model DEHM model. However, two different sets of emissions are used as input to DEHM. In figure 4.2 the general model setup is illustrated.

In the analysis of projected ozone chemistry over three centuries (chapter 6, the model setup includes emissions from the GEIA, EMEP, EDGAR databases and in the analysis of the signal from climate change vs the signal from emission change (chapter 7 the RCP4.5 emission scenario has been used. Both sets of emissions are described more detailed in chapter 3.

The first experiment concentrate on the impacts of climate change and therefore the anthropogenic emissions provided by the GEIA, EMEP, and EDGAR databases are kept constant at a year-2000 level. On the contrary

the biogenic emissions are calculated interactively within the model by the the GEIA emission model [Guenther et al., 1995] (see section 3.3.1 for details).

In the second experiment both the impacts of climate change and emission change have been simulated. As part of this experiment agin the siganl from climate change on the future air pollution has been calculated but in this experiment thee RCP4.5 projections (section 3.2.2) have been used and fixed at a 2000 level. At the time the first study was performed the RCP emission scenarios were not available and therefor there is this difference between the two experiments. Nevertheless analysis of the two projections have shown, that the differences effectuated in the DEHM output are extremely small due to constant GEIA-EMEP-EDGAR emissions vs the RCP4.5 emission and from now the simulations driven with different sets of emission is treated as if they were identical and to limit the number of figures only one of the simulations will not be shown in this thesis.

The DEHM-ECHAM climate setup have been evaluated thoroughly in earlier studies [Hedegaard, 2007; Hedegaard et al., 2008] against observations from the EMEP observation network over Europe and against similar model setups with known performance. According to these evaluations the DEHM-ECHAM climate setup has shown to perform well with respect to annual mean values and seasonal variation based on monthly mean values of various different chemical species (see [Hedegaard, 2007; Hedegaard et al., 2008]).

5 The ECHAM5/MPI-OM Climate Model

The climate simulation used in this study were a part of the 4th IPCC Assessment Report (AR4) multi-model ensemble study (run4). It is based on the coupled atmosphere-ocean model ECHAM5/MPI-OM, which is a global state of the art climate model developed at the Max Planck Institute in Hamburg [Roeckner et al., 2003, 2006]. The climate simulation is forced with emissions, based on realistic estimations until year 2000 and emissions according to the SRES A1B scenario in the period 2000-2100. In the final period 2101-2200 all the emissions have been fixed at a 2100-level.

The ECHAM5/MPI-OM consists of an Atmospheric General Circulation Model ECHAM5 [Roeckner et al., 2003, 2006] and the ocean-sea-ice model MPI-OM [Marsland et al., 2003]. The atmospheric model ECHAM5 is horizontally defined in a spectral grid with truncation T63 and uses hybrid sigma-pressure coordinates in the vertical. It is a global model system with a top layer at 10 hPa. State-of-the-art parameterizations are used for shortwave and long wave radiation, stratiform clouds, boundary layer and land-surface processes and for describing gravity wave drag in the model. Details about the description of the aerosol effect in this specific simulation can be found in May [2008].

The ocean-sea-ice model has a horizontal resolution of $1.5^\circ \times 1.5^\circ$ and is vertically discretized into 40 z-levels. The model operates on the primitive equations for a hydrostatic Boussinesq fluid with a free surface. Along-isopycnical diffusion, horizontal tracer mixing by advection with unresolved eddies, vertical eddy mixing, near-surface wind stirring, convective overturning, and slope convection are all parameterized in the ocean model. Concentration and thickness of sea ice are treated interactively in the model by a dynamic and thermodynamic sea-ice model. For further details of the ocean-sea-ice model, see Marsland et al. [2003].

The atmosphere and ocean/sea-ice components are interactively coupled by the Ocean-Atmosphere-Sea Ice-Soil (OASIS) coupler [Valcke et al., 2003] and exchange information about sea-surface temperature, sea-ice concentration

and thickness, wind stress, heat and freshwater once a day. Further details of the coupling can be found in Jungclaus et al. [2006]. The model does not employ flux adjustments. The coupling of the atmosphere and ocean model have been tested by Jungclaus et al. [2006] and it is found to perform well with respect to sea surface temperatures, sea-ice conditions and the meridional heat and transport of freshwater and is in good agreement with observational data [Jungclaus et al., 2006].

ECHAM5/MPI-OM is a state-of-art climate model widely used within both the international climate community and with respect to its modelled climate within the impact research community. It was part of the multi-model ensemble CMIP3 of the last IPCC report (AR4) and will contribute to the next IPCC report (AR5, to be published 2013) as well. The ECHAM model have been evaluated in several model inter-comparison project and the overall performance is good. In Walsch et al. [2008] the performance of 15 models from the CMIP3 project have been evaluated against observations over the Arctic region. The ECHAM5 model is among the top two highest ranking models in projecting surface temperature over Alaska, Greenland and in the northern hemisphere in general.

The SRES A1B scenario that the ECHAM5/MPI-OM model has been forced with in the simulations for this thesis work is described in section **??**. For ozone, only the stratospheric ozone is prescribed according to the A1B scenario. The tropospheric ozone concentration varies annually according to a cyclic distribution based on observations [May, 2008]. It should be noted that the SRES A1B forcing only applies to the projected meteorology. The anthropogenic emissions used for the DEHM model is different as described above.

5.1 Meteorology by ECHAM5/MPI-OM

In the following, the output from the simulation used to drive the DEHM model in all the research performed in this thesis, is described. The temperature, humidity and precipitation are direct output from ECHAM5 simulation whereas the mixing height is derived from simple energy balance considerations and the radiation is calculated from the cloud cover (for details see Hedegaard [2007]). The snow cower and sea ice are defined as a fraction between one and zero in each grid cell. One indicates total snow/sea ice cover and zero indicates that no snow/sea ice is present in the current grid cell.

5.1.1 Temperature

The climate simulation used in this study where a part of the 4th IPCC Assessment Report (AR4) multi-model ensemble study. In the current simulation the global temperature is predicted to increase by 3.03 $\circ C$ by the end of the 21st century and $4.27^\circ C$ by the end of the 22nd century, both relative to the period 1971-2000 [May, 2008]. This increase is a little higher than the average value ($2.65^\circ C$ and $3.36^\circ C$, respectively) predicted by the multi-model ensemble following the SRES A1B scenario in the AR4 [Meehl et al., 2007a]. However, it is well within the standard deviation of the IPCC AR4 multi-model ensemble by the end of the 21st century.

In figure 5.1 the mean temperature of the four decades considered in this study is plotted together with the absolute change between these decadal mean values and the significance of these changes using a student's t-test [Spiegel, 1992]. Temporally the temperature is increasing significantly in the two future decades (2090s and 2190s) compared to 1990s. The ECHAM5/MPI-OM model simulation generally also predicts a temperature increase in the 20th century (represented by the difference between the 1990s and the 1890s), however, this increase is only significant in the tropics and a temperature decrease is predicted over the North Atlantic storm tracks.

The absolute largest temperature increase is found in the 21st century (see centre plot of Fig. 5.1 (2090s minus 1990s)). This is in line with results from May [2008] who found that the changes in the global annual mean near-surface temperature is largest around 2060 with a warming rate of more than $4.5^\circ \frac{C}{century}$. This high warming rate is due to a strong increase in all greenhouse gases except methane and a marked reduction in the anthropogenic sulphur emissions according to the SRES A1B emission scenario. Focussing on the 21st century (2090s-1990s) geographically the temperature increase is largest in the Arctic region where it locally exceeds 9 degrees. Over land areas in general the temperature increase ranges from $3^\circ C$ to $6^\circ C$ and over the ocean the increase is more modest in the range $1^\circ C$ to $4^\circ C$.

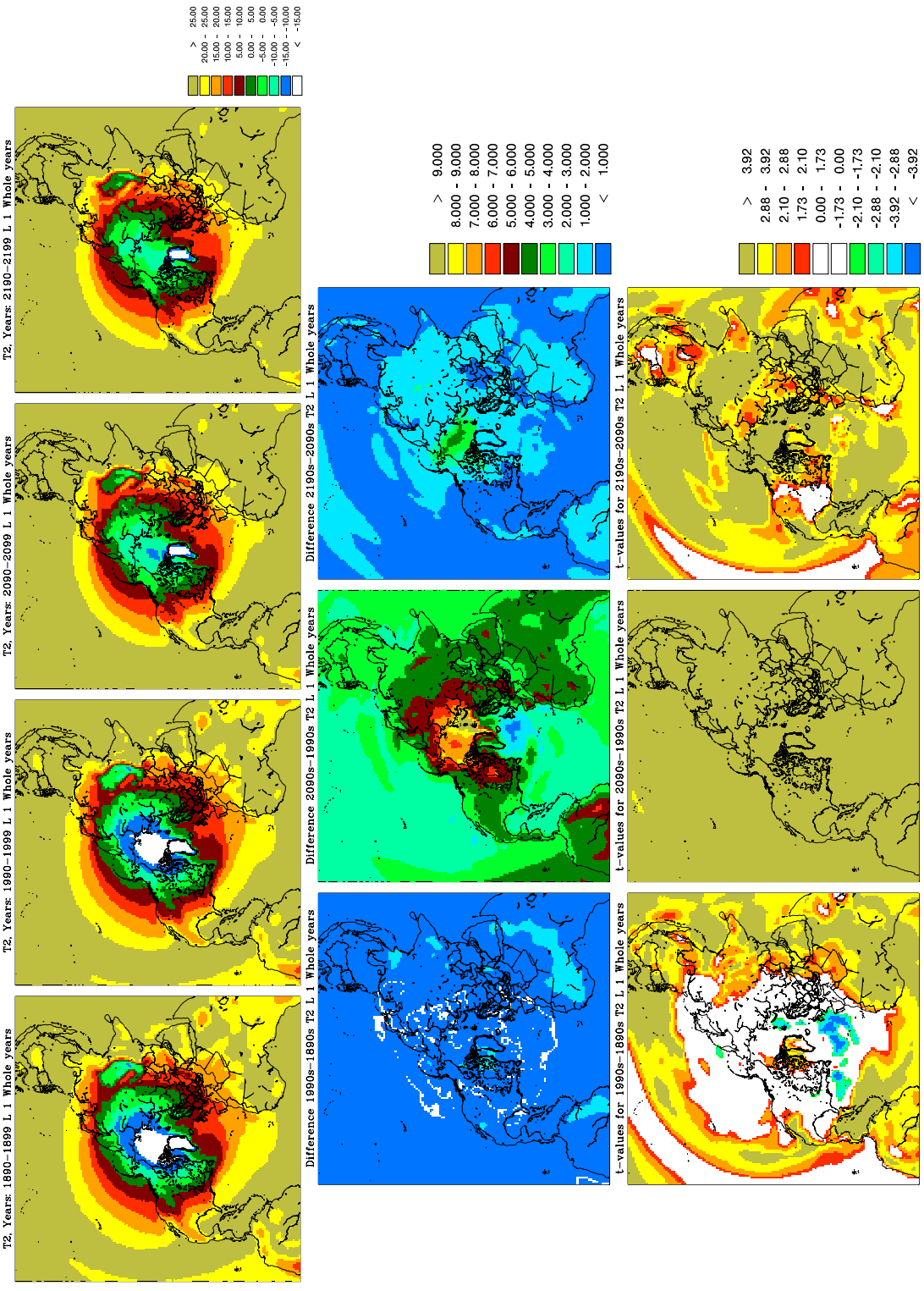

Figure 5.1: Top panel: Decadal mean temperature of the lowest model in °C of the decades; 1890s, 1990s, 2090s and 2190s. Middle panel: The difference in °C. Bottom panel: The significance of the differences according to the students t-test [Spiegel, 1992]. The threshold value for significance is chosen to 10% (white areas indicates no significant change)

5.1.2 Specific humidity

In figure 5.2 results for the specific humidity is shown. The specific humidity is closely related to the temperature. At saturation the specific humidity is a quasi-exponential function of temperature according to the Clausius-Clapeyron equation [Goosse et al., 2009]. This exponential dependency implies that the change in humidity is significantly largest at low latitudes (where the highest temperature is projected). The specific humidity distribution follows the latitudes very closely both for the means of the four decades (upper panels of figure 5.2) and for the changes between these decades (middle panel of figure 5.2). As the temperature plot (figure 5.1) the specific humidity also shows the absolute largest changes within the 21^{st} century (middle panel of figure 5.2). In the 20^{th} century the predicted change in specific humidity is only significant in the tropical region. Vertically the largest change in specific humidity is confined to the lowest part of the troposphere (approximately the lowest 2 km) where most water vapour in the atmosphere is found, in contrast to the vertical profile of temperature change, which is rather uniform.

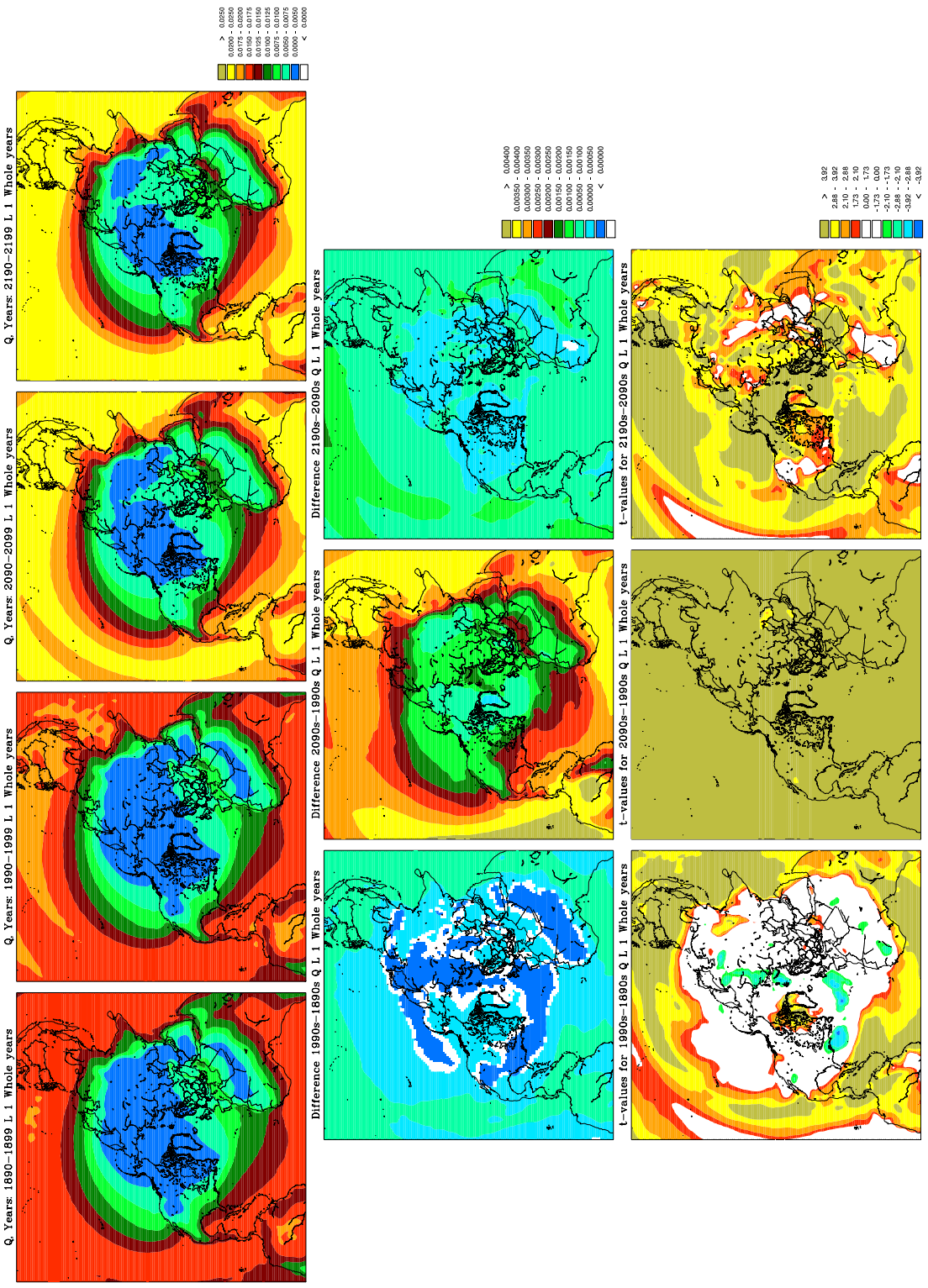

Figure 5.2: Average decadal specific humidity in the lowest model layer in $\mathrm{Kg\,Kg^{-1}}$. Setup the same as Fig. 5.1

5.1.3 Shortwave radiation

The shortwave radiation depend on both space and time and is derived from the cloud cover calculated by the ECHAM5 according to the method used in Hedegaard [2007]. In figure 5.3 the shortwave radiation of the four decades is shown together with the difference and the significance of these differences. The largest changes are predicted in 21st century, where the shortwave radiation is predicted to increase in the southern mid-latitudes and the subtropics. This is in line with the general idea that the earth in the future will experience longer and more persistent periods with drought and high temperatures in the subtropics [Christensen et al., 2007]. In contrast to the temperature and specific humidity, the change in shortwave radiation is only significant in the 21^{st} century (see lower panel, figure 5.3). The predicted change is highly dependent on latitude and increasing everywhere in the domain, except over the tropical Pacific.

Since the shortwave radiation is derived from latitude and ECHAM5 cloud cover, the area of decreasing shortwave radiation over the tropical Pacific most likely is due to an increase in cloud cover in the climate simulation. The ECHAM5/MPI-OM simulation has been part of the multi-model ensembles of 4th IPCC report (AR4), which confirms a general increase in cloud cover over the tropical Pacific [Meehl et al., 2007a]. In central and southern Europe the shortwave radiation is predicted to increase more than 20%, which is in good agreement with the theory of longer and more persistent periods of dry warm summers in the future at these latitudes [Vautard & Hauglustaine, 2007; Stott et al., 2004].

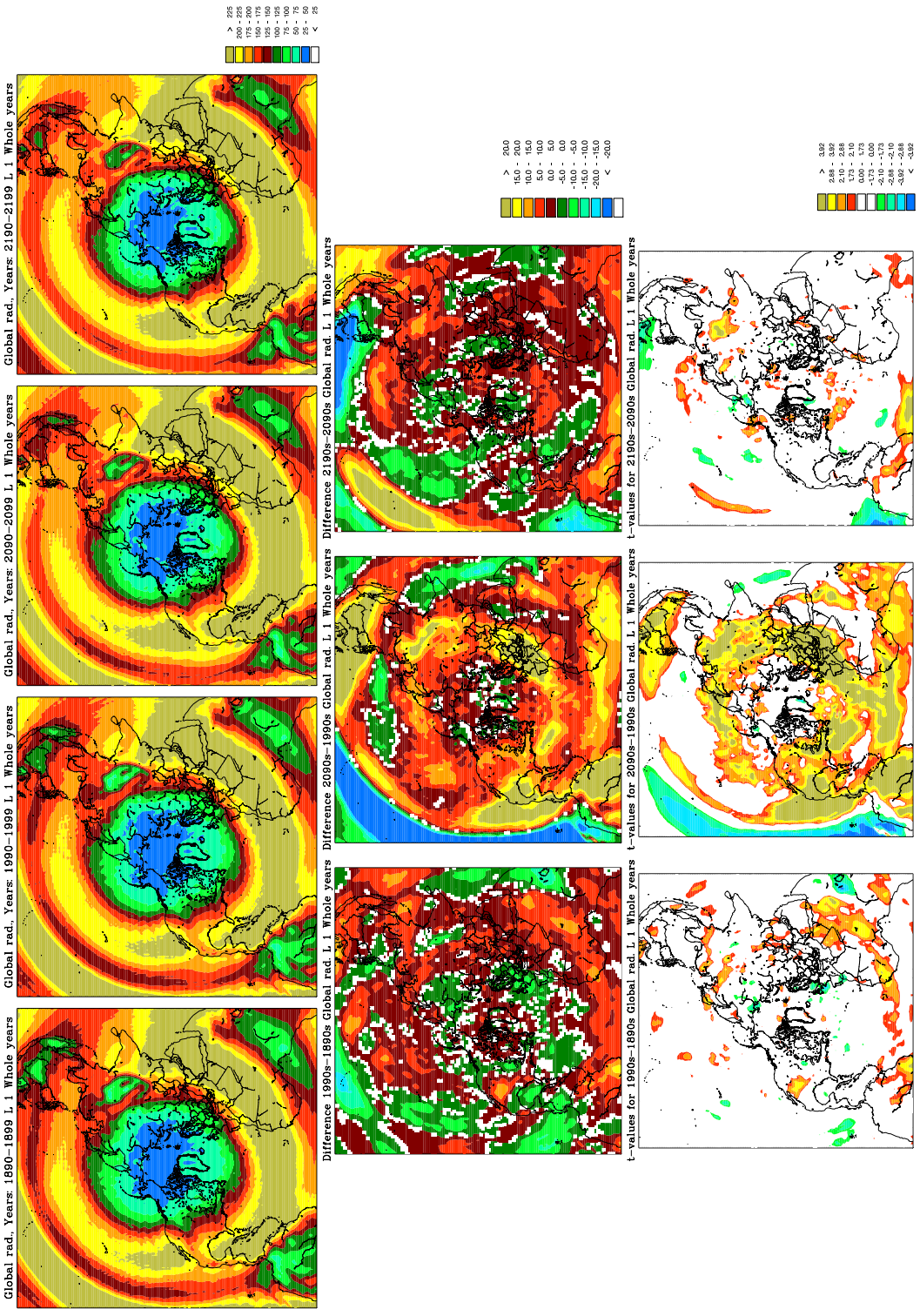

Figure 5.3: Average decadal shortwave radiation in the lowest model layer in W m^{-2}. Setup same as Fig. 5.1.

The following illustrations of the meteorological output are limited to display the levels of the 1990 decade and the 2090 decade, the difference and the significance of these differences according to the Students t-test [Spiegel, 1992].

5.1.4 Precipitation

In figure 5.4 the precipitation frequency is shown. The precipitation frequency is more interesting than the amount of precipitation with respect to deposition of air pollutants, since the most particles are washed out of the atmosphere in the beginning of a precipitation event. For example a whole week with showering rain results in more cleaning of the atmosphere than one full day with frontal rain surrounded by some dry days. The threshold value for precipitation in a given six-hour interval is set 1 mm and the ten-year mean precipitation frequency is shown figure 5.4 defined as a fraction between 0 and 1, where one indicates precipitation in a given grid cell at in a given six-hour time interval. The choice of 1 mm as a threshold value for precipitation is based on the parameterizations of the in- and below-cloud scavenging in the DEHM model, for further details see Hedegaard [2007].

Figure 5.4 shows the a) decadel mean precipitation frequency in 1990s, b) in the 2090s, c) the difference between the 2090s and the 1990s and finally in d) the significance of the difference between the two decades according to the students t-test. The white colours indicates no significant change and the threshold value for significance is set to 10 %. In general the precipitation frequency is projected to increase at high an low latitudes and increase at mid-latitudes. Focusing on Europe the precipitation frequency is projected to decrease significantly in the Southern Europe and oppositely in Scandinavia, Finland, Iceland, Greenland and the precipitation frequency is projected to increase. In general the precipitation frequency is projected to increase North of about $60°N$ and decrease significantly in subtropical part of the Pacific and Atlantic Ocean, the Caribbean, Mexico and the Central South America and in Western Africa.

5.1.5 Mixing Height

Figure 5.5 shows the mixing height in meters. The Mixing height is calculated from simple energy balance equation for the internal boundary layer according to the methods described in Christensen [1997]. Figure 5.5 is illustrated the same way as the precipitation frequency where a) is shows the 1990s decadal mean mixing height, b) the 2090s decadal mean, c) the difference in meters and c) the significance of this difference. In South eastern Europe the mixing height is projected to increase in the range 50 m to above 100 meters which is the relative change in the order of 20%. Small increases

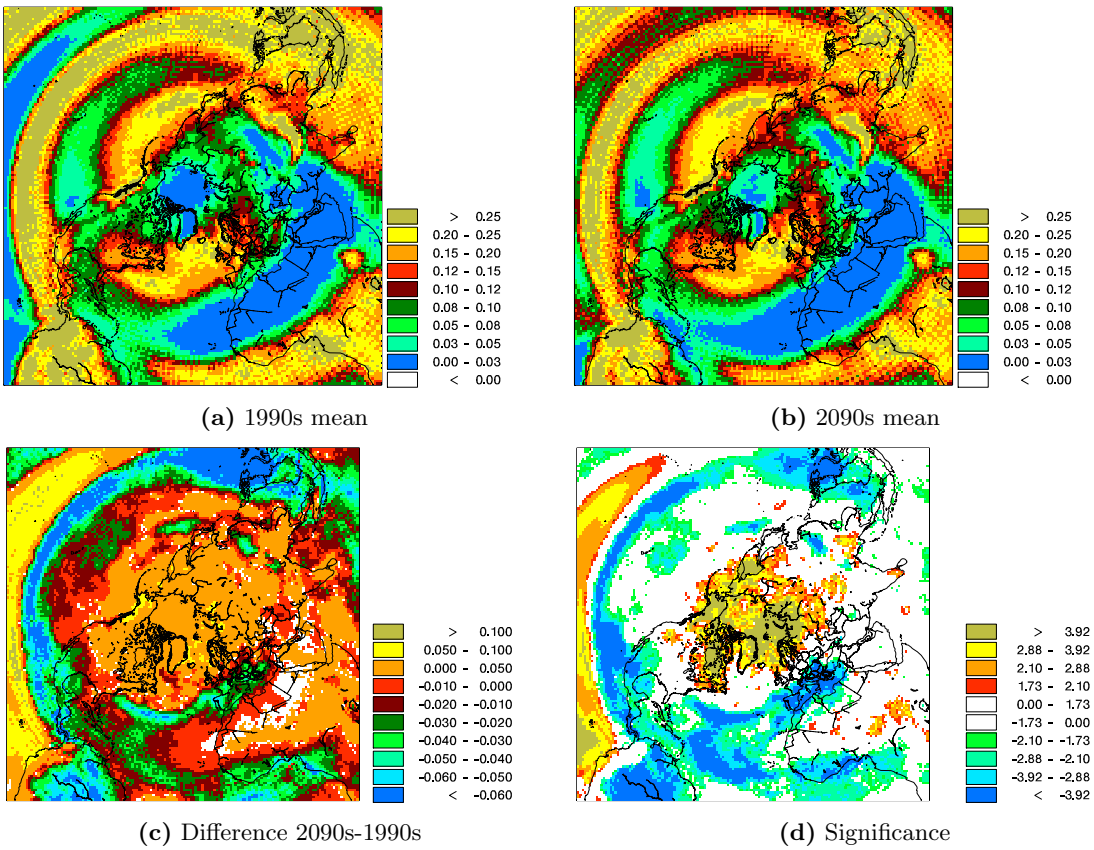

(a) 1990s mean **(b)** 2090s mean

(c) Difference 2090s-1990s **(d)** Significance

Figure 5.4: Precipitation frequency: Defined as a fraction between 0 and 1, the threshold value for precipitation in a given six-hour interval is 1 mm. Figure a) shows the mean precipitation frequency during 1990s decade and b) during the 2090s decade. In figure c) the difference between the 2090s and the 1990s is shown and finally figure c) illustrates the difference between the two decades, white colours indicates no significant change and the threshold value for significance is set to 10 %

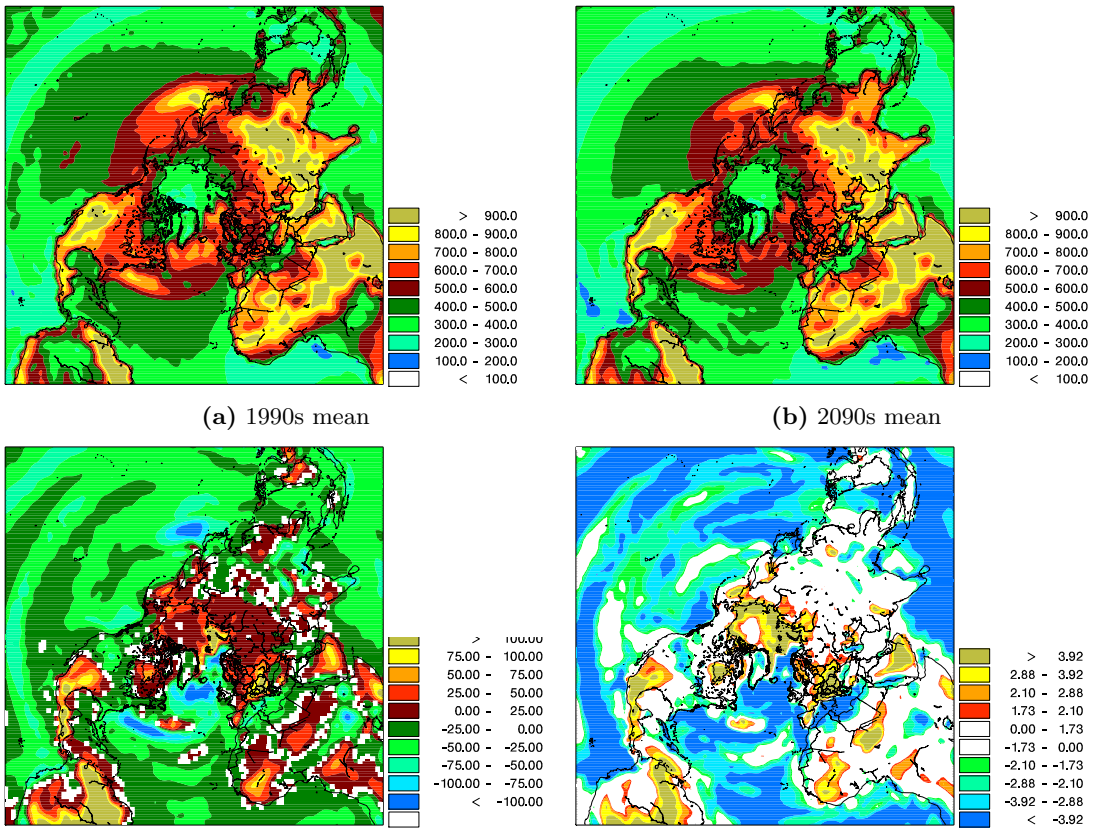

(a) 1990s mean **(b)** 2090s mean

(c) Difference 2090s-1990s **(d)** Significance

Figure 5.5: Mixing height in meter: Illustrated as in figure 5.4

(0-25 meters) are found in general over Eurasia and the Arctic Ocean. In Mexico, the Caribbean and in Central South America the mixing height is also projected to increase in the range 50 to above 100 meters. In general the mixing height is projected to decrease over marine areas. The projected increase in mixing height over the American continents and in Southern Europe is coincident with areas with decreased precipitation frequency, which maybe is an artefact of the derivation of the mixing height.

5.1.6 Snow and Sea Ice

In figure 5.6 and 5.7 the snow cover and sea ice is displayed similarly to the mixing height above (figure 5.5). Both snow cover and sea ice is defined as a fraction between 0 and 1 and they are both decreasing from the 1990s to the 2090s due to climate change. For example the snow cover in the Alps is projected to disappear completely by the end of the century by the used ECHAM5 simulation and the snow cover the Himalaya is projected to be

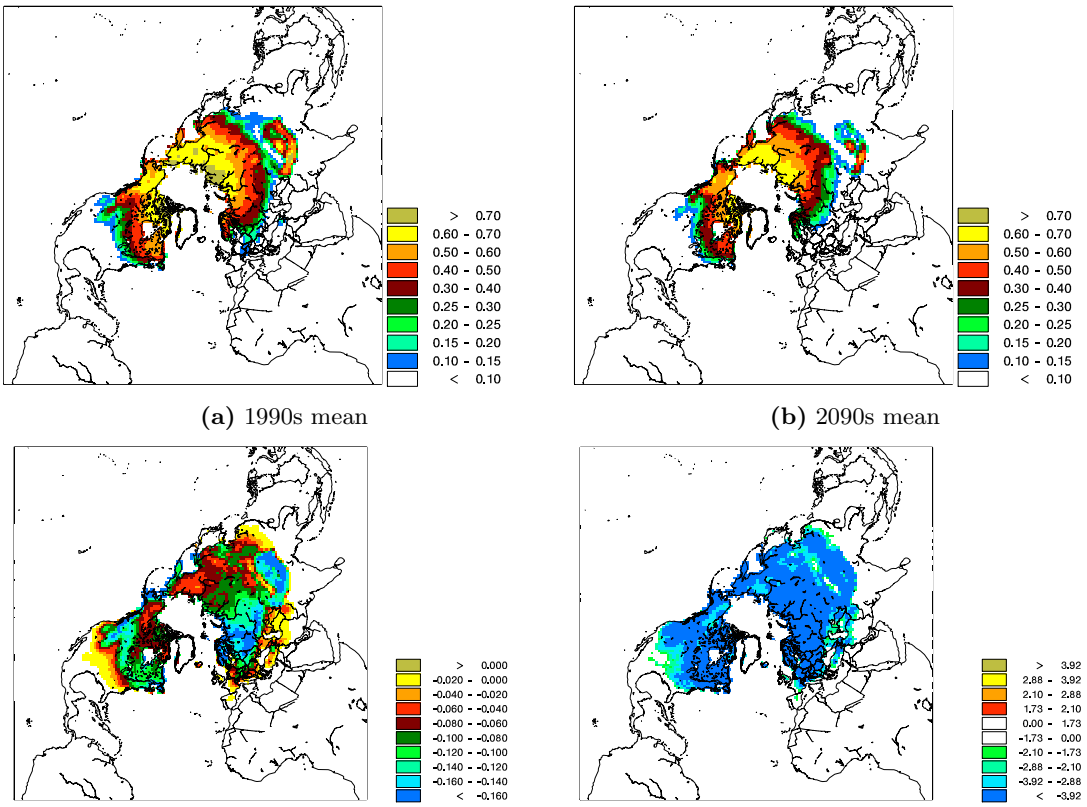

(a) 1990s mean **(b)** 2090s mean

(c) Difference 2090s-1990s **(d)** Significance

Figure 5.6: Snow cover: Illustrated as in figure 5.4

significantly reduced. Large reductions in the snow cover are also found in the United States where the border of snow is estimated to lie in Canada.

The large reductions are found in the sea ice extent. The sea ice extent shown in figure 5.7 only indicates if there ice present in the given grid cell or not and do not carry any information on e.g. sea ice thinning. The sea ice in general decreasing an is by the end of century completely disappeared from Gulf of Bothnia, the Greenland and Bearings Sea and only present in the absolutely northern part of the David Strait. Further the seasonal means are shown, however in the summertime (JJA) the sea ice are projected to disappear completely by the end of the century. Note that the largest decadal mean by the end of the century is between 0.8 and 0.9 and only in the central part of the Arctic basin.

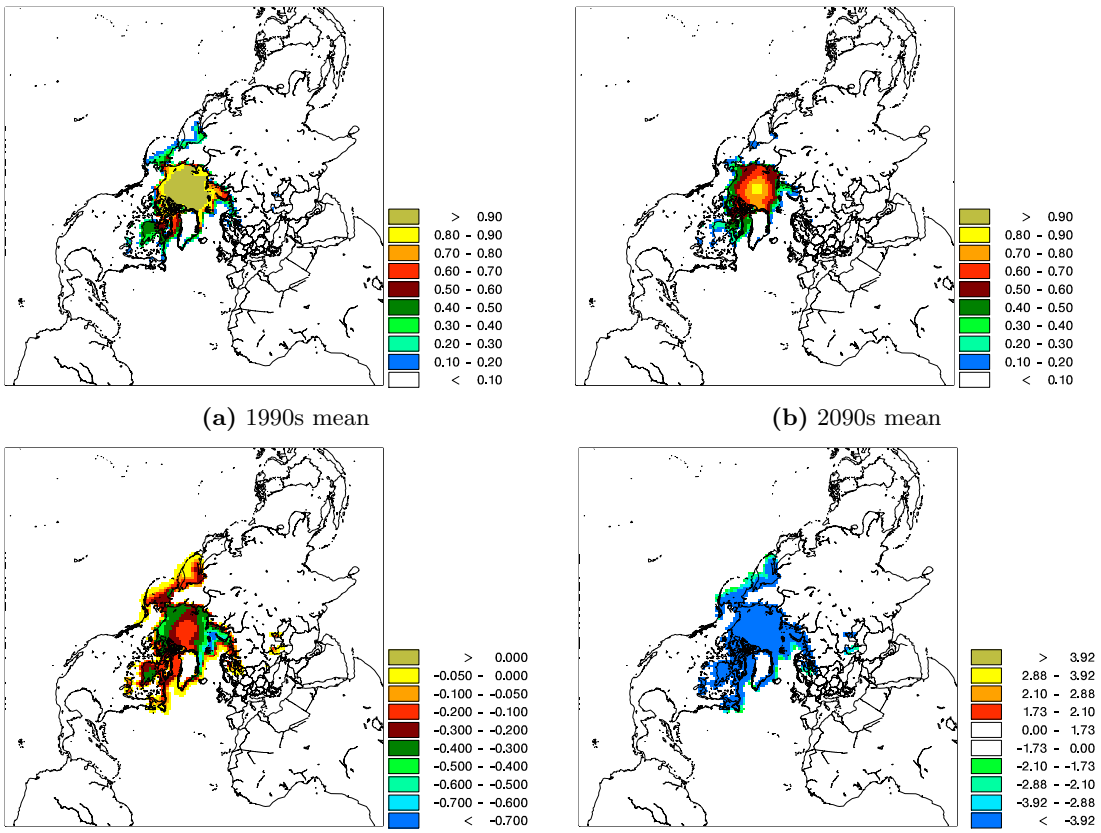

(a) 1990s mean

(b) 2090s mean

(c) Difference 2090s-1990s

(d) Significance

Figure 5.7: Sea Ice: Illustrated as in figure 5.4

6 Impact of climate change on ozone chemistry over three centuries

The aim of this chapter is to analyse the climate change impacts on the ozone concentrations over three centuries. In previous studies [Langner et al., 2005; Murazaki & Hess, 2006; Hedegaard et al., 2008; Tagaris et al., 2007; Liao et al., 2007; Wu et al., 2008a,b; Pye et al., 2009; Lam et al., 2011], the focus has solely been on the 21st century, where a significant change is found. In the current study the aim is to determine if the observed change is present only in this century. Secondly the chemical and physical mechanisms behind the changes in the ozone concentrations are investigated in order determine and understand the governing mechanisms behind the projected changes. Relative to the study carried out in 2008 [Hedegaard et al., 2008] this study is based an updated version of the whole model system including the use of the newly developed emission scenarios; Representative Concentration Pathways (RCP4.5) (see section 3). In section 6.1 below the experimental design is described for this particular experiment. This is followed by a thorough description of the results in relation to the chemistry included in the model. The results are discussed continuously in this chapter and an overall discussion can be found in chapter 10.

6.1 Experimental setup

In this study the Danish Eulerian Hemispheric Model (DEHM), is driven on six-hourly meteorology input simulated by the coupled Atmosphere-Ocean General Circulation Model ECHAM5/MPI-OM (see section 5) and constant anthropogenic emission from the year 2000. The faith of 58 chemical species and 9 classes of particulate matter has been simulated in four decades (1890s, 1990s, 2090s and 2190s) to examine the evolution of air pollutants over three centuries. Here the focus is on ozone and its precursors. The performance of the total model system with ECHAM5/MPI-OM model coupled to the

DEHM model system has been thoroughly tested in earlier studies [Hedegaard, 2007; Hedegaard et al., 2008].

The emissions of the primary pollutants consist of data from the GEIA, EDGAR and EMEP emissions databases (see description in 3.3) fixed on a 2000-level in order to isolate the signal from climate change on air pollution. The isoprene is calculated dynamically in the model according to the GEIA natural VOC emission model [Guenther et al., 1995] described in section 3.3.1. Other naturally emitted VOCs like for example terpenes are not yet included in the model.

6.2 Results and discussions

In figure 6.1 the distribution, the differences and the significance of the ten-year average O_3 concentration in ppbV is plotted. From the upper panel it can be seen that the O_3 concentration in the lowest model layer in all four decades is highest in the subtropics and the tropics over land, especially close to the anthropogenic precursor sources and downstream from these.

The life-time of ozone depends strongly on the latitude, time of year, solar radiation and vertical placement in the atmosphere. Because free oxygen and O_3 molecules (together called "odd oxygen") are rapidly interconverted an individual lifetime of O_3 is often irrelevant with respect to atmospheric transport. Considering atmospheric long-range transport this interconversion makes the lifetime of odd oxygen more interesting. The lifetime of odd oxygen is ranging from a few days in the lower troposphere and up a month or more in the middle and upper troposphere [Lollar, 2007]. The relative longer lifetime of odd oxygen is the reason O_3 is considered as a long-range transported specie.

O_3 is not directly emitted, but produced from its precursors, which is of both biogenic and anthropogenic origin. A local measured ozone concentration consists of a local, an inter-continental and a background contribution, which depend on the distance to the precursor sources, the local photochemical conditions and the transport pathways. The concentration distribution plotted in figure 6.1 reflects these features well.

The increase of the ozone concentration is due to a combined effect of increased temperature, solar radiation, humidity, isoprene chemistry and anthropogenic VOC pollution as well as influence from NOx. The trend in ozone concentration has the sign in all three centuries. However, most pronounced in the 21^{st} century with a general decrease over the ocean and very remote areas (as e.g. the desert of Sahara and central Asia) and with an increase over the densely populated areas and areas where biomass burning relatively often occurs. The change in the concentrations over the Arctic

Ocean differs from the above pattern. Here a significant increase in the 21st and 22nd century (cf. Fig. 6.1 middle and lower panel) is found.

The major contributor to tropospheric ozone is the termolecular recombination

$$O(^3P) + O_2 + M \longrightarrow O_3 + M \qquad \text{(R 6.1)}$$

where M is an inert atom or molecule in the atmosphere primarily O_2 and NO_2. $O(^3P)$ is formed in the photolysis of NO_2:

$$NO_2 + h\nu \longrightarrow O(^3P) + NO \qquad \lambda \leq 424 \text{ nm} \qquad \text{(R 6.2)}$$

Some of the formed O_3 is destroyed by reactions with NO:

$$O_3 + NO \longrightarrow NO_2 + O_2 \qquad \text{(R 6.3)}$$

It can be seen that Reactions R 6.1 - R 6.3 are a closed cycle where all the products also are reactants.

In the troposphere reactions (R 6.1) through (R 6.3) illustrates the most important cycle for O_3, however since the cycle is closed, not all tropospheric O_3 stems from this cycle. The oxidation of VOC and CO plays a central role for this extra contribution to the O_3 budget. O_3 is important since it is a major source of hydroxyl radicals (OH), which determines the oxidation capacity of the atmosphere:

$$O_3 + h\nu \longrightarrow O(^1D) + O_2 \qquad 290\ nm \leq \lambda \leq 319 \text{ nm} \qquad \text{(R 6.4)}$$

$$O(^1D) + H_2O \longrightarrow 2\,OH \qquad \text{(R 6.5)}$$

The main source of OH formation is Reaction R 6.5. In relation to climate change it is important to note that $O(^1D)$ can either react as reaction (R 6.5) or collide with N_2 or O_2 and quenched to ground state oxygen $O(^3P)$. As the temperature and water vapour increases in the future due to climate change (Figs. 5.1 and 5.2) reaction R 6.5 is in more favourable than the formation of $O(^3P)$ which in the remote and clean areas leads to a decrease in the ozone concentration. This can be observed in Fig. 6.1, where a decrease of ozone in the 21st century over the ocean and in the Sahara is predicted. The concentration of H_2O is increasing in this century (Fig. 5.2) and it is regions with low NOx where the destruction of O_3 according to reaction R 6.4 will be dominant.

Figure 6.3 shows the changes of OH concentrations. Since the hydroxyl radicals determine the oxidation capacity of the atmosphere, they are important when considering pollution levels; e.g. fate of primary emitted pollutants,

formation of ozone and secondary particles. In Fig. 6.3 (lower panel) there is an increasing tendency in the 21st century over the ocean, in large part of Europe, including Greenland, Arabia, central Asia and to some extend over the ocean in the vicinity of the major international ship routes. The significant increase over the southern part of the domain over the Pacific can be explained by changes projected in the global radiation figure 5.3. On the contrary the hydroxyl radical levels are decreasing elsewhere in the domain of interest. These projections are in agreement with what is expected from the theory described above.

In the 20th and 22nd century the picture is more mixed with both significant increasing and decreasing areas, which most likely can be explained by the less significant changes in the solar radiation in these centuries (see figure 5.2).

6.2.1 Impact of Volatile Organic Compounds (VOCs)

Non-methane Volatile Organic Compounds (VOCs) can be split into anthropogenic VOCs (AVOCs) ($\sim$10% of total) and Biogenic VOCs (BVOCs) ($\sim$90% of total) (e.g. Goldstein & Galbally [2007]). Here the discussion is limited to concern alkanes and alkenes ignoring the emission and chemistry of oxidized VOC's, alkynes and aromatics, though they are important VOC's in the troposphere.

AVOC is dominated by saturated VOCs (alkanes) and BVOC is dominated by unsaturated VOCs (alkenes) but fractions play important roles in tropospheric chemistry. Alkanes can be transported over long distances due to their chemical stability. Hydroxyl radicals react via hydrogen abstraction of both a terminal and an internal carbon atom followed by addition of O_2 and thereby forming alkyl peroxy radicals (RO_2):

$$RH + OH + O_2 \longrightarrow RO_2 + H_2O \qquad (R\,6.6)$$

These alkyl peroxy radicals (RO_2) are highly reactive and can react with NO forming NO_2:

$$RO_2 + NO \longrightarrow RO + NO_2 \qquad (R\,6.7)$$

which through reactions R 6.1 and R 6.2 produces additional O_3 compared to the photostationary state presented by Reactions (R 6.1) to (R 6.3).

Approximately 40% of BVOCs is emitted as isoprene [Fall, 1999; Goldstein & Galbally, 2007]. Isoprene emissions are in the DEHM model calculated by the GEIA emission modul, which is a parameterization describing the isoprene emission as a function of temperature and sunlight [Guenther et al., 1995]. The tropospheric lifetime of isoprene C_5H_8 due to its reaction with

OH, nitrate (NO_3) and O_3 is 1.4 h, 1.6 h and 1.3 days, respectively (summarized in Hedegaard [2009]). Due to this relatively low atmospheric lifetime the highest isoprene concentration (top panel of figure 6.4) is found close to the emission sources in especially the tropical areas. Tropical broadleaf trees contributes with almost half of the global isoprene emissions [Guenther et al., 2006].

The main degradation pathway of alkenes are OH addition to the double bond (e.g. isoprene has two double bonds) rather than hydrogen abstraction as is the case for alkanes. OH adds to one of the double bonds followed by addition of O_2 creating a peroxy radical. For further details of these reaction pathways see e.g. Seinfeld & Pandis [2006] or for recent results Paulot et al. [2009].

6.2.2 Ozone and NO_x

As described in reaction R 6.1-R 6.3, NO_2 reacts with ozone to form nitrate radicals which photolysis fast during the day and thus is of little importance.

However, during night time substantial concentrations can build up and affect the NOx chemistry. Moreover it is suggested from field studies that NO_3 reactions can be a major contributor to isoprene loss at night [Rollins et al., 2009; Skov et al., 1992]. NO_3 react by addition to isoprene at C_1 or C_4 carbon atom followed by addition of O_2 to make a 1.4 addition to form a nitrate peroxy radical isoprene adduct. In the model these peroxy radicals reacts with NO and thus will lead to ozone production at dawn through the photolysis of NO_2 (reaction R 6.2). This contribution is however of minor importance. There is discussion in the literature of what will be the fate of these RO_2 radicals. They might self react, react with NO_3 radical or with OH as discussed by Rollins et al. [2009].

In this study it is difficult to isolate the exact impact of NO_3, O_3 and OH on isoprene because many other reactions also occur simultaneously in the simulations and most of the areas with a high emission load of isoprene also to some extent are influenced by anthropogenic sources (reaction R 6.8).

6.2.3 Production and loss reactions of hydro- and organic peroxy radicals

The main source of organic peroxy radicals is from AVOCs and BVOCs. The inorganic peroxy radical can be formed either from the simplest aldehyde:

$$\mathrm{HCHO} + 2\,\mathrm{O_2} + \mathrm{h}\nu \longrightarrow 2\,\mathrm{HO_2} + \mathrm{CO} \qquad 290\ nm \leq \lambda \leq 340\ nm \quad \text{(R 6.8)}$$

$$HCHO + h\nu \longrightarrow H_2 + CO \qquad 290\ nm \leq \lambda \leq 360\ \text{nm} \qquad \text{(R 6.9)}$$

$$HCHO + OH + O_2 \longrightarrow HO_2 + H_2O + CO \qquad \text{(R 6.10)}$$

or from various reaction of OH with inorganic oxides (O_3, H_2O_2, SO_2 and CO) and the photolysis of carbonyl containing compounds.

HO_2 is removed either from the reaction with NO:

$$HO_2 + NO \longrightarrow OH + NO_2 \qquad \text{(R 6.11)}$$

or by its self reaction:

$$HO_2 + HO_2(^{+}H_2O) \longrightarrow H_2O_2 + O_2 + H_2O \qquad \text{(R 6.12)}$$

Reactions (R 6.11) and (R 6.12) are competing reactions where the first dominate in NOx rich areas exposed to high emission from combustion processes and the latter is dominating in the free troposphere and in marine environments. Reaction (R 6.11) will be followed by Reaction (R 6.1) and (R 6.2) to form additional ozone whereas (R 6.12) will lead to loss of odd oxygen and by that loss of O_3 (see figure 6.1).

Figure 6.5 shows that the largest increase in hydroperoxy radicals is found in the 21st century in the "semi-remote" areas, which has a high fraction of vegetation and industry, and in the subtropical and tropical areas. However a significant increase is also found over most of the domain in 22nd century. Only in the 20th century the hydroxy radical concentration is predicted to decrease over the North Atlantic, western Europe and parts of Siberia. The increase due to vegetation is explained above (section 6.2.1). The increased concentration of hydroperoxy radicals in the regions with high emissions from vegetation and regions with high emissions from anthropogenic sources, is caused by the increased level of water vapour and isoprene emissions in the future decades. When the water vapour content increases, the OH concentration increases, due to photolysis of ozone (reaction R 6.4). The hydroxyl radicals can then be converted to hydroperoxy radicals as described above (reaction R 6.10).

In figure 6.6 the concentration and the difference of organic peroxy radicals over the three centuries are shown. From the 1890s to the 1990s the largest increase is found in the Tropics. The general tendency is also increasing elsewhere, though the projections are less significant here. The 21st century exhibits significant increases in most of the domain, whereas the projections for the 22nd century are less significant but still increasing. The increase in organic peroxy radicals can be explained by the same parameters as for hydroperoxy radicals.

6.2.4 The effects of NO_x

NO_x consist of and NO and NO_2 and the projected concentrations throughout the three centuries are shown in figure 6.8 and 6.7, respectively. NO has a short lifetime in the atmosphere and quickly inter-convert with NO_2 according to reaction R 6.2-R 6.3. NO_2 (figure 6.7) reacts with ozone to form nitrate radicals which photolysis rapidly during the day and thus are of little importance. However, during night time substantial concentrations can build up and affect the NO_x chemistry. NO_3 reacts rapidly with a series of alkenes among which are isoprene and dimethyl sulphide. NO_3 reacts also with NO_2 to form N_2O_5 which hydrolyses heterogeneously with water to form nitric acid. This last reaction accounts for about the same removal as the reaction between OH and NO_2 at mid latitudes.

In figure 6.7 the decadel average concentration in NO_2 is shown for the four decades. The picture is mixed with respect to increase and decrease but the most significant changes are again found in the 21st century. Most of the increase is in both the 21^{st} and 22^{nd} century found over the parts of the North Atlantic Ocean, the Arctic Ocean and the northern part of the pacific ocean. In contrast NO_2 mostly decrease over southern Europe, South America and Africa in all three centuries.

Figure 6.8 displays the concentration of NO over the North western part of Europe (Benelux and surrounding) there are an excess of NO. This area is having the highest NO_x density in the world which explains the difference from this area compared to other dense populated areas with high NO_x emissions. This also means that the ozone concentration is low, since O_3 is used to convert the emitted ozone to NO_2 (see eq. R 6.3).

6.2.5 Development of ozone in the future related to its precursors

In the future, the radiation, temperature and water content of the atmosphere are projected to increase according to ECHAM5 simulations applied in this study (chapter 5). These parameters will increase the OH formation due to reaction R 6.4 which initiates the cycle described in reactions (R 6.1)-(R 6.6). Increasing amount of OH, HO_2 and RO_2 are also to some extent observed in the model runs (Figs. 6.5 and 6.6), and can explain the higher ozone concentrations observed in the simulations over the densely populated areas (US, central and southern Europe and parts of Asia), see figure 6.1.

Over the north western part of Europe high concentrations of NO was found and the concentration decreases significantly between the 1990th decade and the 2090th due to the impacts of climate change. The decrease in NO emission is in good agreement with the projected increase in ozone in the same area (figure 6.1).

In a clean atmosphere, where the NO_x and VOC load is low, isoprene reduces the ozone concentration, which is reflected in the projected changes over the the oceans (figure 6.1). However, in regions with moderate to high NO_x levels, the interaction between the emitted NO and the formed isoprene peroxides from OH, increases the concentration of HO_2 (Fig. 6.5) and NO_2 (Fig. 6.7), which then enhances the ozone formation. This can explain the higher ozone concentrations in Africa south of Sahara, Southeast Asia and South America. In addition these areas are covered with a large proportion of tropical plants and tropical rainforest, which emits a large fraction of the ozone precursor, isoprene. Moreover, the BVOC emission itself is expected to increase under changed climate conditions, which can further amplify the signal in the future ozone concentration.

In the Arctic the ozone concentration is predicted to increase throughout all three centuries. However the change is most significant in the 21st century. From analysis of each season it is found most significant during the winter season. In the Arctic region there is no sun in the winter months, and hence not any ozone degradation due to photolysis (reaction R 6.4). But since the length of Arctic winter nighttime does not change over the centuries and there is no significant change projected in the global radiation over the Arctic region, further analysis of the ozone related species cannot explain the change over the Arctic region.

Over land the ozone dry deposition increases (figure 6.2) which explains the decrease in the concentration of O_3 (figure 6.1). Deposition to vegetative surfaces is much larger than to snow covered surfaces and it is found that the snow cover decreases significantly between the two periods (figure 5.1.6).

Over the Arctic Ocean the temporal and spatial extent of sea ice decreases between the two decades (figure 5.1.6). Ozone does dry deposit to water surfaces in the model [Asman et al., 1994; Hertel et al., 1995] and the deposition is larger for ice surfaces than for water, which results in a decrease in the dry deposition. This is good agreement with the results of the dry deposition (figure 6.2), which decreases over the areas of the Arctic ocean, were sea ice is decreasing. However, horizontal transport from the source areas may also contribute to the observed increase over the Arctic Ocean. If this is the case more ozone are transported into the Arctics from the source areas where increased ozone levels are calculated. This additional ozone is compensated by increased deposition over land but amplifies the increase in concentration over the ocean due to a decrease in dry deposition.

Finally vertical downward transport could also increase the concentration of the surface ozone concentration. In figure 6.9 the change in ozone between the 1990s and 2090s is compared at three vertical levels; the surface layer, a layer situated at approximately 2 km altitude and one at approximately 5 km altitude. When entering the free troposphere the trend in ozone evolution has a more zonal pattern with a highly significant increase within and north

of the subtropics and a highly significant decrease in the tropics. In the free troposphere the concentration levels are less influenced by local gradients in emissions and therefore local features are less pronounced. Since the ozone concentration in general are increasing at higher levels, this could contribute with additional ozone at the surface in the future. With the current model the stratosphere-troposphere exchange of ozone cannot be expected to be simulated in detail. First of all the model only extents to 100 hPa and secondly the model resolution in the high level is relatively poor. Nevertheless, the model includes a rough description of the ozone layer (with high ozone concentrations in the stratosphere) and more ozone can be produced in the model at at the higher levels (below 100 hPa) due to climate change and transported downwards increasing ozone concentration at lower levl.

The results in this study indicate that a given change in ozone concentration due to climate change depends on two competitive processes; Ozone destruction due to increased water vapour in the atmosphere (see reactions R 6.4 and R 6.5) and ozone formation due to increased levels of ozone precursors. The increase in precursors is in this study solely due to an increase in biogenic isoprene emissions, since the anthropogenic emissions and other natural emissions has been kept constant. Below the mixing height, the increase of ozone due to the increase of isoprene is only happening in the presence of sufficient available NO_x. The ozone distribution in the free troposphere (last plate of figure 6.9) indicates that the increase in ozone concentration due to increased isoprene concentration exceeds the decrease in ozone concentration due to increased water vapour at higher latitudes, while the opposite is true in the equatorial regions.

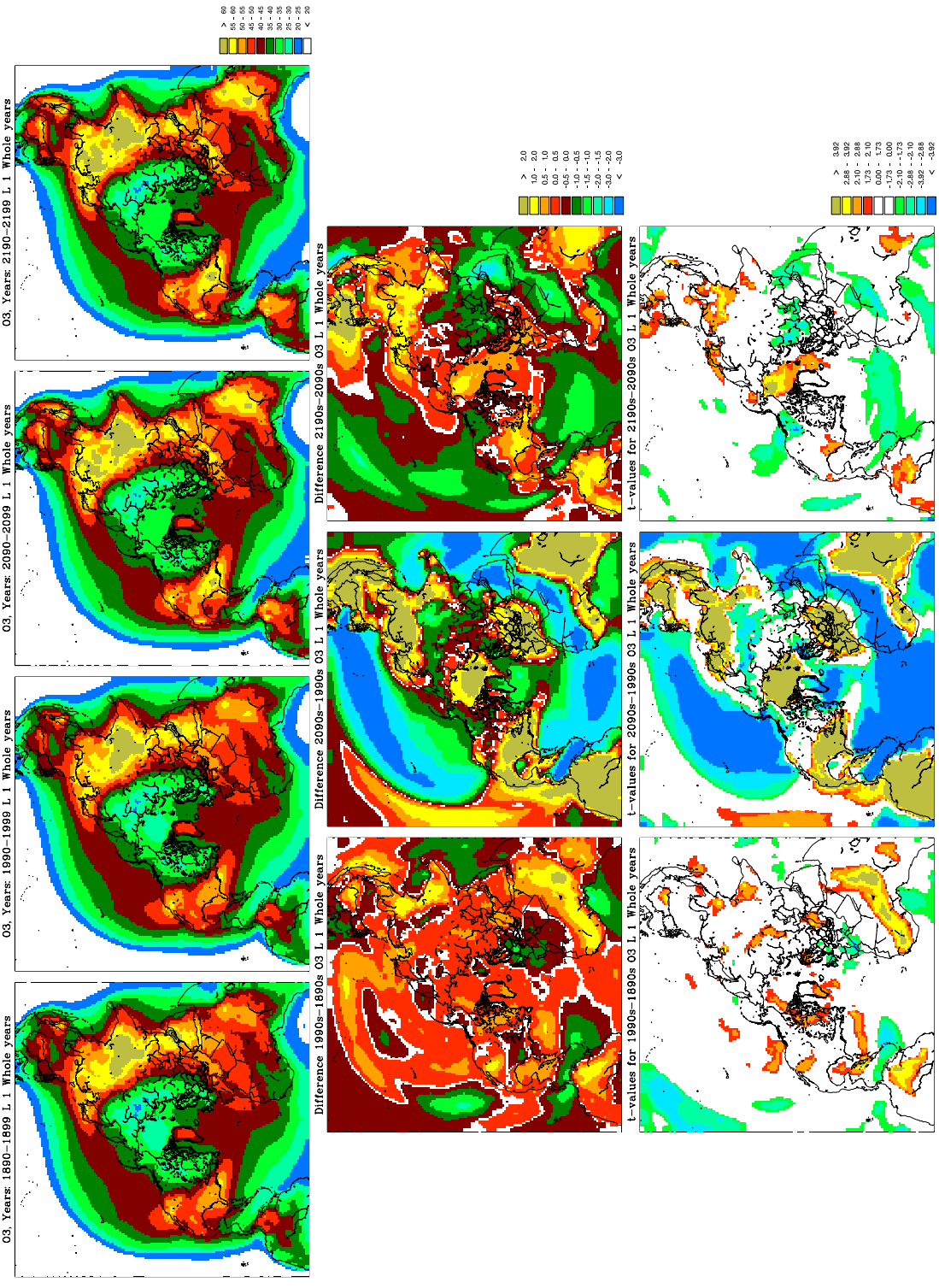

Figure 6.1: Top panel: Decadal mean surface ozone concentration in ppbV for four decades (1890s, 1990s, 2090s and 2190s). Middle panel: The difference in ppbV. Bottom panel: The significance of the differences according to the students' t-test. The threshold value for significance is 10% (white areas indicates no significant change).

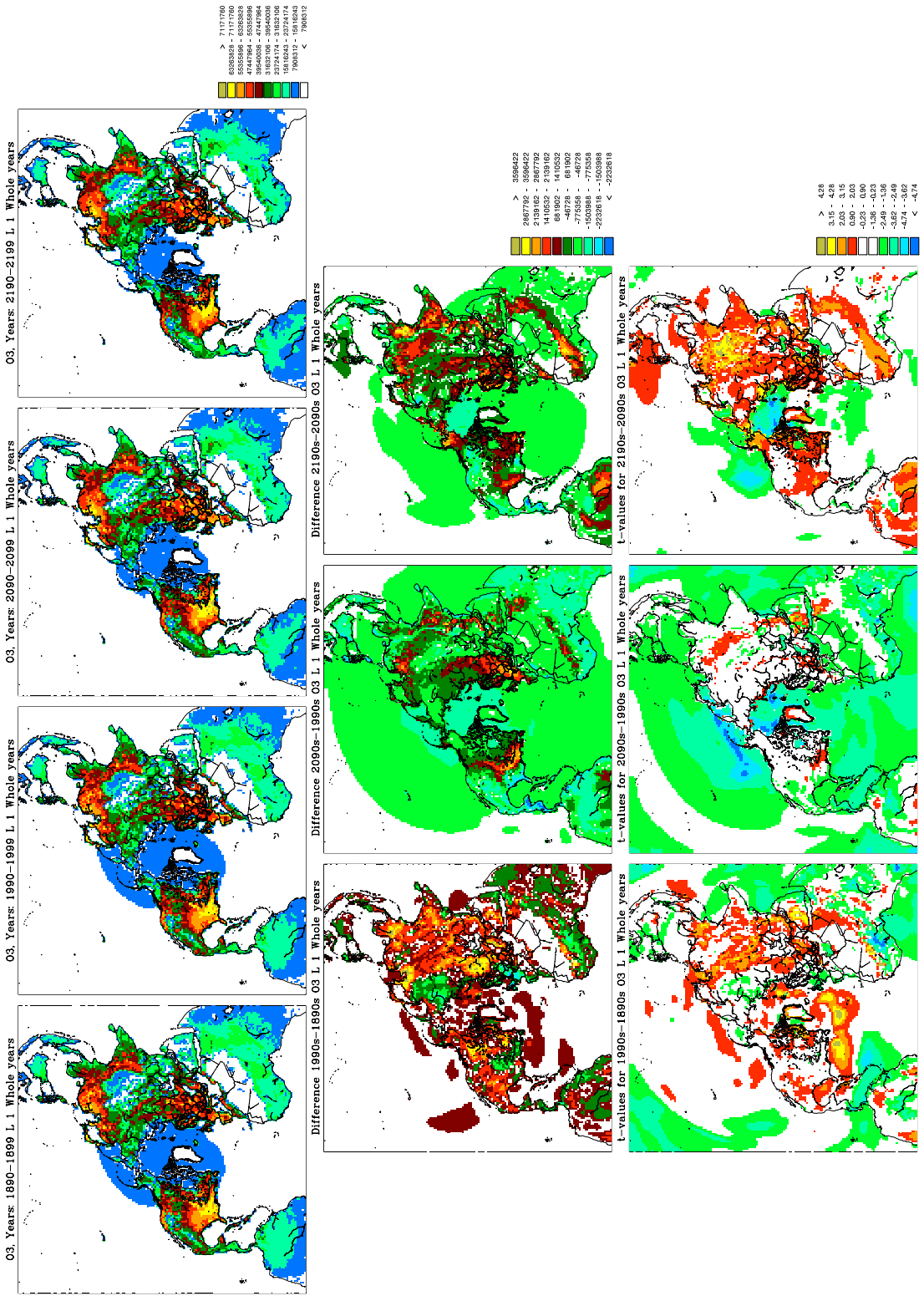

Figure 6.2: Average decadel ozone dry deposition in $mg/m^{-2}/year$. Setup as in figure 6.1.

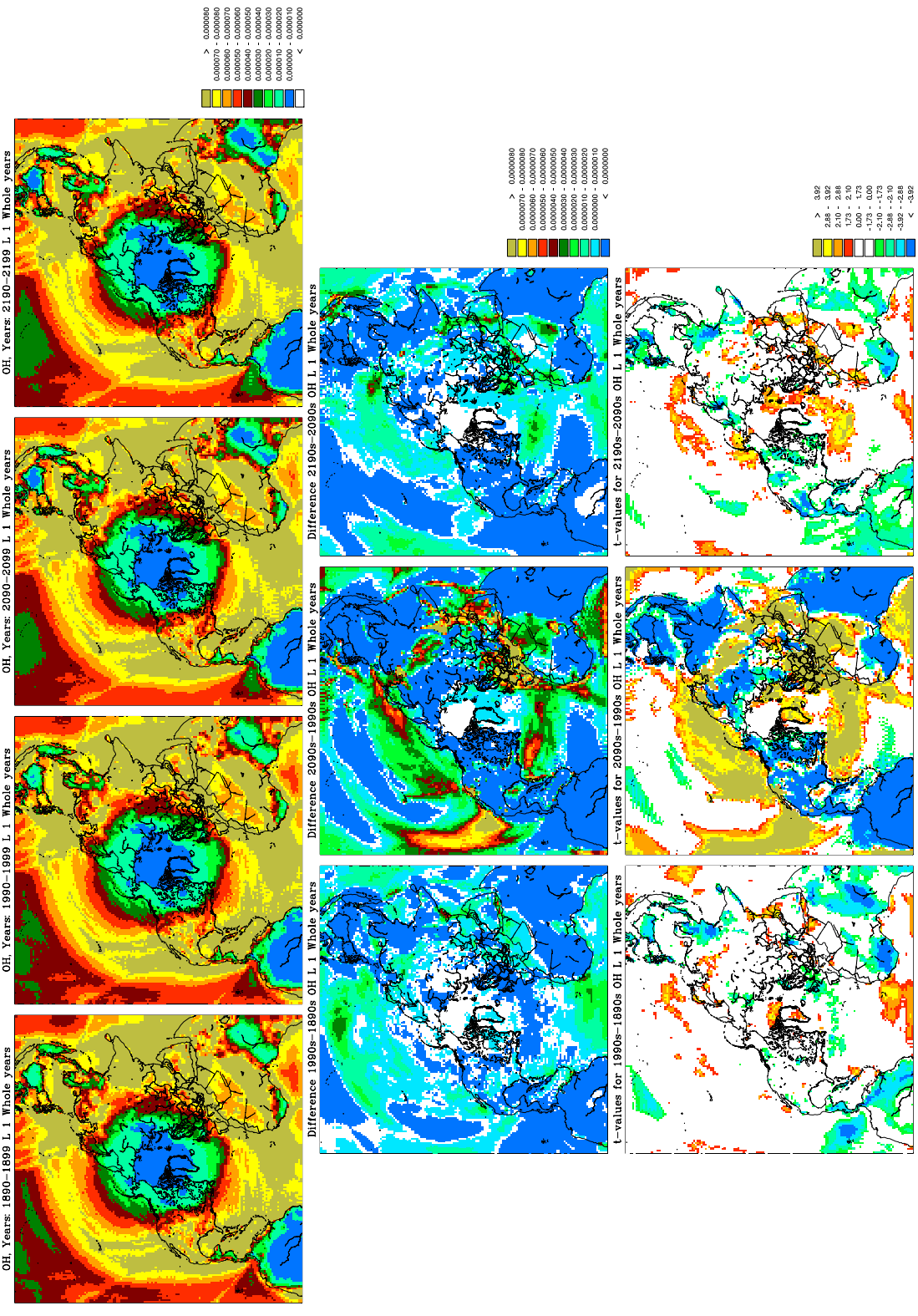

Figure 6.3: Average decadal concentration of hydroxyl radical (OH) in the lowest model layer in ppbV. Setup the same as in figure 6.1.

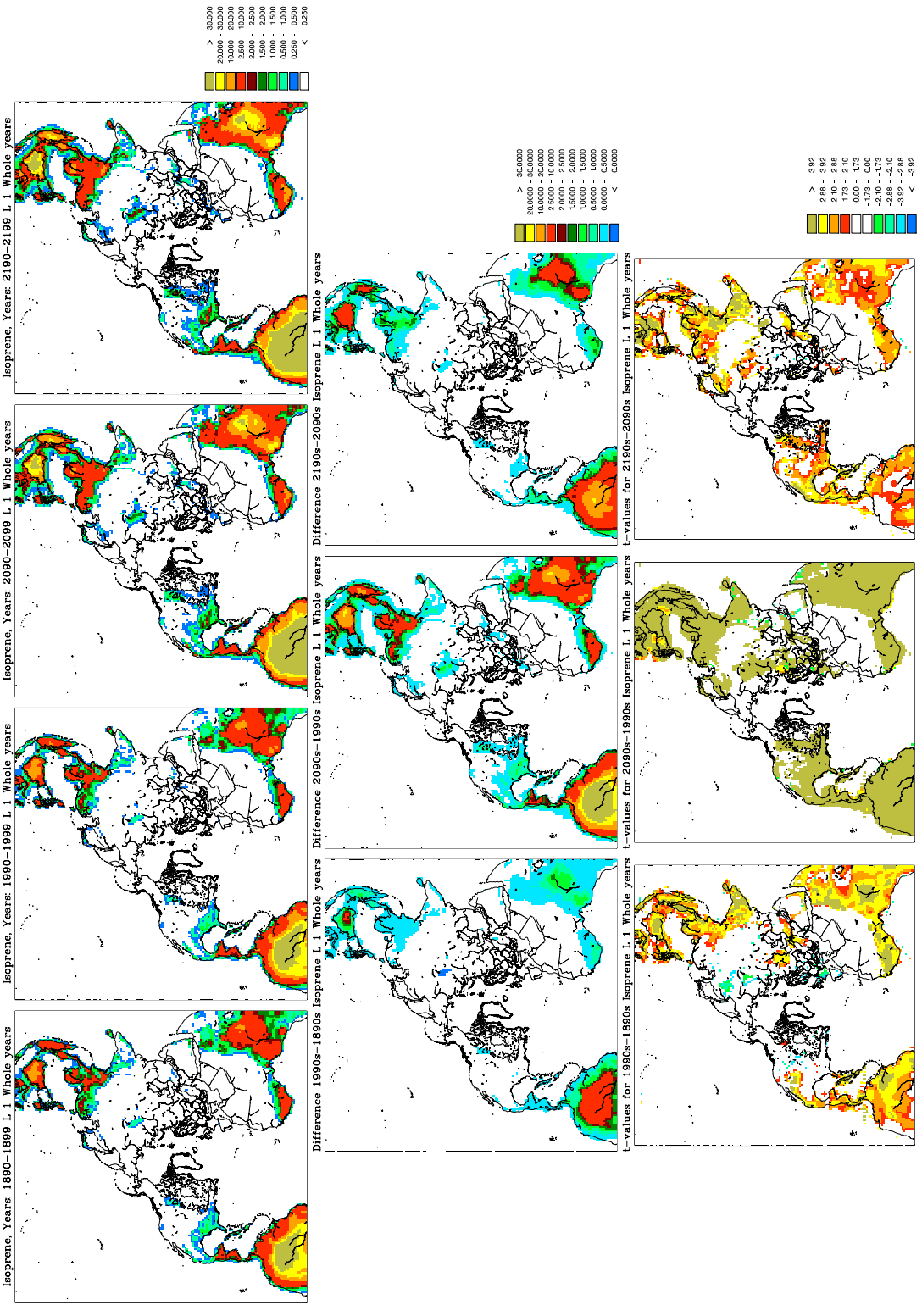

Figure 6.4: Average decadal concentration of isoprene (C_5H_8) in the lowest model layer in ppbV. Setup the same as in figure 6.1.

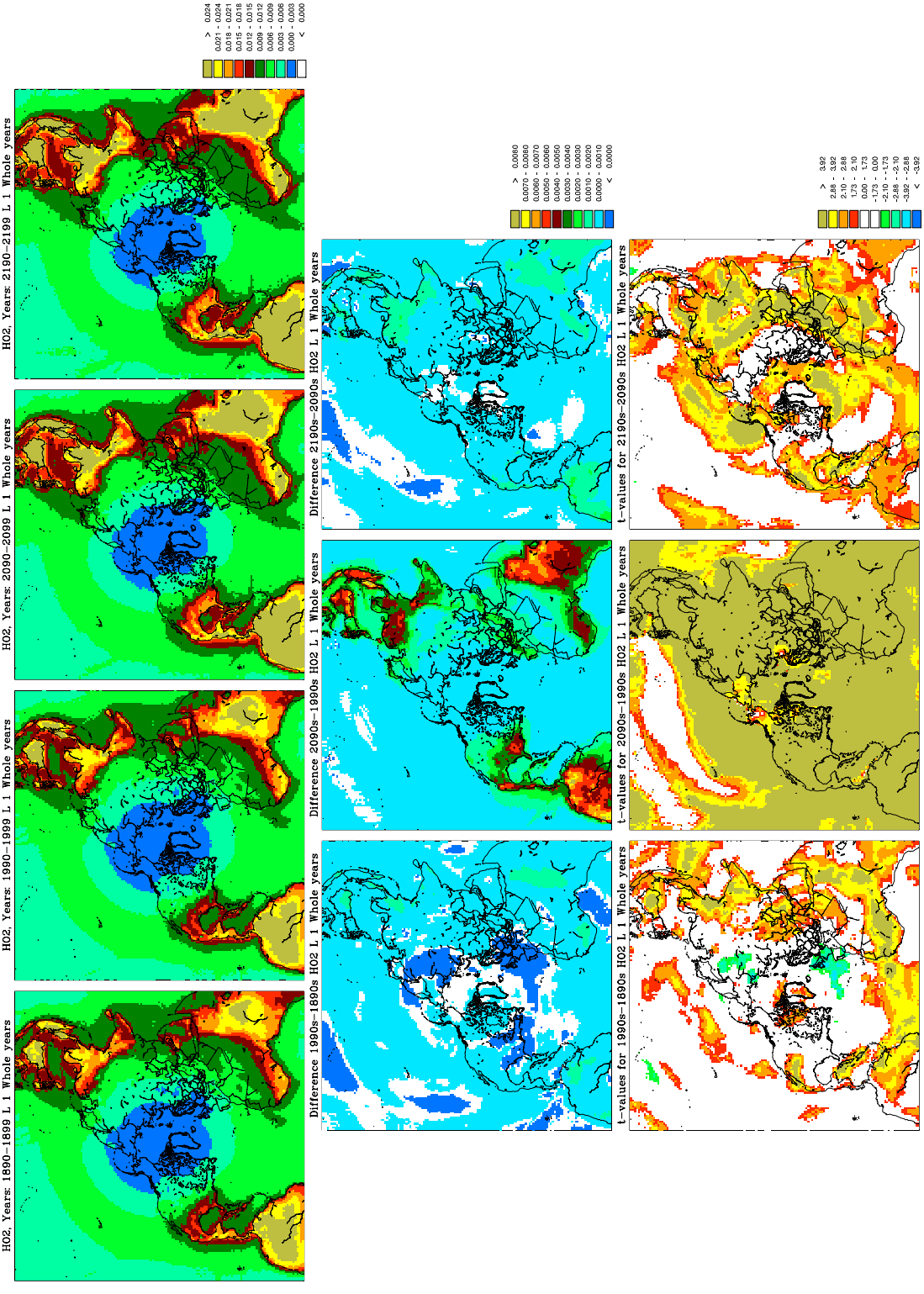

Figure 6.5: Average decadal concentration of hydroperoxy radical (HO_2) in the lowest model layer in ppbV. Setup the same as in 6.1.

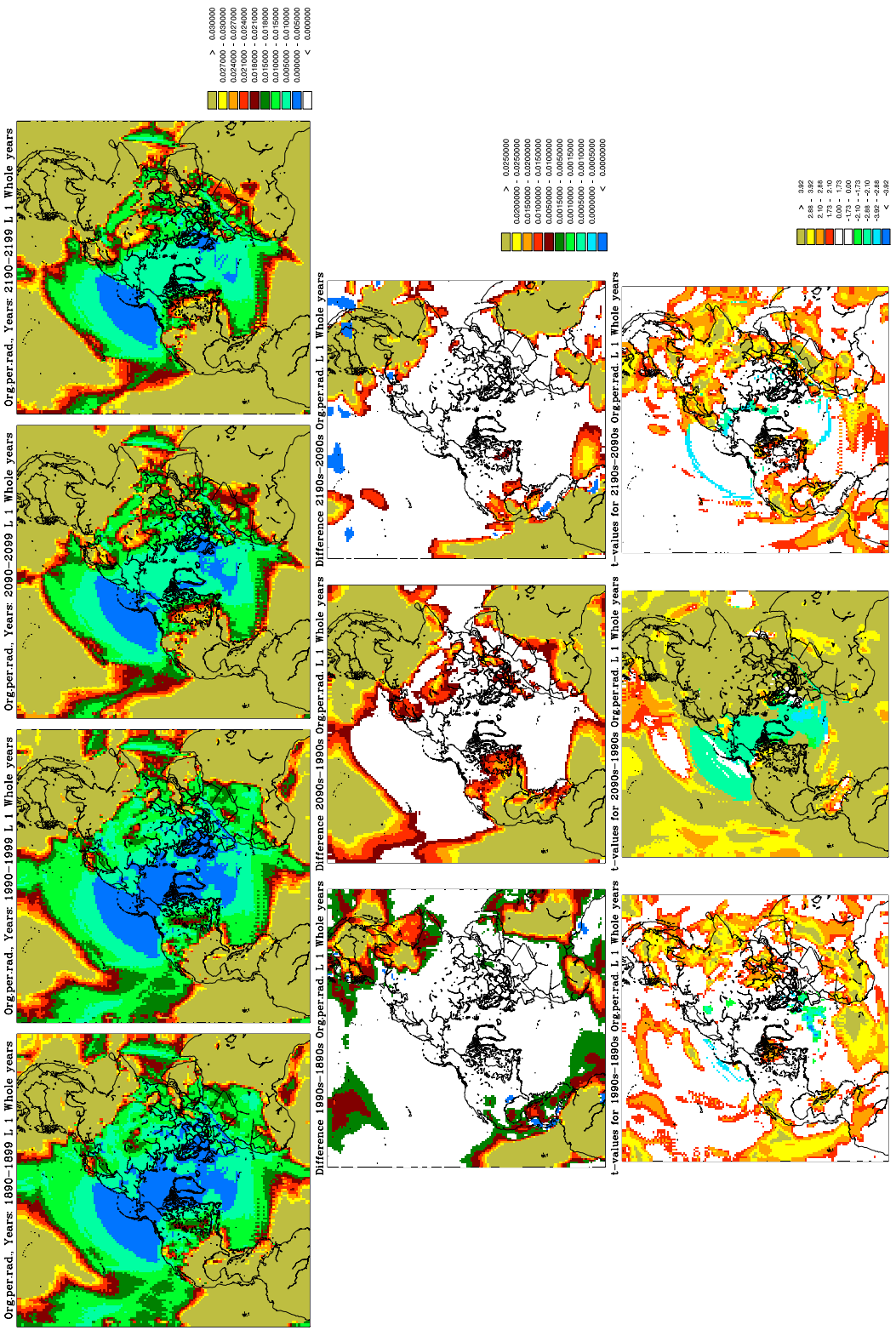

Figure 6.6: Average decadal concentration of organic peroxy radicals in the lowest model layer in ppbV. Setup the same as in 6.1.

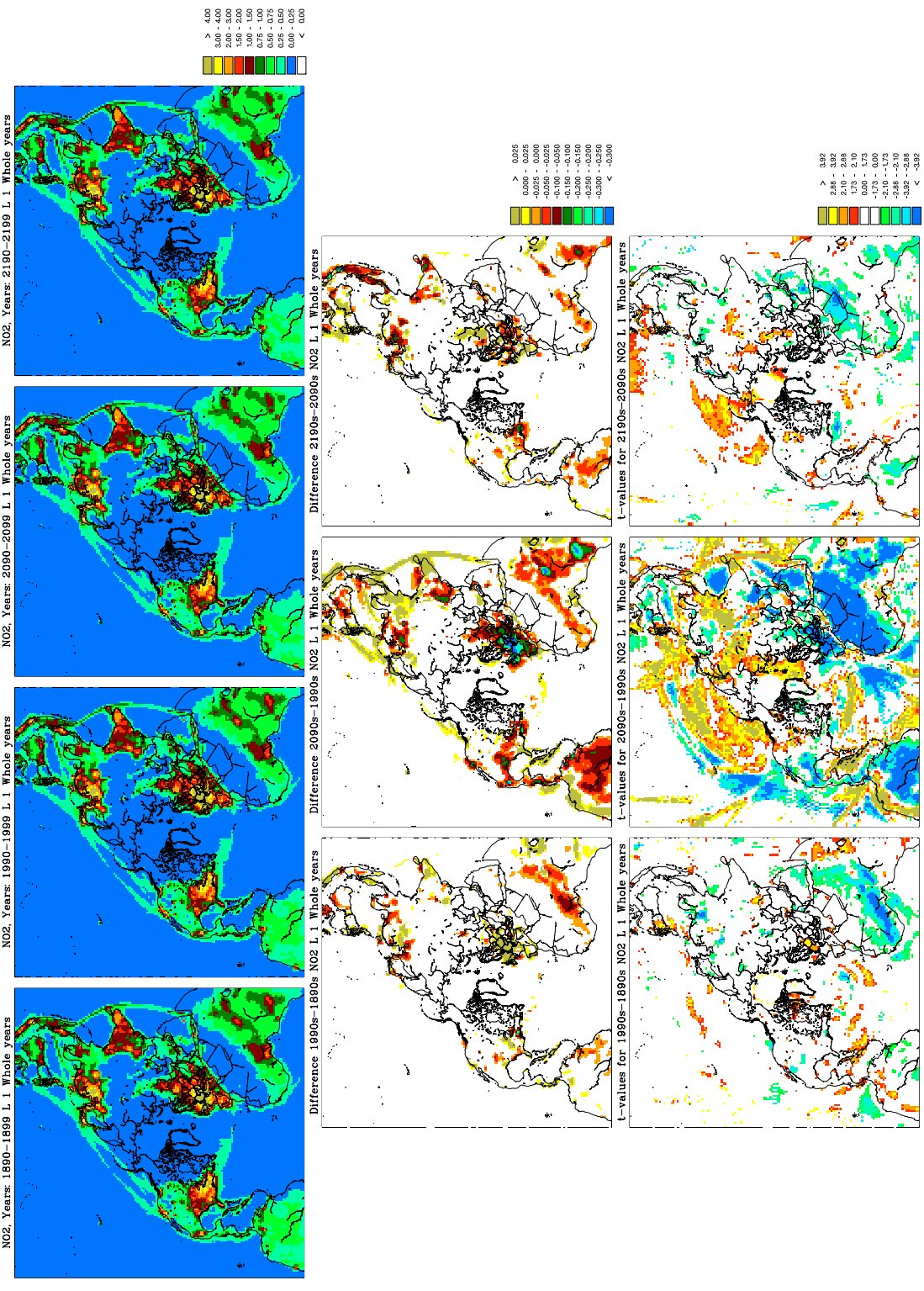

Figure 6.7: Average decadal concentration of nitrogen dioxide (NO_2) in the lowest model layer in ppbV. Setup the same as in 6.1.

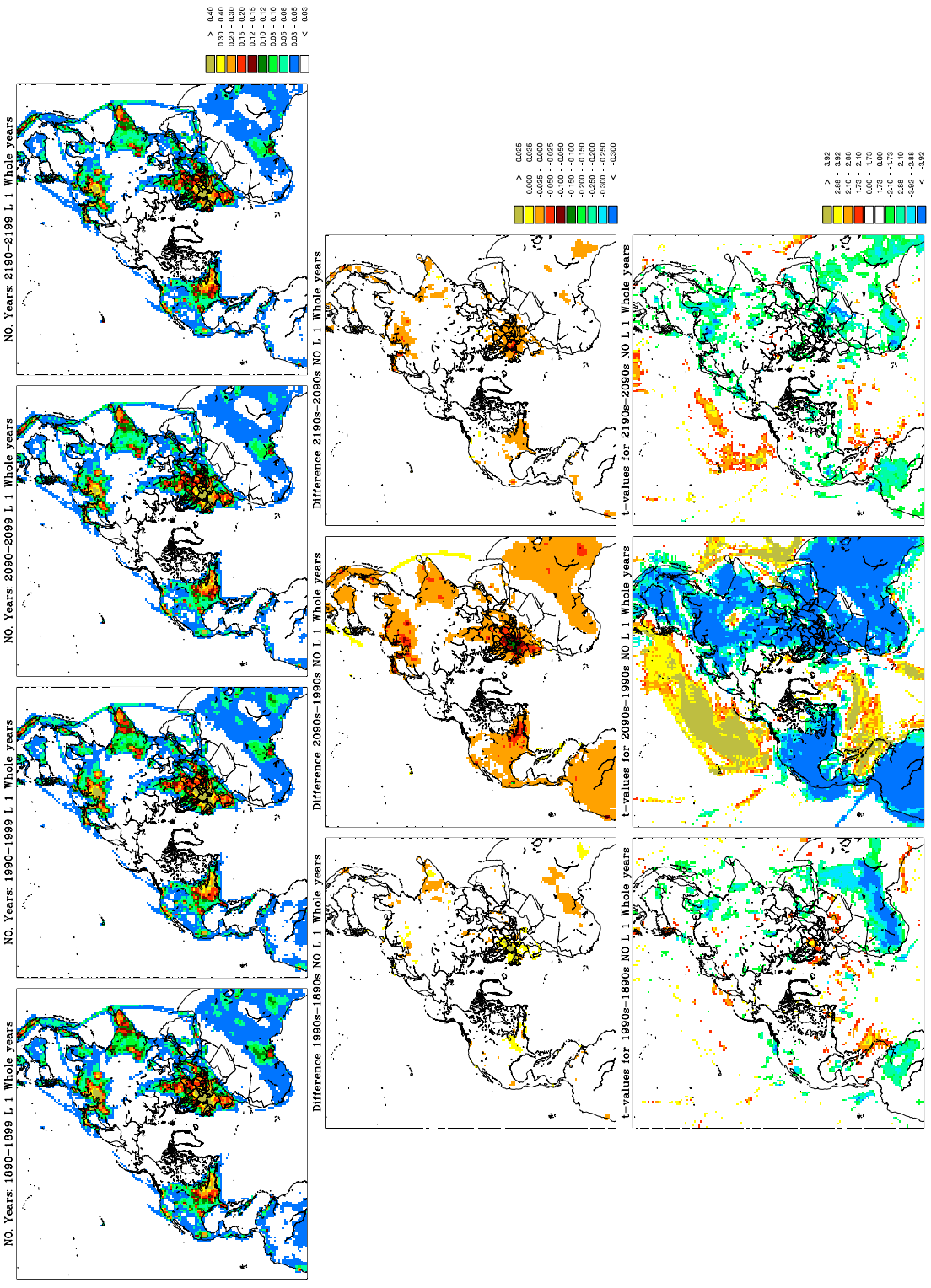

Figure 6.8: Average decadal concentration of (NO) in the lowest model layer in ppbV. Setup the same as in 6.1.

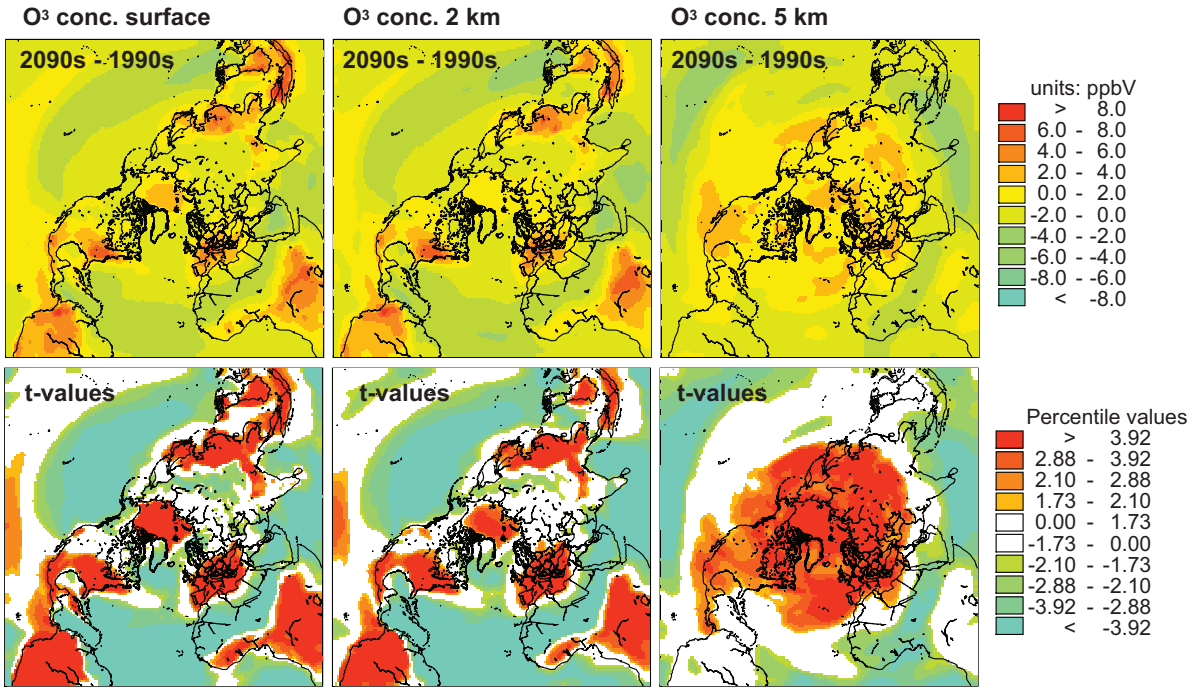

Figure 6.9: Changes in ozone concentration in ppbv between the 1990s to the 2090s and the significance of these changes the surface layer, layer 12 ($\sim$2100 m) and layer 15 ($\sim$4750 m)

7 Quantification climate signal vs. anthropogenic emission

Emissions of air pollutants impacts the future air pollution levels both on a global, regional and local scale. However also changes in the future climate conditions have significant effects on the local, regional and global air pollution levels. Most recent studies have concentrated either on the signal from emissions reductions or the signal from climate change [Langner et al., 2005; Murazaki & Hess, 2006; Hedegaard et al., 2008, 2011] and only a few have compared the two signals over a limited areas [Tagaris et al., 2007; Wu et al., 2008b; Pye et al., 2009; Racherla & Adams, 2009]. In this study we hypothesis that climate change can in some areas have significantly impact air quality in relative to the impacts from changes in emissions. The signals from changes in climate conditions and emissions might cancel out, damp or even amplify each other depending on the sign of the individual contributions. We aim to estimate the size and sign of the impact from changes in climate and changes in emissions relative to each other and relative to the total predicted change.

All meteorological parameters do effect the chemistry and physics of the atmosphere either directly or indirectly through various chemical and physical interactions and feed-back mechanisms. Since the last IPCC report [Pachauri & Reisinger, 2007] it had become clear that climate change is already occurring and will continue in the future which means that the global, regional and local meteorological conditions will change in the future. Furthermore emissions will change due to population growth and technology evolution. Since the mid 1970s when the first global pollutant problems were discovered[1] national and international air pollution legislations were formulated and enforced. New legislations are formulated every year in order to prevent future atmospheric pollution levels to amplify or to clean

[1] Arctic haze were (re-)discovered in the early 19070s and and after some years it became clear that it has its origin from Asian and European pollution. Air Pollution was no longer a local or regional problem but had turned in to a global problem

up past and present pollution in the purpose of returning to cleaner atmospheric conditions. Therefore large changes in both climate conditions and emission levels and distributions are to be expected in the future.

The atmospheric chemical composition is only a sub-agent of the full atmospheric system and furthermore the atmosphere is only a sub-domain of the full climate system. All possible climate agents that might alter the climate system needs to be accounted for in order to predict the future atmospheric composition and climate conditions. Because of the large uncertainties that still are connected to climate change and atmospheric processes itself this is a very difficult task. The non-linear nature of atmospheric chemistry might enforce new threads or benefit from one chemical species due to emission reduction in another chemical species and in order to make reasonable air pollution reduction strategies it is important to know if the signal from climate change should be accounted for in the legislations. Moreover changes in the chemical composition if the atmosphere leads to altered forcings on the climate system and vice versa. However the radiative imbalances in the climate system is beyond the scope of this paper and needs fully integrated air pollution- climate models to be investigated.

We have in this study carried out a sensitivity study to investigate if the signal from climate change is important relative to the signal from changes in emissions and this is a first step in the direction of predicting the overall Climate Change - Air quality Interactions.

7.1 Experimental setup

To study the relative importance of impacts from climate chance and changes in anthropogenic emissions several simulations has been carried out with different combinations of meteorology and emissions. The climate simulation used in the current experiment is the same as in the former study (chapter 6) and the simulation and the meteorological output are described in 5. The DEHM model is here after driven on the projected meteorology. The anthropogenic emissions used as input to DEHM model are based on the newly developed RCP4,5 emission scenario [Clarke et al., 2007; Smith & Wigley, 2006; Wise et al., 2009], which is described in chapter 3.2. The experiment is setup as a time-slices experiment in order to save computing time and storage space. To avoid any confusion the setup is illustrated in figure 7.1. The dehm model is driven on six-hourly meteorology projected by the ECHAM5 climate simulation, which in the period 2000-2100 has been forced with the SRES A1B emission scenario [Nakicenovic et al., 2000], described in chapter 3.1.

The faith of 58 chemical species and 9 classes of particulate matter has been simulated for the 1990s and the 2090s by the DEHM model. The

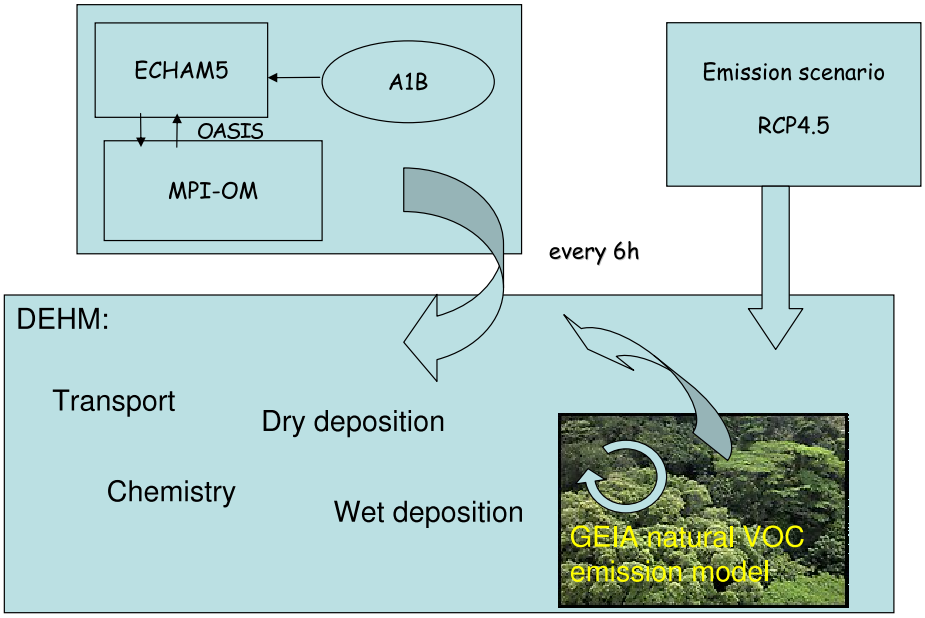

Figure 7.1: Model setup: The ECHAM5-OM is driven the SRES A1B scenarío, the governing meteorological parameters are saved at a three hour interval. After that the DEHM model driven on the saved ECHASM5 Meteorology and antropogenic emmission projected by the newly developed RCP4.5 scenario

model is driven on six-hourly meteorology input simulated by the coupled Atmosphere-Ocean General Circulation Model ECHAM5/MPI-OM. The ECHAM5 climate simulation has been forced the SRES A1B scenario whereas the DEHM model receives emission input based on the newly developed RCP4,5 emissions. It was not possible to use a climate simulation which also were based on the RCP scenarios, since the such simulations simply did not exist at the time this research began.

The decade from 1990-1999 (met1990a) and from 2090-2099 (met2090s) is chosen to give a first estimate of the changes during the 21st century. As a reference period the 1990s decade has been simulated with meteorology predicted by the ECHAM5/MPI-OM model for the same period (1990-1999) and constant 2000 emission. The reference simulation is from now denoted $x(met1990s, emis2000)$ where x is the concentration or deposition of a specific chemical specie like eg. ozone. In order to separate the signal from climate change, a simulation with constant 2000 emissions and future meteorology for the period 2090-2099 has been carried out and is denoted $x(met2090s, emis2000)$. Similarly the signal from changes emissions is identified by a simulation with present day meteorology 1990-1999 and and scenario emissions from year 2100, denoted $x(met1990s, emis2100)$. Finally the best guess of the future predicted by these models arise from a simulation

with future meteorology 2090-2099 and scenario predicted emissions from year 2100 and this is denoted $x(met2090s, emis2100)$.

From these simulations the current and future emissions can be combined with current and future meteorological in a number of ways and even more information can be extracted from the data by subtracting and dividing these simulations in several ways. In the current study 4 combinations have carefully been selected in order to describe the individual contributions from climate and emission change, respectively.

The signal from climate change relative to the reference period is illustrated by:

$$climate\,signal = \frac{x(met2090s, emis2000) - x(met1990s, emis2000)}{x(met1990s, emis2000)} \quad (7.1)$$

where x is a given parameter (like e.g. ozone concentration or nitrogen deposition) and $x(met2090s, emis2000)$ represent the level of the given parameter x due to future meteorology for the period 2090-2099 and constant 2000-level emission derived from RCP4.5 emission database. This means that in equation 7.1, the signal from climate change have been isolated by keeping the anthropogenic emissions constant at a present-day level (year 2000) and using projected meteorology of the two decades 1990s and 2090s.

For $climate\,signal > 0$: The given parameter increase due to climate change
For $climate\,signal = 0$: The given parameter does not change due to climate change
For $climate\,signal < 0$: The given parameter decrease due to climate change

The signal from emission change relative to the reference period:

$$emission\,signal = \frac{x(met1990s, emis2100) - x(met1990s, emis2000)}{x(met1990s, emis2000)} \quad (7.2)$$

The signal from emission change for a given parameter x is obtained by keeping the meteorology constant and force the simulation with the RCP4.5 emission scenario (subfigure 7.2(b)).

For $emissionsignal > 0$: The given parameter increase due to emission change
For $emissionsignal = 0$: The given parameter does not change due to emission change
For $emissionsignal < 0$: The given parameter decrease due to emission

change.

The total signal from climate and emission change relative to the reference period:

$$total\,signal = \frac{x(met2090s, emis2100) - x(met1990s, emis2000)}{x(met1990s, emis2000)} \tag{7.3}$$

The total signal is shown in 7.2(c). For all the chemical reactive species the signal from climate change plus the signal from emission change do not equal the total signal from climate and emission change due to the non-linear nature of the atmospheric chemistry. Furthermore in order to quantify the size of the signals relative to each other the following fractions have been calculated:

$$\frac{climate\,signal}{emission\,signal} = \frac{x(met2090s, emis2000) - x(met1990s, emis2000)}{x(met1990s, emis2100) - x(met1990s, emis2000)} \tag{7.4}$$

Equation 7.4 express the size of the climate signal relative to the emission signal. Whether the two signal amplify or oppose each other can be seen from individual signal plot of the climate signal (eq. 7.1) and the emission signal (7.2). This means;

For $\frac{climate\,signal}{emission\,signal} = 1$: The climate and emission signal is of equal size and sign and the sign can be determined from eq. 7.1 and 7.2.
For $\frac{climate\,signal}{emission\,signal} > 1$: The size of climate signal is larger than the size of the emission signal and both effects are either both positive (increasing) or both negative (decreasing) and therefore results in an added effect on a given concentration or deposition (x).
For $0 < \frac{climate\,signal}{emission\,signal} < 1$: The emission signal dominates and both the climate signal and the emission signal has the same operational sign. The sign of the two signals can again be determined from equation 7.1 and 7.2 (subplots 7.2(a) and 7.2(b)).

7.2 Model results

In the following the projection of O_3, BC, total $PM_{2.5}$ including secondary inorganic particles primarily emitted particles (mineral dust, OC and BC), total SO_4 and total N are shown. The findings are briefly discussed while as they presented and further discussed together with the rest of the results of this thesis in chapter 10. The overall conclusions can be found chapter 11.

7.2.1 Ozone and ozone related species

In figure 7.2 the changes in ozone surface concentration due to impacts of climate change and changes in the anthropogenic emissions between the 1990s and 2090s are shown (eq. 7.1-7.4). In subfigure 7.2(a) the signal from climate change is displayed. This is similar to the results shown in chapter 6, where the ozone concentrations due to climate change are projected to increase over the Arctic, the densely populated areas and the terrestrial tropics. Elsewhere the ozone concentration will decrease considering only impacts of climate change.

The increase in Arctic is likely to be due to increased transport of ozone from the source areas in combination with reduced amount of sea ice in the future, since O_3 in the model, dry deposit more effectively to sea ice than to open water. In densely populated areas and over the tropics both the NO_x and VOC level in general are high and the changed climate leads to enhanced productions of BVOCs and hence higher ozone levels over these areas. In the rest of the domain the effect from increased water vapour in the atmosphere enhances ozone destruction and this process is dominating in the areas with lower NO_x and VOC concentrations.

Subfigure 7.2(b) illustrates the changes in the ozone concentration due to changes in the anthropogenic emission between the two decades 1990s and 2090s. The anthropogenic emissions are for the 1990s based on the RCP4.5 emission scenario year 2000 emissions and for the 2090s based on the RCP4.5 year 2100 emissions. In most of the domain the emission signal is opposing the signal from climate change. The model estimates a decrease in the current ozone concentration in the order of 20% between the 1990s decade and 2090s decade solely due to changes in the anthropogenic emissions. The tendency is different over northwestern Europe. In the Benelux countries and in the vicinity of this area the ozone concentrations are calculated to increase due to changes in the anthropogenic emissions. This is also the case in Africa south of Sahara.

The projected increase in ozone concentrations in the future in these areas can be explained by the emission inventory. The NO_x emissions are general prescribed to decrease in the future (not shown). In the Benelux area the NO_x emissions are also projected to decrease (not shown), however this area is different from the rest of the densely populated areas. The largest density of NO_x emissions is found in Benelux and the surrounding areas and the area is characterized by urban area chemistry. The ozone present in the area is used to convert the emitted NO to NO_2 (see R 6.3) which is called the ozone titration effect or urban deficit [Fowler et al., 2008]. This means that lowering the emissions of NO will increase the amount of ozone and hereby change the chemical regime.

In Africa a large increase in the future O_3 concentration is found (figure 7.2)

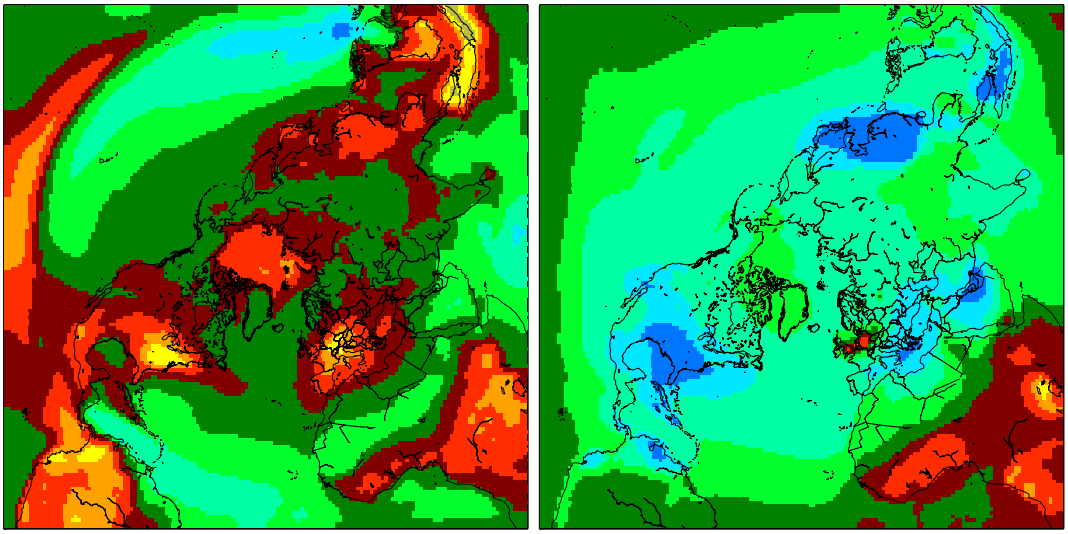

(a) O_3: Climate signal (see eq. 7.1)

(b) O_3: Emission signal (see eq. 7.2)

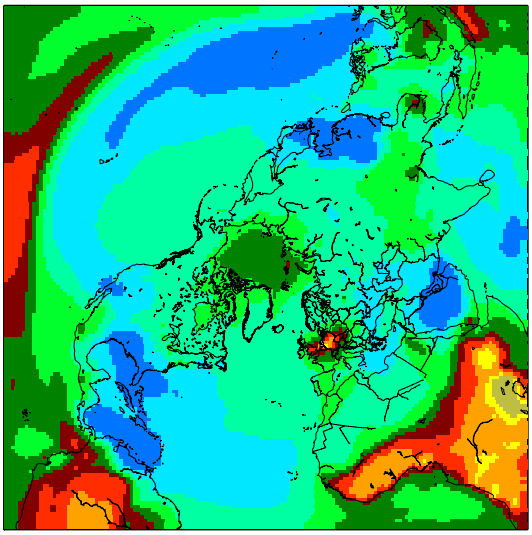

(c) O_3: Total signal (see eq. 7.3)

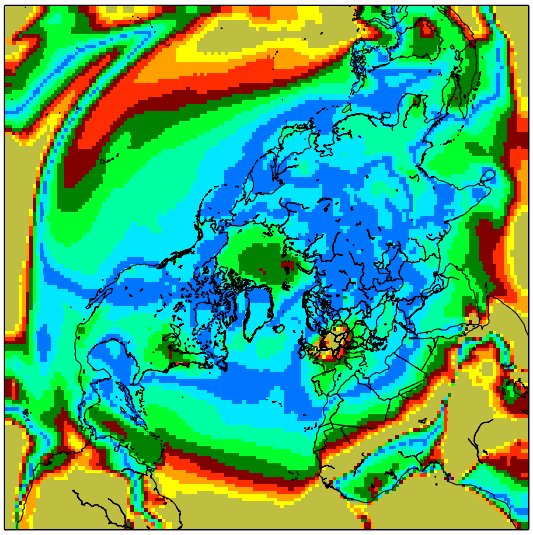

(d) Climate signal/Emission signal (see eq. 7.4)

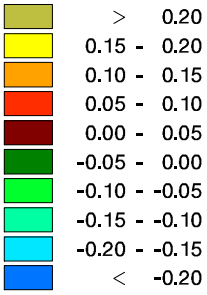

(e) Legend for a,b,c (fraction)

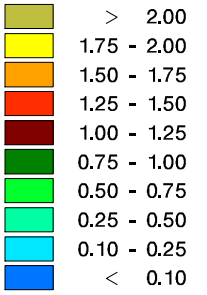

(f) Legend for d (fraction)

Figure 7.2: O_3: The signal from a) climate change, b) emission change, c) the total change on the surface ozone concentration and d) the climate signal relative to the emission signal. a) The climate signal, simulated with constant year-2000 emissions and ECHAM5 meteorology, b) The signal from changes in the anthropogenic emissions, simulated with projected RCP4.5 emissions and constant 1990s meteorology ECHAM5, c) The total signal from both changes in climate and emissions, simulated with projected emissions (RCP4.5) and future meteorology by ECHAM5.

which is explained by a large increase in the anthropogenic NO_x emissions combined with general higher biogenic VOC (BVOC) levels in the tropics (figure 6.4). About half of the global isoprene emissions originate from tropical broadleaf trees [Guenther et al., 2006] and the tropical meteorological conditions are highly conductive for isoprene emissions, which together with the tropical meteorological conditions is the reason for general high biogenic VOC levels in the tropics.

In subfigure 7.2(c) the combined effect on the future ozone concentration from both changes in anthropogenic emissions and changes in the climate is shown. As noted previously, the total change is not equal to the addition of the two contributors due to the non-linear nature of the chemical processes included in the model. The ozone concentration decrease due to impacts from changes in both the future anthropogenic emissions and climate, except over the continental tropics and northwestern Europe where this impacts will increase the future ozone concentration, according to the model.

Subfigure 7.2(d) shows the relative importance of the two individual signals. This is illustrated by the fraction: "Climate signal" divided by "Emission signal" (see 7.4). Sand/orange colours indicate areas where the climate signal dominates and blue and light green colours indicate area where the change in the future emissions are dominating. In the areas with dark red and dark green colours the two signals contribute approximately equally in the future to the ozone concentration. Subfigure 7.2(d) shows that the increase in surface ozone concentration in the continental tropics and northwestern Europe are mainly due to the impacts of climate change. The climate signal dominates and is more than twice the size of the impact from changes in the anthropogenic emissions.

The minor decrease in the estimated ozone concentration over the Arctics is a composite of two opposing signals. The impacts of climate change leads to a 5-10% increase (figure 7.2(a)) and the reduction in emission of ozone precursors imply a 5-10% decrease (figure 7.2(b)). The total signal displayed in figure 7.2(c) shows a minor overall decrease in the Arctic by the end of the 21st century and in figure 7.2(d) it can be seen that the climate signal is a little weaker than the emission signal (0.75-1.00).

7.2.2 Black Carbon and $PM_{2.50}$

Black Carbon (BC) is in the model an inert tracer, which means that it does not interact chemically with other species in the atmosphere. In figure 7.3 the change in BC surface concentration due to changes in a) climate, b) anthropogenic emissions and c) changes in both climate and anthropogenic emissions is shown. The latter is equal to the addition of a) and b), since BC is an inert tracer and do not react chemically with other species in the

atmosphere. In subfigure 7.3(d) the climate signal is illustrated relative to emission signal.

In figure 7.3(a) the relative projected changes due to impacts of climate change is shown. The concentration is projected to decrease in the Arctic, in Scandinavia, over Eastern Europe and Russia and over large parts of the Pacific Ocean (red, blue and green colours). A increase is found nearly elsewhere. Since BC is an inert tracer in the model and the emissions are kept constant at a year 2000 level, only changes in the physical (e.g. meteorological) conditions can be the explanation of the projected changes.

In figure 7.4 the isolated effect from climate change on the BC a) wet deposition, b) dry deposition, c) atmospheric concentrations and finally d) the total deposition is shown. The plots display the significance of the changes in decadel mean values between the 1990s and the 2090s. Over the Arctic, Northern Scandinavia, Siberia and the North Atlantic and Pacific Ocean the atmospheric concentration is found to decrease significantly due to impacts of climate change. The decrease over the Arctic region is to a large extend in agreement with the increased precipitation frequency in this area (figure 5.4). When the precipitation frequency increases, particles will be washed out of the atmosphere and hereby lowering the atmospheric concentration of particles, in this case BC. There are some differences over the Canadian part of the Arctic. Here the wet deposition decrease despite the increase in the precipitation frequency and therefore changes in the precipitation pattern between the 1990s and 2090s cannot explain the calculated decrease in the atmospheric BC concentration. However analysis have shown that the mixing height in this area increases (figure 5.5), which leaves more air for the same amount of particles to mix in and hence the concentration in the column of air decrease.

In and south of the Mediterranean Sea, along the east coast of North America and Asia and in general over the low latitudes the atmospheric concentration of BC is found to increase due to climate change. In the Mediterranean area there is a close relation between decreased precipitation frequency (figure 5.4) and decreased wet deposition despite the increased atmospheric concentrations of BC. Over the US East coast, on the contrary, the concentration in the air increases, due to a decrease in the mixing height (5.5). Over the tropical Pacific a distinct belt of significant changes is found in most of the plots displayed in this thesis. This feature originates from the ECHAM climate simulation. The ECHAM model has been described in some model inter-comparisons to fail in capturing the low level clouds over the Pacific Ocean correctly and this feature can be seen in all the plots and hence will not be given any particular attention in the analysis of the atmospheric compounds in this study.

Going back to figure 7.3, subplot 7.3(b) shows the relative contribution from the impact of changes in anthropogenic emissions on the atmospheric BC

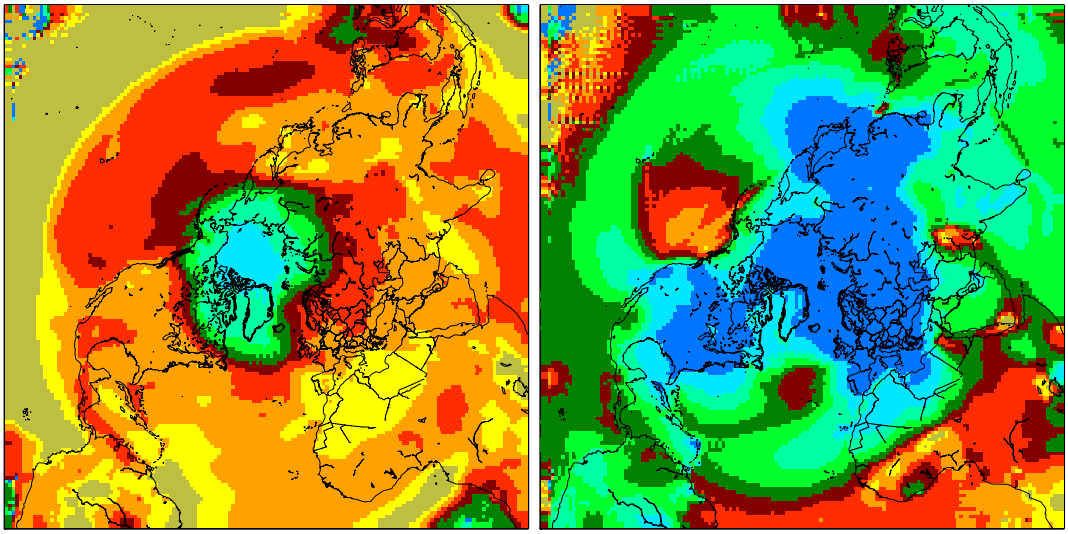

(a) BC: Climate signal (see eq. 7.1)

(b) BC: Emission signal (see eq. 7.2)

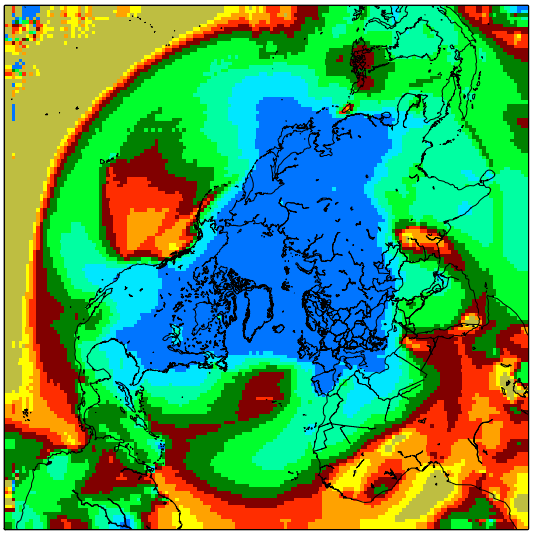

(c) BC: Total signal (see eq. 7.3)

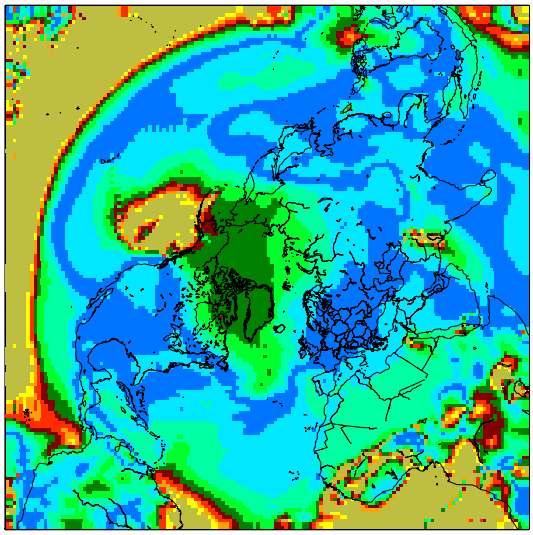

(d) Climate signal/Emission signal (see eq. 7.4)

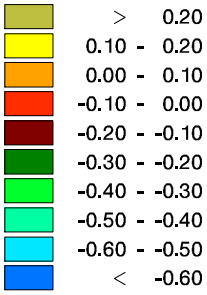

(e) Legend for a,b,c (fraction)

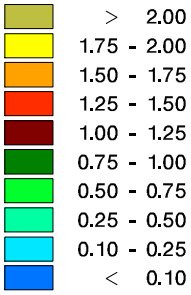

(f) Legend for d (fraction)

Figure 7.3: Black Carbon (BC): The signal from a) climate change, b) emission change, c) the total change on the surface BC concentration and d) the climate signal relative to the emission signal. a) The climate signal, simulated with constant year-2000 emissions and ECHAM5 meteorology, b) The signal from changes in the anthropogenic emissions, simulated with projected RCP4.5 emissions and constant 1990s meteorology ECHAM5, c) The total signal from both changes in climate and emissions, simulated with projected emissions (RCP4.5) and future meteorology by ECHAM5.

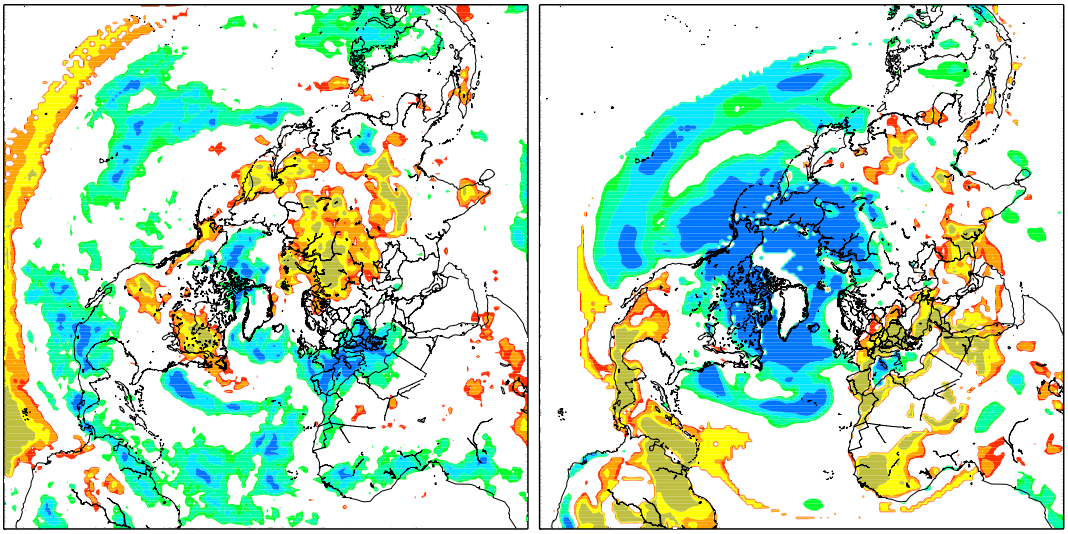

(a) BC:wet deposition $mg/m^2/year$

(b) BC: Dry deposition $mg/m^2/year$

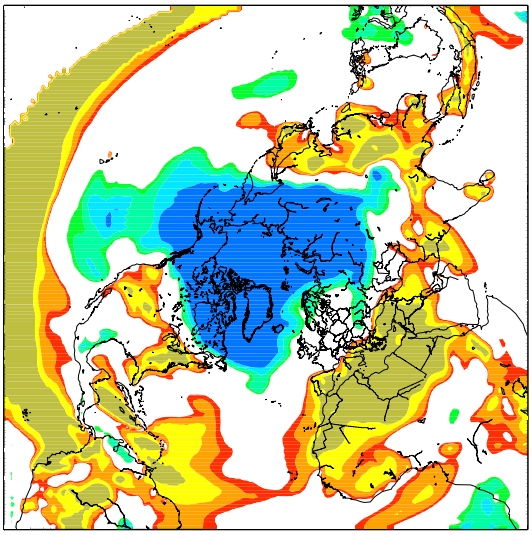

(c) BC: Concentration

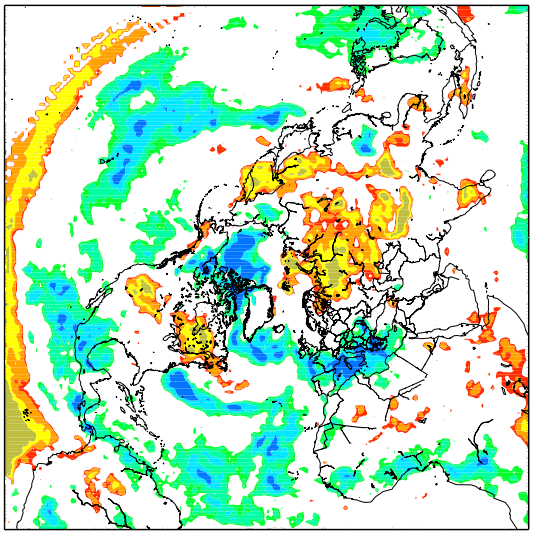

(d) BC: Total deposition $mg/m^2/year$

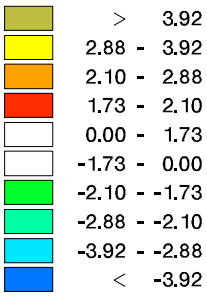

(e) Significance

Figure 7.4: Black Carbon (BC): Changes due to impacts of climate change: The significance of change of decadal mean values between the 1990s and 2090s in a) wet deposition and b) dry deposition c) concentration and d) total deposition. The significance is calculated according to the students t-test, the threshold for significance is set to 10%. White areas indicate no significant chance, yellow/red areas indicate significant increase and blue values indicate significant decrease.

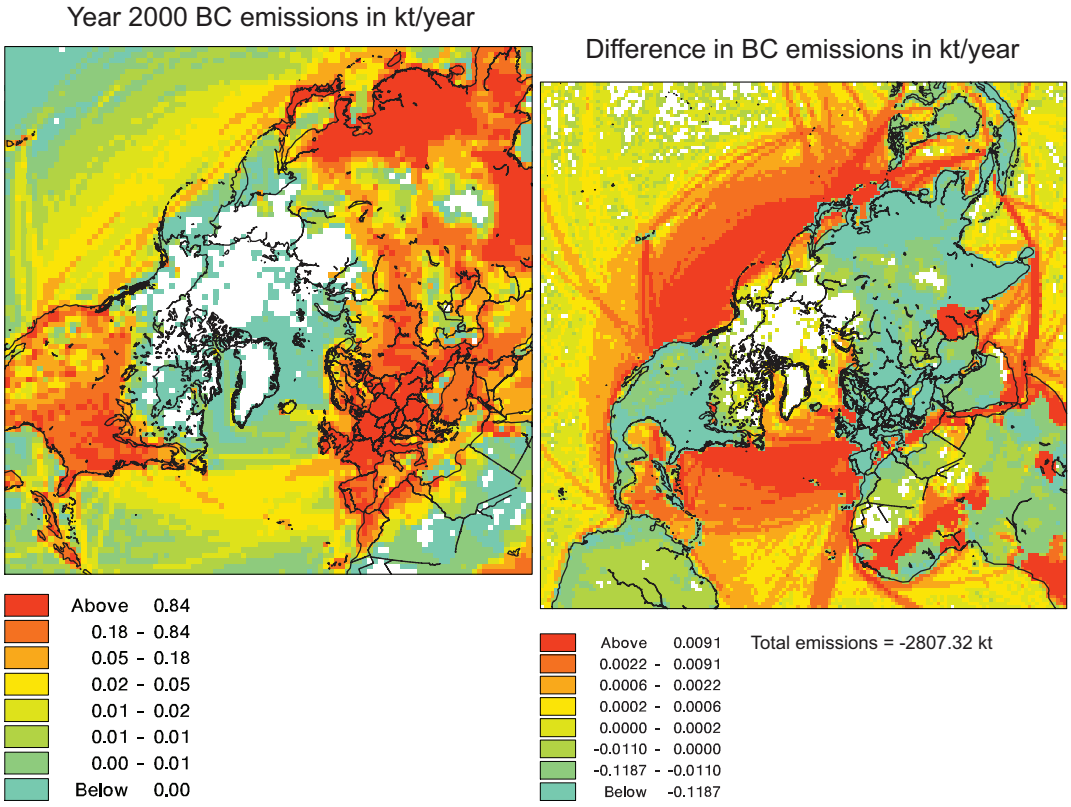

Figure 7.5: RCP4.5 total Black Carbon emission a) the 2000 BC emissions for all sectors b) the difference between the 2100 and the 2000 total emissions. Details of the emission from each of the 12 emissions sectors can be found at www.iiasa.ac.at/web-apps/tnt/RcpDb.

distribution. The contribution from emission change leads to a decrease in BC in the majority of the domain, though there are some differences in the size of the signal. Since the meteorology is kept constant in this simulation (to isolate the impact from changes in the emissions) only change in emissions size and spatial distribution can explain the pattern of figure 7.3(b). For comparison the total RCP4.5 emissions of BC for year 2000 and the difference between year 2100 and year 2000 (2100 minus 2000) is shown in figure 7.5.

The majority of BC emissions stems from the transportation, industry, residential and biomass burning sectors and BC is therefore mainly emitted in and near the terrestrial areas (figure 7.5(a)). In the future these emissions is prescribed by the RCP4.5 scenario to decline significantly (figure 7.5(b)). In contrast the emissions over the ocean are prescribed to increase. This increase originates from increased aviation and shipping activities in the re-

mote marine areas, see www.iiasa.ac.at/web-apps/tnt/RcpDb for emissions from the individual sectors.

In figure 7.3(c) the total signal on BC from changes in both emissions and climate conditions is shown and further the climate signal relative to the emission signal is given in figure 7.3(d). From the latter figure it can be seen that the area south of the Aleutian are strongly dominated by the signal from climate change. In this area the signal from climate change results in a decrease the future BC concentration due to an increase in the mixing height (figure 5.5). In this way the climate signal oppose the projected rise due to changes in the anthropogenic emissions from ships and aviation. Elsewhere at high and mid-latitudes the total concentration of BC will decrease due to a combined effect of climate change and emission changes, though the impact from changes in emissions dominates.

In figure the 7.6 the absolute concentrations for the 1990s and the 2090s decades are shown together with the calculated change between 2090s and 1990sdue to both climate change and emission change. The overall BC distribution are found to decrease in the future except over parts of Central and West Africa. From this figure it can be seen that the distinct pattern south of the Aleutians results in extremely small changes (changes below 1/1000 of the mean concentration are set to zero and indicated in the figures with white). In general it can be concluded that the changes due to impacts of climate change on an inert tracer like BC is small compared to the impacts from changes in the anthropogenic emissions which are absolutely dominating. The BC concentration will decrease due to a general reduction in the future BC emissions.

Figure 7.7 is similar to figure 7.3 and shows the relative impacts from a) climate change, b) emission change and c) total change, d) the climate signal relative to emission signal. For the total $PM_{2.5}$ concentrations the pattern in the changes of $PM_{2.5}$ looks to a large extend like the distribution of BC described above and the same is valid for the change in the total sulfate (not shown). $PM_{2.5}$ is particulate matter with a diameter below 2.5 μm and include both secondary inorganic particles and primarily emitted particles (mineral dust, BC and OC).

The patterns of $PM_{2.5}$ (figure 7.7) look very similar to the distributions of BC shown in figure 7.3 except that the structure is more smooth and e.g. the distinct pattern South of the Aleutians is not evident in the total $PM_{2.5}$ changes. Again the low latitudes experiences less improvement in the air quality in the future compared to higher latitudes mainly due to either increased or less reduced anthropogenic emissions in the future. This means again that the impact from changes in the emissions dominate in the future (figure 7.7(d)) and the overall signal from climate change and emissions change work in same direction and therefore amplify each other. A smaller difference compared to BC is seen in the Arctic, where the decrease in $PM_{2.5}$

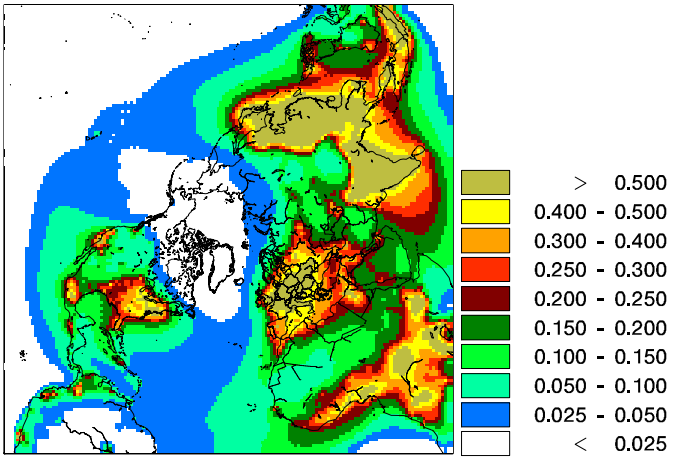

(a) BC concentration mean concentration in the 1990s in ppbV

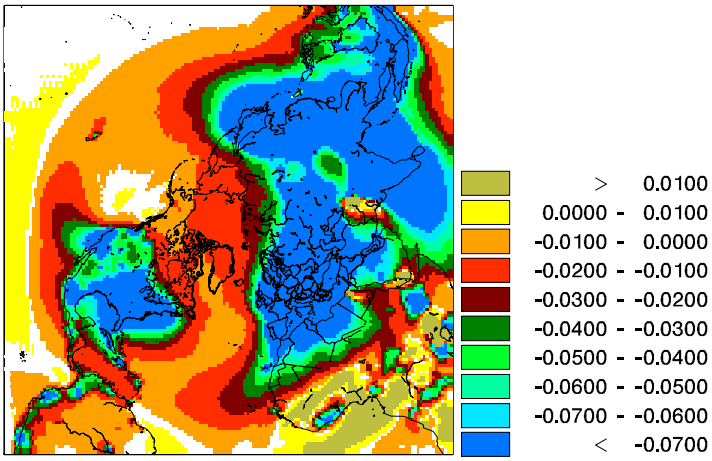

(b) BC difference 2090s-1990s in ppbV

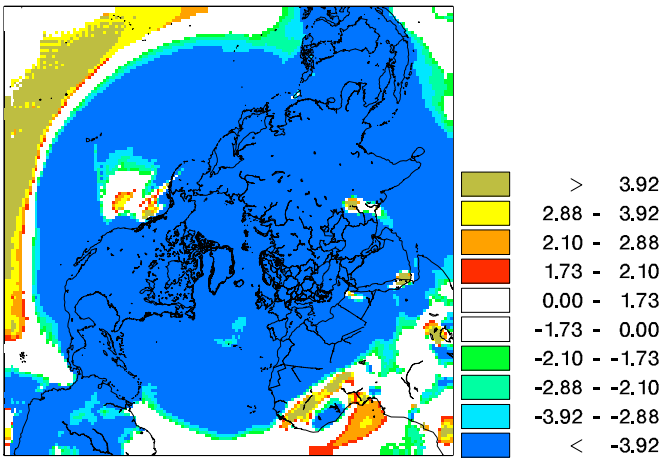

(c) Significance of the difference

Figure 7.6: Black Carbon (BC): The signal from both climate change and emission change a) 1990s concentration b) difference (2090s-1990s) in ppbV, c) the significance of the differences calculated according to the Students t-test and significance is chosen to be within a 10% threshold.

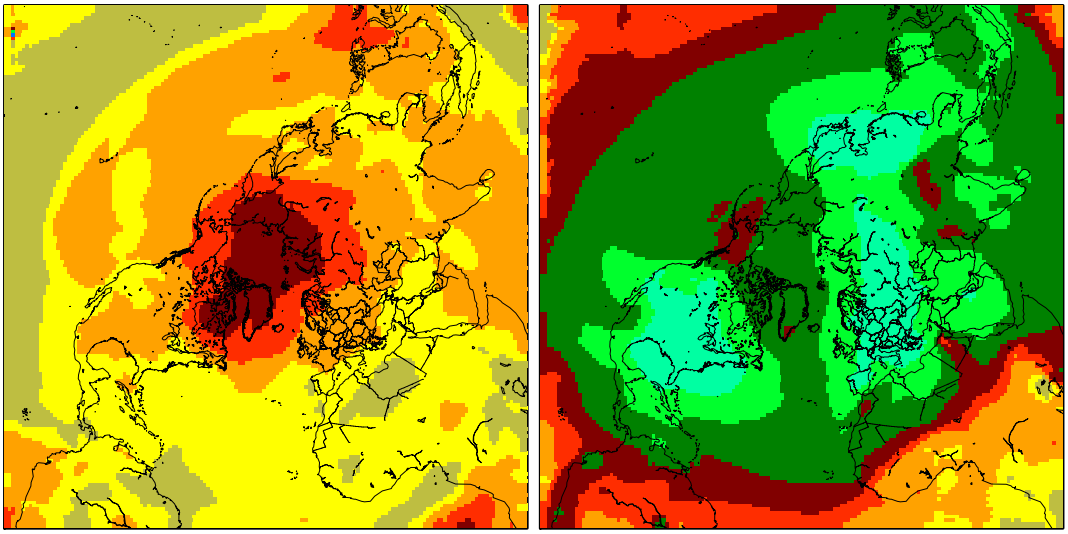

(a) $PM_{2.5}$: Climate signal (see eq. 7.1)

(b) $PM_{2.5}$: Emission signal (see eq. 7.2)

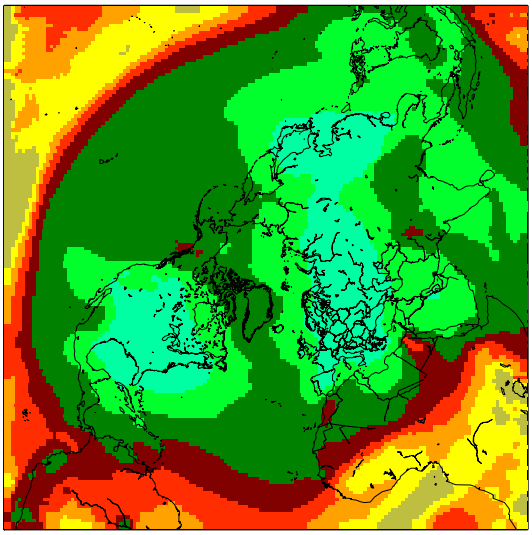

(c) $PM_{2.5}$: Total signal (see eq. 7.3)

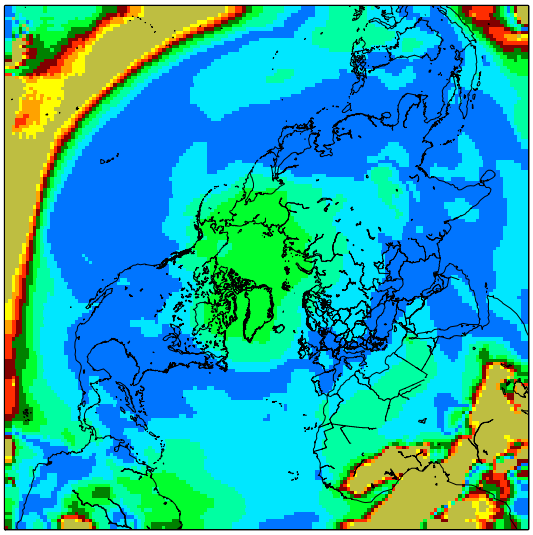

(d) Climate signal/Emission signal (see eq. 7.4)

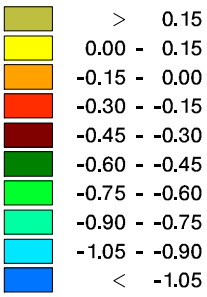

(e) Legend for a,b,c (fraction)

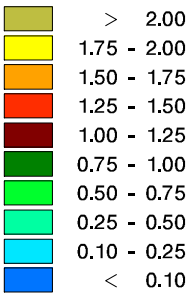

(f) Legend for d (fraction)

Figure 7.7: Total PM 2.5 ($PM_{2.5}$): The signal from a) climate change, b) emission change, c) the total change on the surface $PM_{2.5}$ concentration and d) the climate signal relative to the emission signal. a) The climate signal, simulated with constant year-2000 emissions and ECHAM5 meteorology, b) The signal from changes in the anthropogenic emissions, simulated with projected RCP4.5 emissions and constant 1990s meteorology ECHAM5, c) The total signal from both changes in climate and emissions, simulated with projected emissions (RCP4.5) and future meteorology by ECHAM5.

concentrations are less compared to BC in the case of climate change only.

7.2.3 Total N

In figure 7.8 the individual contributions to the projected changes in total nitrogen concentration is shown. This figure is similar to figure 7.7 and 7.3. Again the impact from emission dominates 7.8(a) and the signals are in general very similar to the changes projected in BC and $PM_{2.5}$. The signal from climate change is to some extent driven by the changes in the global precipitation distribution and in a few areas also the changes in mixing height (see e.g. central South America figure 5.5(d) and 7.8(c). Since Total N contains both NH_x and NO_y the total N distribution is also dependent on chemistry like e.g. oxidation capacity of the atmosphere.

Since nitrogen deposition can have harmful effects on the marine and terrestrial ecosystems, the absolute concentration in year 2000 is shown in figure 7.9 together with the differences in total nitrogen deposition and the significance of those differences. Over Europe and down wind from there and in the eastern part of North America the future nitrogen deposition is estimated to decrease between 0-10%. The decrease is even larger over the ocean, where the projected reduction of 10-20% in the total nitrogen deposition is evident. However at low latitudes, especially in the western US, in Africa and large parts of Central and South Asia, the depositions are found to increase due to changes in both emissions and the climate conditions. The areas in the Arctic that from figure 7.8(a) are controlled by the impacts of climate change are at the same time areas with extremely low nitrogen concentrations (not shown) and hence the changes due to climate change are also very low.

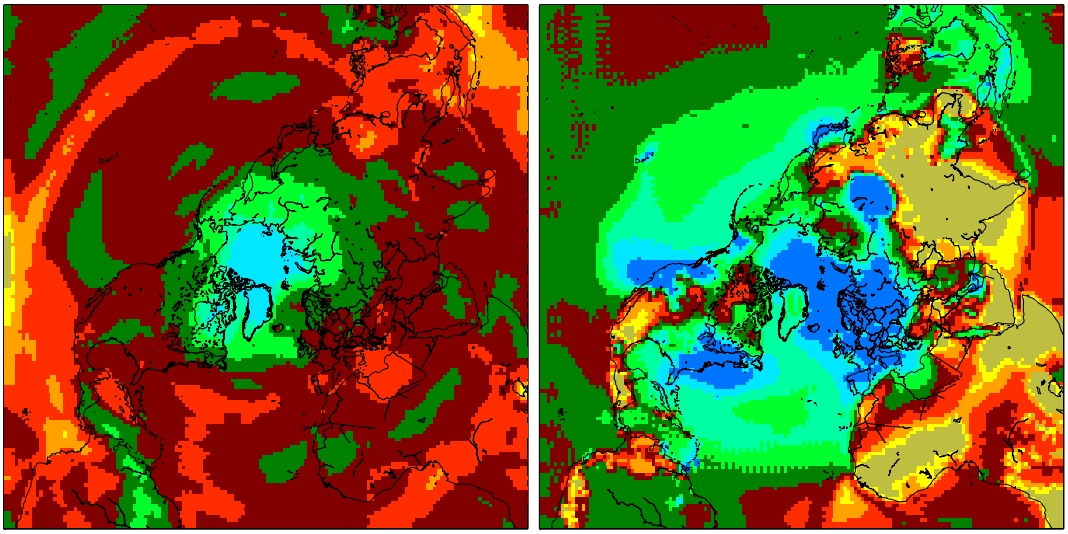

(a) Total N: Climate signal (see eq. 7.1)

(b) Total N: Emission signal (see eq. 7.2)

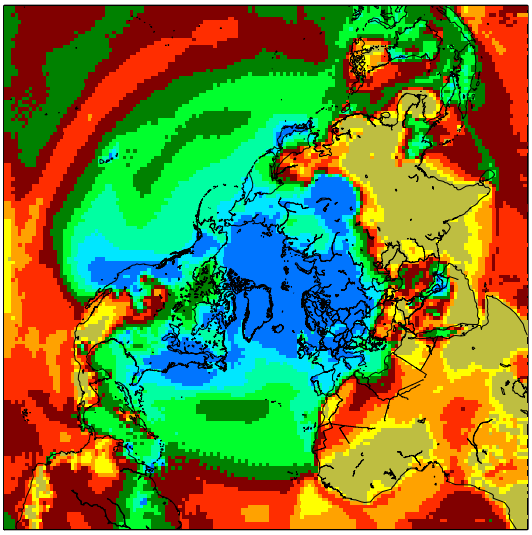

(c) Total N: Total signal (see eq. 7.3)

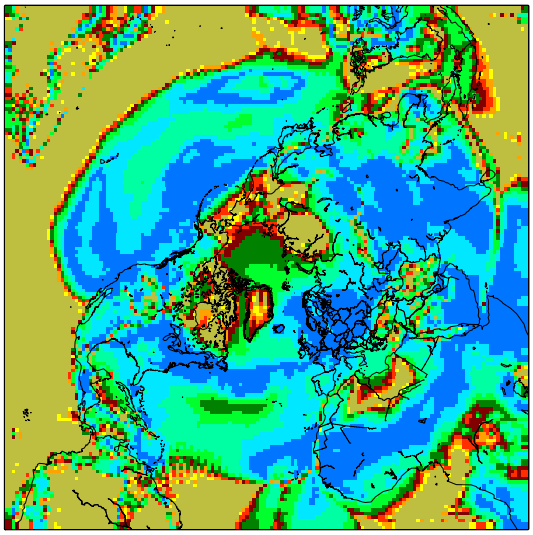

(d) Climate signal/Emission signal (see eq. 7.4)

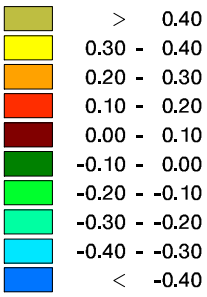

(e) Legend for a,b,c (fraction)

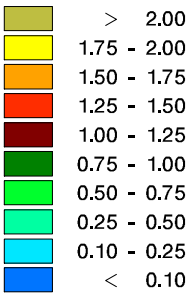

(f) Legend for d (fraction)

Figure 7.8: Total nitrogen (N): The signal from a) climate change, b) emission change, c) the total change on the surface nitrogen concentration and d) the climate signal relative to the emission signal. a) The climate signal, simulated with constant year-2000 emissions and ECHAM5 meteorology, b) The signal from changes in the anthropogenic emissions, simulated with projected RCP4.5 emissions and constant 1990s meteorology ECHAM5, c) The total signal from both changes in climate and emissions, simulated with projected emissions (RCP4.5) and future meteorology by ECHAM5.

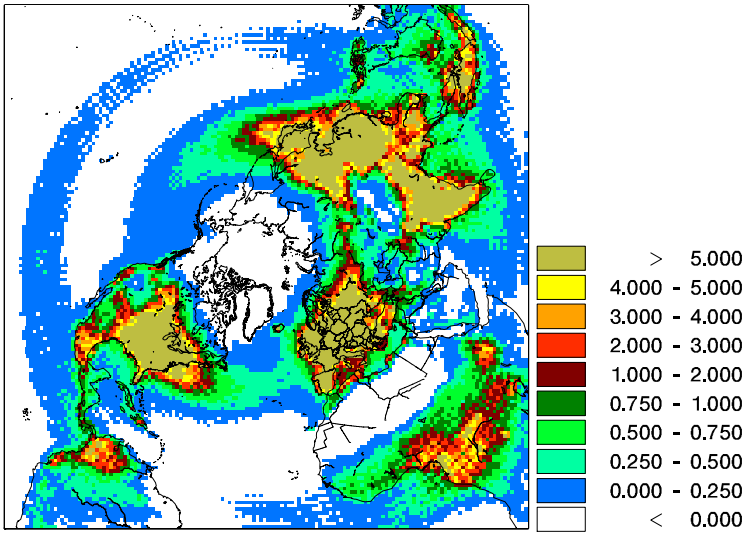

(a) Total mean N deposition in the 1990s in $mg/m^2/year$

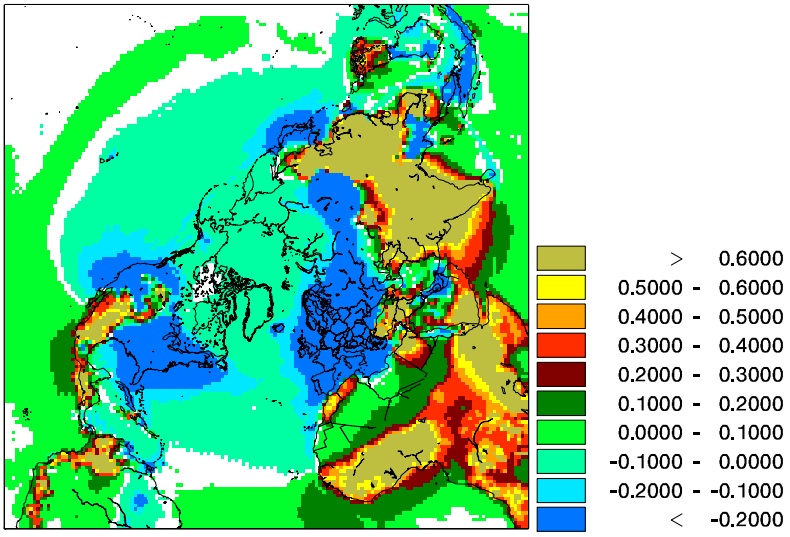

(b) Total N deposition: difference 2090s-1990s in $mg/m^2/year$

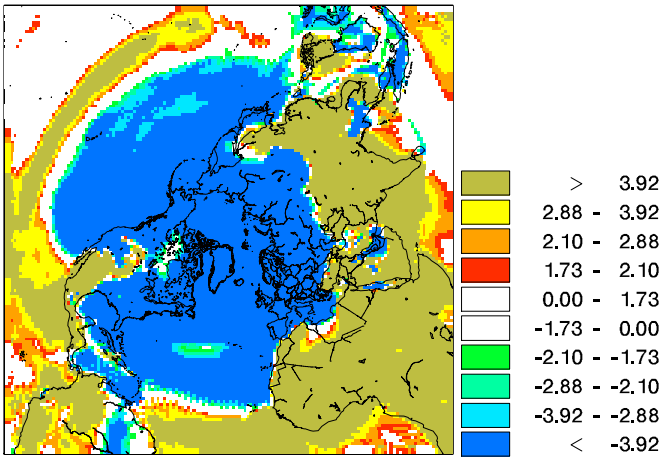

(c) Significance of the difference

Figure 7.9: Total nitrogen deposition in $mg/m^2/year$.

8 Evaluation of Time-sliced experiments

The research described in the former chapters is an example of the use of climate model data to describe impacts of climate change. In general, climate impact research uses data from climate models for a wide range of purposes and sometimes the constraints and limitations of climate model data are either toned down or un-purposely forgotten. The effects of climate change on the biosphere, human health, agriculture or infrastructure are other example of such impacts studies that deals with detailed models which limits the climate change experiments to be cut down to comparison of shorter time-slices.

Historically the World Meteorological Organization (WMO) defined thirty years as the minimum time period when dealing with climate trends in order mask out any seasonal, annual or decadal variability. However, thirty years is just a choice based on the amount of continuously measured data available at the time WMO introduced "Climate Standards" [Baddour & Kontongomde, 2007]. In climate impact studies, it is common to assume that a decade of model simulated data can represent a much longer time period. The difference between the first and the last decade of a century are assumed to a give a reasonable estimate of the change expected by the end of the given century.

Some impact studies use even shorter periods. The studies by Tagaris et al. [2007]; Liao et al. [2007]; Wu et al. [2008a,b]; Pye et al. [2009] and Lam et al. [2011] are all examples of time-sliced experiments within the field of air pollution and climate change interactions, where time-slices of only one to three years are used to project what will happened by year of 2050 and these papers are all published in well reputed scientific journals. The time-slice method is used when data from relative short measuring campaigns or computationally expensive models are applied. Governments and private companies urge for specific information on e.g. sea-level rise, precipitation and emissions of various chemical compounds to plan future infrastructure and to establish new emission legislations of both greenhouse gases and air pollutants. So far research results from time-slice experiments are the

best first guess with respect to centennial projections which encourages the impact community to carry out these experiments. Moreover some impact researchers are unaware of the problems related to model climate data (and maybe even unfamiliar with the statistics needed to handle such problems) and therefore do not state the necessary assumptions and limitations clearly enough together with the final impact results.

In contrast the climate model community consider the time-slice assumption crude since natural year-to-year and decadal variability exist. Therefore it is natural to question; if impact/assessment research based on short time-slices can provide scientifically sound impacts of climate change results? And further; how long should the time-slices be when studying impacts of climate change in order to provide useful and scientifically sound results? These questions are difficult to answer and the answers depend strongly on the particular data set and output data of interest. In the following a method to analyse climate data intended to be used in impacts of climate change experiments are described. The conclusions of this investigation, do not give any definitive answer to how long time-slices should be when working with time-sliced impact studies. Conversely the method can be considered as a recipe on how to determine an appropriate length of the time-slices and further how to select the most representative time-slices from the full data set for an impact study. In Section 8.1 the overall method is sketched and in section 8.2 and 8.3 the statistical tools used to do the analysis is described. The climate data used in this thesis is analysed with respect to inter-annual and decadal variability and results are shown in the next chapter.

8.1 Method

If a given ten-year period of climate data should represent a full century of climate data, it is important that the given period do not differ significantly from the overall atmospheric pattern of the full period. Both inter-annual and decadal variability do exist in both nature and model data and when 10 years of data is taken out of the full data set there is the possibility that exactly those ten years contain some or even ten extraordinary years relative to the full period. With respect to impact research it would be very unfortunate to pick out such a decade since the results would not represent the most likely outcome of the future but instead an extreme case, which cannot be associated with the overall evolution.

The climate simulation used in this thesis was part of the 4th IPCC Assessment Report (AR4) multi-model ensemble study (run4). It is 340 years long spanning over the period 1860-2200 and is based on the coupled atmosphere-ocean model ECHAM5/MPI-OM. Details about the climate model and the simulation can be found in chapter 5. The output from the climate sim-

ulation consists of a large set of meteorological parameters ranging from 3-hourly to annual values. In this study monthly 500 gph is analysed which over the 340-year long period results in 120 temporal values per decade and 34 decades in total.

The domain covers Europe, the North Atlantic Ocean and some of the Arctic Ocean and is bounded by the coordinates $90°W - 35°E$ and $25°N - 87°N$ (see e.g. figure 9.1). This is the region where the North Atlantic Oscillation (NAO) takes place[1]. The NAO pattern is the only teleconnection that is visible all year around in the Northern Hemisphere however most pronounced in the winter month where the atmosphere in the area of interest is most dynamically active. For this reason December, January, February and March have been selected (i.e. winter) to represent the variability of the full period and the "the full data set" refer to an average over the full period of these months and each decade (e.g. 1860-1899) is an average over the same months average over ten years denoted e.g. "1860" for period 1860-1869. Furthermore to avoid analysing the known climate trend in the data, the full data set has been de-trended by fitting a third-order polynomial and subtracting this from the data.

The 500 gph is governing the surface meteorology since it carries information of both temperature and dynamics and has a strong connection to the low-level pressure systems. The main focus of this thesis is the future air pollution level. The governing parameters with respect to atmospheric air pollutants are pressure/wind fields, temperature, humidity and insolation. These parameters are through atmospheric dynamics more or less directly connected to the placement of the 500 gph. A continuous data set of any air quality parameter like e.g. ozone are not available and therefore the analysis of the time-slices vs. the full period is based on the z500 gph field which originates directly from the climate model output. The z500 gph are assumed to be strongly connected to the surface ozone concentration. This assumption is investigated further in section 9.2.

This method can be applied to any feature impacted by climate change. However it is not necessarily the z500 gph field that should be analysed. For example if thunder clouds or simply convection, is the research topic, it would be better to analyse the instability or humidity projected by the climate model and in this way assure that the time-slices are able to capture the correct decadal variability with respect to exactly these governing meteorological parameters. Another example could be black carbon, which in the atmosphere acts as an inert tracer. In this case one might investigate the low level wind or pressure pattern with respect to the decadal variabil-

[1]The North Atlantic Oscillation is an index originally defined by the difference in MSLP over the Azores and Island. When the MSLP is high over the Azores and low over the Island the NAO is defined to be in a positive mode and vice versa. For further details see e.g. Hurrel et al. [2003]

ity. Or to work with a smother field; the z500 pressure distribution could be analysed in contrast to the z500 gph, since this also contains information about temperature which might be redundant with respect to the transport of a tracer.

EOF analysis (see section 8.2) has been used to identify "the centre of action" with respect variability in the data set. The aim is to investigate the spatial variability of the full data set vs. the individual decades. It is well known that the NAO pattern exists and evidence from literature indicates that it is likely to have existed for at least the last millennium [Hurrel et al., 2003] and therefore probably will continue to exist into the next two centuries. This implies that a climate model should be able to simulate this phenomenon both within the individual decades and within a full 340-year long period in order to capture the variability of the atmosphere correctly.

Practically in this study, the EOF analysis has been performed on both the full de-trended period and on the 34 individual decades. The first EOF of each decade is now correlated with the first EOF of the full period, surrogate data are created and compared with the results and the final results are presented in the following chapter.

8.2 Empirical Orthogonal Function (EOF) analysis

In atmospheric science, multivariate statistical techniques are commonly used. They are particularly useful to identify and understand mutual dependencies of one or more parameters and to analyse changes in trends and means of these parameters. The Principal Component Analysis (PCA) method was originally described by Pearson [1902], however it was introduced into atmospheric Science in 1956 by Lorenz [1956] under the name Empirical Orthogonal Functions (EOF). Actually Lorenz used the EOF technique to describe the NAO phenomenon [Lorenz, 1951, 1956].

The EOF technique was developed to identify and examine variability in large and complex data sets. The technique can identify patterns of simultaneous variation. One of the advantages of the EOF technique is that it can reduce a data set of the observed or modelled system to a much smaller subspace (often represented by the first two or three EOFs). This subspace represents the most of the dynamics of the original observed system. In climate research it is often reasonable to assume that the subspace with maximum variation coincides with the dynamically active subspace [Storch & Zwiers, 1999]. Mathematically, EOF analysis is performed by expanding the anomalies from a data series of a given parameter into a finite series. This series consists of k time-coefficients multiplied by k fixed EOF patterns.

These patterns are mathematically constructed to be orthogonal. The patterns can be thought of as "modes of variability" and the corresponding Eigen values describe the time fraction each pattern is represented in the data. For a more complete description see e.g. Storch & Zwiers [1999].

Climate variability is often described as an anomaly from a mean state. The same is done in the EOF analysis where the technique is performed on the anomaly data. The anomalies are simply the deviation from any mean state and here the mean state refers to an average value over a decade and over the full 340-year period, respectively.

The EOF technique results in a 3-dimensional array containing the EOF patterns, the principal components (PCs) and the Eigen Values. The latter describes how much of the total variability each EOF explains. The first EOF is the variability pattern with the highest degree of explanation (e.i. with the largest Eigen value). From analysis of measured MSLP data (Iceland vs. Azores MSLP) among others Hurrel et al. [2003] found that the first EOF constitutes of approximately 1/3 of the total variance.

When working with EOF data it is important to keep in mind, that it is mathematically constructed. This means that the first EOF do locate the areas of the largest physical variability and because of the strong dynamic nature of the NAO, this area is expected to express the NAO in the domain chosen here. However, the second EOF is constructed to be mathematically orthogonal to the first EOF and at same time describe areas of the second most variability in the data set. The orthogonality implies a non-physical structure to the patterns and the higher EOF (EOF3, EOF4, EOF5.... etc) one investigates, the less physics the pattern represents.

8.3 Correlations and surrogate data

To investigate if a given ten-year period resembles the full period, the first EOF of each of the ten-year periods has been correlated with the first EOF of the full period. This correlations is denoted χ and is plotted as a function of the corresponding Eigen value of appertaining decade. It is assumed that the all 34 decades has the pattern recognized as the NAO represented in the first EOF. For example the dynamics of one decade could for some unknown reason have been altered and therefore oscillates most of the time in another mode of variability (another EOF pattern). This means that the EOF pattern showing the NAO-like structure would move down and be represented in maybe the second or third EOF. In this case it would be more correct to correlate the first EOF of the full period with second or third EOF of that particular decade. This feature is analysed in section 9.2 where the correlation of the 500 gph vs. the surface ozone concentration is

evaluated, however in the full analysis of the length of the time-slices, it is assumed that the first EOF represent the NAO-like pattern in all decades.

The correlations between each decade and the full period result in a span of correlations between -1 and 1. The sign of the correlation indicates if a given EOF pattern are displayed in their negative or positive mode and therefore it is the size of the correlations that is interesting in the current study. Another issue is to determine if an absolute correlation of e.g. 0.8 is good enough in order to state; that the particular decade do contain the same variability as the full period. A general rule of thumb says; that all correlations above 0.8 is high [Rogerson, 2010]. Nevertheless this is a useless rule since the threshold for acceptance of correlation values depends highly on the data, the method and the scientific question in mind. The correct answer to ask is; if it is possible to obtain similar correlations with artificial data?

Artificial or surrogate data can be constructed in many different ways, though it is important to preserve the statistical features of the original data. This means that the surrogate should hold the same mean, spread and spatial de-correlation length as the original data set.

One way to construct surrogate data, that features the mean and spread of the original data set, is to take the map (in this case of the first EOF), cut it into pieces and mix these pieces differently. To preserve the spatial de-correlation length it is important that the length of each piece is long enough to preserve any possible spatial de-correlation of the original data set. The spatial de-correlation length (also called block length) can be calculated by correlation of the time-series (in this case the principal component) of each point with the time-series of all the surrounding points. This results in a correlation-map and from that, the block length is determined as the mean distance to a point where the correlation has decreased to $\frac{1}{e}$. [2] Alternatively, more simple one can inspect the plot of the first EOF for the full period and make an educated guess, which is the approach used in the next chapter 9.

There are many ways to create surrogate data most of them is complex and time consuming and it is beyond the scope of this thesis to go further into details with these statistical method. Instead the "shift" command in IDL has been applied to create a surrogate data set that preserves the statistic features of the original data set. The "shift" command moves every grid point in the map a specified number of grid points ("x") in the east/west and north/south direction depending on the sign of the input value "x" and the points at the edge of the map is wrapped around and re-appears in other side of the map. The input value "x" has to be greater than or equal to the block length in order to preserve the spatial correlation of the original data set. In the current study 100 surrogate data sets of the full 340-year long

[2] $1/e$ originates from fitting the exponential function to the autocorrelation functions.

period have been created and each EOF analysed. The first EOF of these 100 data sets is correlated with the 34 decades and the resulting $100 * 34 = 3400$ correlation coefficients are plotted as a histogram in figure 9.4 from where the significance level of the original data can be determined.

9 Results of the time-slice analysis

This chapter is divided into two parts. First the results from the investigation of the lengths of time-slices based on analysing the z500 gph field is shown in section 9.1, followed by an analysis of the connection between surface O_3 concentration and z500 gph (section 9.2).

In order to determine, if the ten-year long time-slices is a scientifically sound to use, an EOF analysis on the full 340-year long time-series has been performed. The analysis is based on the de-trended z500 gph field, since the changes in this field is expected to control the changes in the O_3 distribution at the surface (see section 9.2).

In figure 9.1 the first four EOFs are shown. Figure 9.2 shows the Eigen value or the "degree of explanation" of the first ten EOFs for the full period. The first EOF 9.1(a) accounts for approximately 35% of the total variance in the data set. The first EOF resembles the NAO pattern well with a centre of action stretching from the US east coast to the central and northern Europe across the Atlantic Ocean and an opposite directed center of action in the vicinity of South Greenland (from from the Canadian east coast across the Labrador Sea and David Strait through south Greenland and further over the Denmark Strait to Iceland). The synoptic scale lows evolves and moves in this season typically in central Atlantic area, forced to the south by persistent highs in the North (e.i. high over Greenland/Iceland) or vice versa and this pattern illustrates the NAO oscillation. Results EOF analysis performed on observational data from this area gives a typical Eigen value of this NAO-like pattern in the range 35% to 40% (see e.g. Hurrel et al. [2003]).

The second, third and fourth EOF explains 15%, 12% and 9% of the total variability, respectively. From the fifth EOF, the degree of explanation decreases steadily to zero. As described in section 8.2 the EOFs are mathematical constructed to be orthogonal. Nevertheless it could be argued that the second EOF could reflect a typical winter time blocking situation, with a persistent high in the east and an active kernel over the Atlantic Ocean

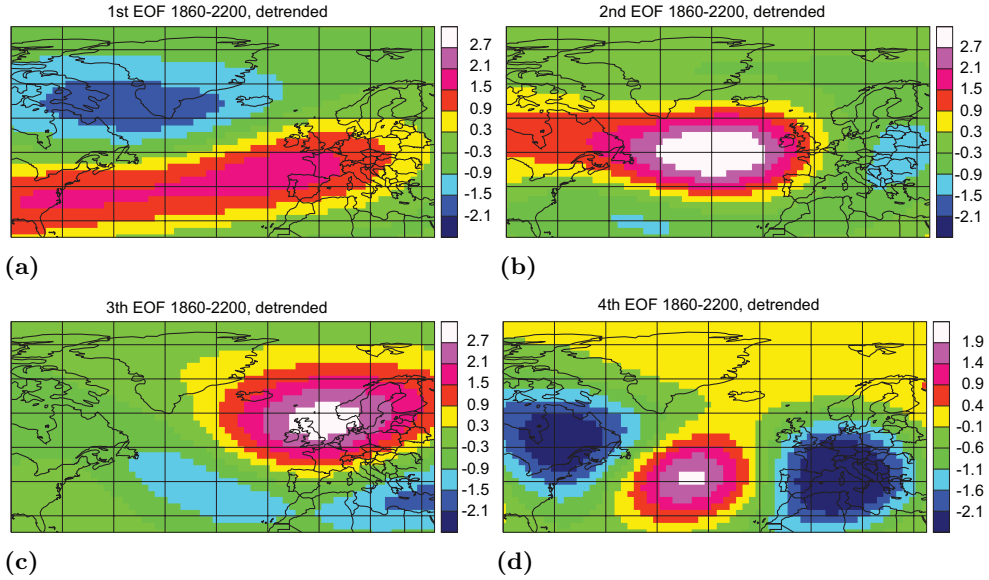

Figure 9.1: The first four EOF of the full 340-year period based on the z500 gph field. The data has been de-trended before the EOF analysis was carried out in order to separate out climate trend. a) shows the first EOF, b) the second EOF, c) the third EOF and d) the fourth EOF. The first EOF resembles the NAO well. The folowing EOFs is mathematical constructed and therefore contains less physics (See text for further details).

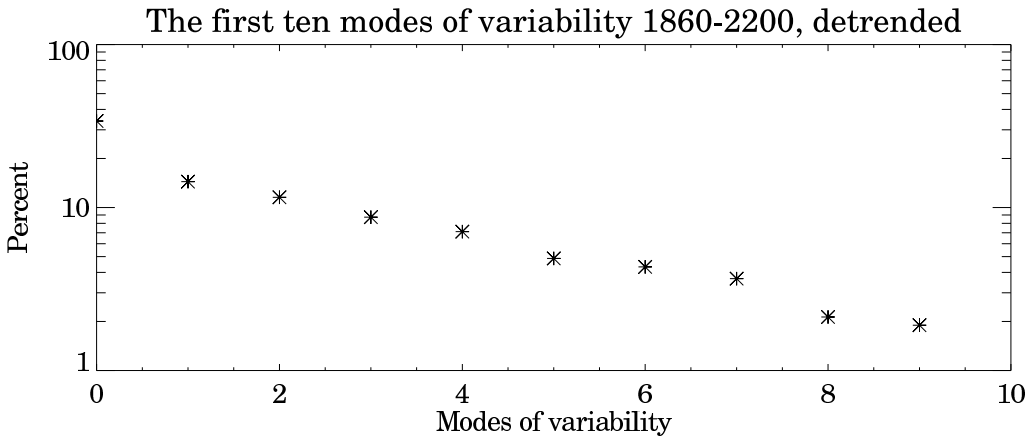

Figure 9.2: The Eigen values or the "degree of explanation" of the first ten EOFs are shown from the full 340-year period based on the z500 gph field. The first four EOFs displayed in figure 9.1 explains approximately 35%, 17%, 12% and 9%.

similar to the one recognised in the first EOF, though shifted to the west. However the blocking events have historical been named "the Scandinavian pattern" (original called Eurasia 1 by Barnston & Livezey [1987]). The Scandinavian pattern consist of a centre of action over Scandinavia accompanied with two weaker centres over western Europe and eastern Russia which cannot be found in any of the EOFs in figure 9.1 due to the choice of domain. However, EOF3 do posses of features of the Scandinavian pattern and a more easterly situated domain might have led to the appearance of this pattern in figure 9.1.

Stevenson et al. [2004] did a similar EOF analysis on 45 years of reanalysis data of the z500 gph field in the Northern Hemisphere. They identified the first EOF as the Pacific-North American (PNA) pattern and the second EOF as the NAO. The two pattern looks similar to the one identified in this thesis 9.1, they are just interchanged. This can be explained by the different domains the EOF analysis has been performed on. In this thesis the focus is on the North Atlantic sector where the PNA oscillation has less influence and is therefore not reflected in the first EOF. Nevertheless the fact that the PNA pattern is stronger in the reanalysis than the NAO indicates that the PNA on a hemispheric scale is a stronger phenomenon in the winter time northern hemisphere.

9.1 Results of z500 gph analysis

To investigate the similarities of the variability in the full period (1860-2200) vs. the 34 individual time-slices an EOF analysis have been performed on every decade and the first EOF of this decade is compared with the full period. The plots can be found in appendix A. It varies how similar the patterns are, though most of them do feature the dipole structure as the first EOF of the full period (9.1). Some of the decades might load differently than the full period meaning that the EOF with the largest "degree of explanation" might be interchanged so it would be more correct to compare e.g. the first EOF of the full period with the second or third EOF of some of the decades. For simplicity it is assumed; that the leading EOF pattern of all the decades is the same as the leading EOF pattern of the full period. The fact that the EOFs are well separated supports this assumption.

In figure 12.6 the Eigen value of the first EOF of each decade is plotted as a function of the absolute correlation between the principal component of the first EOF of the full period and the principal component of the first EOF of the individual decades. The absolute correlation is defined as the numeric value of the correlation ($absolutecorelation = |correlation|$). The four decades of interest with respect to the chemistry modelling work of this thesis is identified with coloured squares. The 1890s, 2090s and 2190s

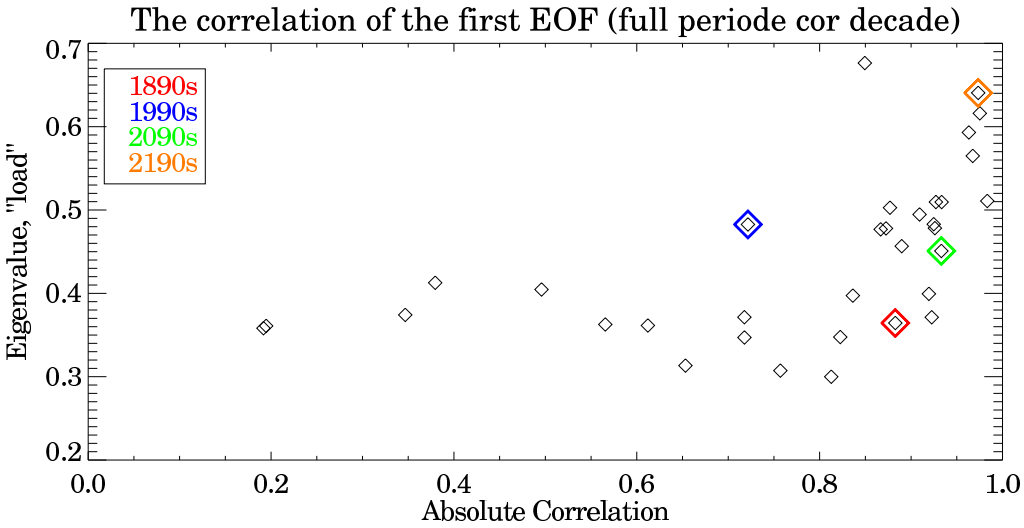

Figure 9.3: The Eigen value of the first EOF of each decade as a function of the absolute correlation between the principal component of the first EOF of the full period and the principal component of the first EOF of the individual decades.The four decades of particular interest marked with a coloured square. The 1990-1999 period posses the lowest correlation with a value of 0.73 and $\sim 23.5\%$ of the decades have a correlation below 0.7.

all have a relative high correlation well above 0.8. Unfortunately the 1990s only correlates a little above 0.7 which degrades it to be questionable with respect to significance by the rule of thumb mentioned in section 8.3. In general 8 out of 34 decades corresponding to $\sim 23.5\%$ have a correlation below 0.7.

The same analysis using time-slices of five and fifteen years respectively, have been carried out and the plots can be found in appendix A. For the fifteen-year case the Eigen values tend to cluster the same way as in the case of the ten-year time-slices except that the fifteen-year correlations in general is higher. The increase in the length of the time-slice increases the correlation between the full period so that only $\sim 13.6\%$ of the correlations is below 0.7 and the four decades of particular interest (1890s,1990s, 2090s and 2190s) all have high correlations in the range 0.82-0.97 in the fifteen-year case. On the contrary the change to five-year long time-slices implies that $\sim 41.2\%$ of the decades correlates with the full period below 0.7, which means that there are only a 58% chance of choosing a five-year period that have captured the variability of the full period.

In summary for the case of ten-year long time-slices it is illustrated that most of the individual decades do posses the same inter-annual variability as the full 340-year period and the decadel variability is not too large with the exception of few decades. These few "outliers" also have relative low

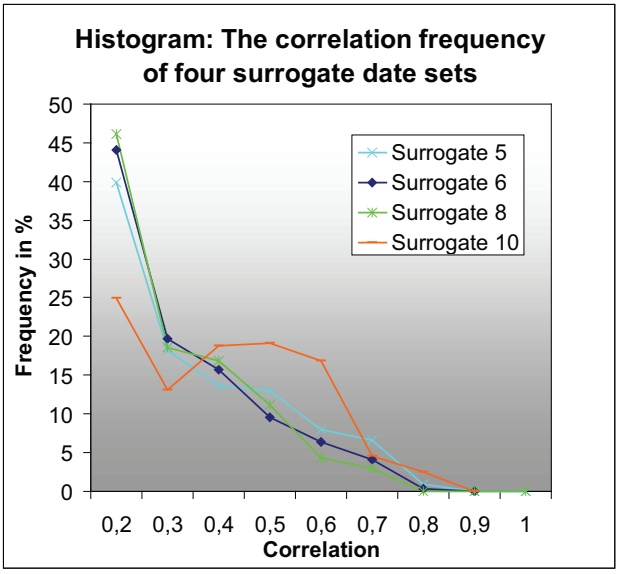

Figure 9.4: This figure shows the Eigen values of the decades as a function of the correlation between each decade and the full 340-year period. Three of different sets of surrogate data with block length 5, 6, 8 do not differ that much. The surrogate data set with block length 10 is significantly different most likely since the block length is relatively high compared to the size of the domain (34x67)

Eigen values for the first EOF and the correlations might have been better if precisely these decades were correlated with e.g. the second EOF or the third EOF of the full period. The four decades of particular interest do resemble the inter-annual variability of the total period with a correlation ranging from ~ 0.73 to ~ 0.98. Furthermore not surprisingly the correlations increase with the lengths of the time-slices. Now, one has to ask; if these correlations are high enough to state that the ten year time-slices do resemble the variability of the full period? As described in section 8.3 to answer this question, it is necessary to determine, if similar correlations could have been obtained from random data?

In figure 9.4 four different surrogate data sets are plotted in a histogram. Each surrogate set is based on 100 random values and is created according to the method described in section 8.3. In figure 9.1(a) there are two "centre of actions". One very elongated structure across the Atlantic Ocean and one with a more circular structure with a centre just east of South Greenland. If both structures were circular like the latter, the block length would have been estimated to be in the order of the radius of that structure, which means a block length of 1000-1500 km. However some caution in the determination of the block length have to be exercised due to the elongated structure of figure 9.1(a). In the North-South direction an educated guess on the block length could be in the order of 500 km in contrast to the East-

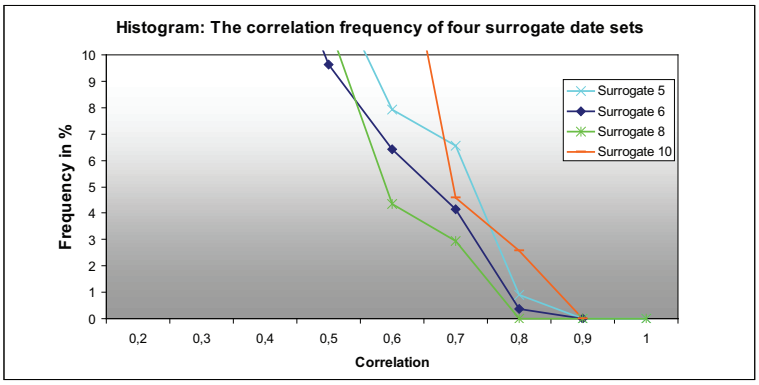

Figure 9.5: The same figure as 9.4 but zoomed in on the lower 10% frequency interval (the higher end of the confidence interval)

West direction, where an educated guess would be about the width of the Atlantic Ocean. Instead knowledge of general synoptic scale meteorology has been used. The typical size of a synoptic low ranges from approximately 1000-2000 km. The z500 gph is connected to these lows and varies according to the synoptic lows, besides it is a smoother field. A smooth field is desirable since it is the large-scale flow which is of interest here. Based on the size of a typical low the first surrogate data is created with a block length of 8 grid points which approximately corresponds to the mean spatial distribution of a synoptic low ($\sim 1600km$). This surrogate data set is the curve denoted "surrogate8" in figure 9.4. Moreover surrogate data with a smaller (surrogate5 and surrogate6) and a larger block length (surrogate10) are also displayed in figure 9.4. The two surrogate data sets with shorter block lengths feature similar histograms as the surrogate8 data set, which indicates that the aim "not to destroy" the spatial de-correlation length is reached. In contrast the surrogate10 data set looks different. It has several maxima and the same was the case when the block length was expanded to 15, 20, 25 and 30 grid points (not shown). This spiky feature of the surrogate10 curve 9.4 is most likely due to the method used. The total domain was only 34 x 67 grid points which is low compared to "a shift" of blocks of the length ten grid point or more. The degree of re-arrangement/disorder of the map is simply too low for a block length of ten and some of the surrogates will look too much like the original data set.

Figure 9.5 is a sector of figure 9.4 and shows the lowest 10% frequency of the histogram of figure 9.5. Recalling that the correlations obtained with the original data for the four decades of particular interest was in the range ~ 0.73 to ~ 0.98 it can now be read off figure 9.5, that these correlations are all significant under a 95 percentile significance level for the surrogate6, surrogate8 and even for the odd looking surrogate10 data set. The surrogate5

data set makes values of ~ 0.7 significant under a 90 percentile significance level and for correlation values above ~ 0.74 this confidence interval increases to 5% (corresponding to the 95 percentile significance level).

This means that four decades (1890s, 1990s, 2090s and 2190s) do resemble the variability of the full period under a 95-percentile significance level in this particular climate simulation and from that it is concluded that it is scientifically sound to use the specific four time-slices to represent the longer climate simulation.

If we decide on a 90 percentile confidence level in the ten-year case, which is common practise in atmospheric modelling. The correlations of figure 12.6 has to be above 0.5 and from figure 12.6 it can be seen that for 30 out 34 decades ($\sim 88\%$ chance), that the variability in the decades relative to the variability in the full period is captured correctly. In the case of fifteen-year long time-slices this chance of reaching a 90 percentile significant level is $\sim 91\%$ and in the case of five-year time-slices it is $\sim 75\%$.

Physically this conclusion means that the four decades, which has been used to drive the DEHM model in the research described in the former chapters of this thesis, are able to simulate the well known phenomena NAO. Nevertheless, the NAO pattern only accounts for approximately 1/3 of the total variability and from the current investigation it is not possible to conclude on the remaining 65% of the variability. On the contrary the NAO is the only well known large-scale pattern in this area, since the domain e.g. do not stretch far enough to the east to include the Scandinavian pattern or large enough to capture the PNA. Further the second EOF of this climate simulation describes only 17% of the variability compared to the 35% for the first EOF (see figure 9.2). In chapter 10 the results of this section are discussed further in relation to the results of this thesis.

9.2 Analysis of the relation between O_3 and z500 hPa gph

In this section the assumption of a connection between the z500 gph and the O_3 surface concentration is investigated. Again the domain covers the North Atlantic sector and most of Europe and analysis is performed on annual averages of the winter months (DJFM). From the chemical transport model DEHM the monthly average surface ozone concentration has been calculated. Each decade has been EOF analysed and the first four EOFs are compared in all possible combinations of O_3 and z500. The results are shown in table 9.1.

The highest correlations in table 9.1 between the PC of the z500 gph and the pc's of the surface O_3 concentrations is marked with red. It is not

1890-1899	O_3: 1. pc	O_3: 2. pc	O_3: 3. pc	O_3: 4. pc
z500: 1. pc	0.678	-0.665	0.221	-0.85
z500: 2. pc	0.107	0.354	0.753	-0.424
z500: 3. pc	-0.076	-0.059	0.494	0.837
z500: 4. pc	0.492	0.318	-0.255	0.310

1990-1999	O_3: 1. pc	O_3: 2. pc	O_3: 3. pc	O_3: 4. pc
z500: 1. pc	-0.456	-0.799	0.011	0.319
z500: 2. pc	0.341	0.137	0.058	0.832
z500: 3. pc	-0.191	0.164	0.727	0.009
z500: 4. pc	0.288	0.045	-0.129	0.071

2090-2099	O_3: 1. pc	O_3: 2. pc	O_3: 3. pc	O_3: 4. pc
z500: 1. pc	0.119	-0.954	0.114	-0.229
z500: 2. pc	-0.704	-0.228	0.008	0.630
z500: 3. pc	-0.171	-0.139	-0.259	0.070
z500: 4. pc	-0.392	0.078	0.543	0.300

2190-2199	O_3: 1. pc	O_3: 2. pc	O_3: 3. pc	O_3: 4. pc
z500: 1. pc	-0.239	-0.078	0.483	-0.320
z500: 2. pc	-0.271	0.024	-0.225	-0.403
z500: 3. pc	0.370	0.321	-0.094	0.563
z500: 4. pc	-0.515	0.365	0.212	-0.266

Table 9.1: The four tables show the correlation between the first four PCs of the z500 gph field correlated with the first four PC of O_3 surface concentration for the decades 1890s, 1990s, 2090s and 2190s. The highest correlations in every decade is marked with red and ranges between 0.5 and $\sim$ 1.0. It is not necessary the first PC of both fields that has the highest correlation. The period 2190-2199 does not have very high correlations (max. $\sim$ 0.5), see discussion in text.

necessarily the first PC of both the parameters that features the highest correlation values. In the 1890s decade the first PC of z500 and the first PC of the O_3 concentration have a correlation of ~ 0.7. Furthermore the first PC of z500 gph is negatively correlated with the second PC for O_3 at a value of ~ -0.7 etc. This just indicates that the two fields are connected in their variability but they do not always have the same sequence of the EOFs. The surrogate data method described in section 8.3 can now be used to determine if the correlation found between the z500 gph and O_3 field are significant. However, to continue this statistical analysis is beyond the scope of this thesis, though the features are discussed more qualitatively in the final discussion (chapter 10).

10 Discussion

So far the results have been presented in the same order as they were carried out during the PhD study. In this chapter the findings of all the research described so far will be summarized, discussed and evaluated in a broader context. As the title of the thesis indicates, the overall aim is to evaluate the sensitivity of air pollution concentrations and depositions to impacts of climate change and changes in anthropogenic emissions. Therefore the discussion here will have this topic as a main focus. In the following some general considerations of the climate system are summarized followed by a discussion of the results of chapter 8 and chapter 9. Next the results are discussed specie by specie followed by an overall recapitulation of the discussion. In chapter 11 the final conclusions of this thesis are put into a future research perspective.

When working with climate change and atmospheric chemical and physical properties a myriad of interacting pathways appear. The atmosphere is an extremely complex system in it itself. Nevertheless it is only sub-parts of the total climate system; here identified as the atmosphere, the hydrosphere, geosphere, cryosphere and biosphere which interact with the atmosphere.

In this thesis the focus has been on the air pollutants. However many air pollutants are also important climate agents having radiative properties that can alter the global, regional or local climate significantly. For example ozone, besides being an air pollutant that has impacts on human health, agriculture etc, is also a strong greenhouse gas due to its ability to absorb infrared light. Other examples are particles, which have both negative and positive impacts on the Earth climate system depending on the particular specie and the environment they are present in. BC is generally believed to posses positive radiative forcing due to its colour that regionally can heat up the air or change the radiative properties of the cryosphere.

In contrast sulphur particles are believed to have a negative radiative forcing, since they shade the earth by reflecting the incoming solar radiation back to space. Further several semi-indirect and direct effects of particles exist through interactions with different cloud types. Nevertheless the properties of the air pollutants just described are a research topic in it self and are not

dealt with in this thesis. To include the feedback processes between the climate system and the chemistry of the atmosphere much more comprehensive model systems, like e.g. earth system models, have to be used.

Focussing only on the impacts of climate change and emission change on air pollutants a number of aims can be achieved, which contribute to knowledge and eventually can lead to a better understanding of the individual processes resulting from humans interference with the natural environment. First of all to investigate the impacts of climate change on air pollutants climate model data are needed. These climate data need to be carefully selected with respect to the ability to capture the natural and known variability of the climate system.

In this thesis the well reputed ECHAM5 climate model has been used. The model have participated in several model inter-comparison projects throughout the years and is a regular member of the Coupled Model Intercomparison Project (CMIP) [Taylor et al., 2009; Meehl et al., 2007b] under the World Climate Research Programme (WCRP). Nevertheless it is important to assure that the specific model simulation used is suitable for the purpose of the study.

This thesis includes simulations with a comprehensive chemical transport model. The storage and computational limitations in the initiation of the phd project in 2007 was the determining factor for limiting the chemical transport simulations to be performed in time-slices of ten years. When working with impact of climate change it is obviously important to use climate data that has been thorough evaluated and performs well with respect to projection by other models (model inter-comparisons) and capture climate events from the past (evaluation against observations/proxy data). Further it is important that the model is able to capture the inter-annual and decadel variability, since the climate simulation is used as input to a time-sliced experiment.

To evaluate the robustness of climate change projections is a difficult task since the true answers lies in the future. One way to analyse climate change data (or any other kind of model data) is to use ensemble predictions, which e.g. was used in the fourth IPCC report [Pachauri & Reisinger, 2007]. When doing ensemble modelling the internal variability, which has been the issue of this study is coped with in another sense. In ensemble modelling there are many models to describe the same climatological parameter in both space and time, which introduces an ensemble mean and deviation from that. One could argue that the ensemble mean represent the "right" internal variability which justifies the use of shorter time-scales when working with ensemble predicted data. As an example 20-year averaged time-slices were used in the last IPCC report (AR4, Pachauri & Reisinger [2007]), which is less than the 30-years recommended by WMO ([Baddour & Kontongomde, 2007]). The physical argument to do that is the fact that ensemble prediction allows

shorter time scales. Another advantage was that the period considered as present day climate was restricted to the period 1980-1999, which probably represents the present better than the period 1970-1999.

There have been several attempts to estimate the robustness of observed data, which can be a complex topic in itself. The focus here has been on the robustness of modelled data and it is therefore reasonable to question if the robustness of modelled result do give any indication of how the real world works? This question is not easily answered since it depends on a large number of variables with various and in some cases unknown uncertainties. The research carried out in this thesis solely shall be considered as a sensitivity study, where the sensitivity of future air pollution concentrations and depositions to climate change and changes in anthropogenic emissions has been studied - hence it is most important that the climate data used, captures the internal climate variability correctly.

One important variability pattern in the North Atlantic region is the NAO. As described in chapter 8 the NAO is a well known phenomenon and literature indicates that it has existed for the last millennium [Hurrel et al., 2003] and it is therefore important that climate models include this internal variability pattern, possibly even in their projections of the future climate conditions. In other parts of the world it can be internal variability like the Indian Monsoon, el niño / La niña-southern oscillation or the Pacific-North American Oscillation (PNA) that are important to capture on a large scale. On the contrary if the impacts study or the climate phenomena of interest is governed by processes going on at smaller spatial or temporal scales it is these processes that need to evaluated in the climate data before the choice of simulations and time-slices is carried out.

A climate model that is evaluated only against observations with respect to a given surface parameter like e.g. temperature could be concluded to perform well. However, the synoptic situations leading to capture the "correct" temperature field could still be wrong if the dynamics of the model is not analysed properly. For example high temperatures and clear sky in a climate simulation can both origins from the well known summertime blocking situations (e.g. the 2003 heat wave) and from e.g. advection of too dry air from the Atlantic Ocean in a longer period of time. This feature obviously affects the rest of the climate system since other features like e.g. transport of pollutants, depth of the mixing layer etc will definitely not be similar in the two synoptic situations, which emphasise the importance of evaluating variability in the climate simulation before using it in impact research.

In this study the EOF method has been used to identify the interval variability over a 340 year long period followed by an evaluation of the internal variability of each decade within this period. This leaves us with 34 different answers on how well the variability of the full period is represented in the individual decades and through surrogate data the decades that are

scientifically sound to use has been identified.

A PhD study is like any other research project a long realisation journey. In the current project four specific time-slices were chosen and used as input to the chemical transport work. During this work the idea arose to do a specific analysis of the four decades of choice. This means that the analysis of the 34 decades from 340 year period has been focused on these specific for time-slices and luckily it turned out that these four decades did capture the overall variability well enough to be used for the current purpose of studying impacts of climate change on air pollutants. Nevertheless it is far from always the case that the climate data used as input to chemical transport models is evaluated with respect to the specific research aims. Indeed picking a shorter period would seem to be inappropriate according to the present thesis work.

In most cases in the literature the climate simulations used are paid little attention and there are not any examples of references or descriptions of studies where an analysis like the current has been performed. For example Wu et al. [2008b,a]; Pye et al. [2009]; Lam et al. [2011] have all investigated the impacts of climate change over the US using the same model simulation and only three year long time-slices in this case using the GEOS-Chem model. They all refer to a study by Wu et al. [2007] where the climate data are thoroughly evaluated. In Wu et al. [2007] the NASA/GISS GCM 3 Rind et al. [2007] climate simulation of the two three-year long time-slices is evaluated with respect to inter-annual and seasonal variability in exactly these six years. The surrounding years are not accounted for and therefore this analysis is not sufficient according to the results of this thesis. Pye et al. [2009] mention in their paper that the climate simulations has been evaluated in ten-year time-slices and refers to Wu et al. [2007], but they only use three-year time-slices for the GEOS-Chem model and the ten-year analysis is not mentioned in the Wu et al. [2007] paper. Other experiments like e.g. Tagaris et al. [2007, 2008]; Liao et al. [2007, 2009] also use only three year long time-slices where as Katragkou et al. [2010]; Hedegaard et al. [2008]; Murazaki & Hess [2006]; Racherla & Adams [2008, 2009] all are examples of impact of climate change on air pollution levels based on time-slice experiments with ten-year long time-slices. Further Giorgi & Meleux [2007]; Meleux et al. [2007]; Engardt et al. [2009]; Andersson & Engardt [2010] are examples of impacts experiments with time-slices as long as 30-years.

The results of the current study can confirm that the four time-slices 1890s, 1990s, 2090s and 2190s do poses the same statistical features as the full 340-year long ECHAM5 climate simulation within a 10% significance level. Therefore, the four decades 1890s 1990s 2190s are considered statistical representative for their period and it is scientifically sound to use these as meteorological input to a chemical transport model. In the analysis leading to

this result, the first EOF of the full period was identified as the NAO pattern and it was assumed that the first EOF of each of the ten-year periods also represented the NAO. The analysis concluded that with a significant level of 10%, 88% of the 34 decades do simulate the variability of the full period sufficiently. Shortening of the time-slices to five years resulted in only 75% of the 68 five-year periods would be able to represent the variability correctly with a 10% significance level. These results depends on the particular climate simulation. It could be interesting to calculate these numbers for the NASA/GISS GCM 3 model Rind et al. [2007] simulations used for the studies including three-year time-slices [Lam et al., 2011; Pye et al., 2009; Wu et al., 2008b,a, 2007].

For simplicity it was assumed that the NAO-like pattern identified as the first EOF of the full period also was the one that would appear as the first EOF of each of the individual decades. If other natural variability patterns have been more dominating in one of the 34 decades than the NAO, this assumption has been violated. This is maybe the case for the decades that have small correlations in figure 12.6. A way to cope with this would be to recombine the variability contained in e.g. the first four EOFs of the full period and then carry out the analysis as done here. This would result in some answers that could explain 73% of the total variability instead of only the 35% explained by the first EOF.

The disadvantage of this method is, that the new combined first EOF would be completely mathematical constructed, meaning that no physical features can be identified by the pattern. Secondly it would imply another and similar assumption: That the first three EOF of the full period are the same three in each of the 34 decades. Alternative the method used comparing the z500 field and the surface ozone concentration 9.2 could be carried out 34 times comparing each decade with the full period for e.g. the first ten EOFs, which would result in a ten by ten matrix from where the EOF combinations correlating the most could be picked out for each decade. These specific chosen EOFs could be recombined into one EOF, which describes the sum of the Eigen values of selected EOFs. In this way the error related to the assumption of leaving out the information of the remaining EOFs would diminish. However, since the NAO-like pattern is a physical property, that can be identified in the EOF maps and similar results from analysis of observation can be found in the literature, the method of using only the first EOF has been used in this study. Moreover 35% is a relative high degree of explanation and it is well separated from the rest of the Eigen values.

Based on the four time-slices 1890s, 1990s, 2090s and 2190s the chemical transport model have been used to simulate the past, present and future impacts of climate change on the atmospheric ozone chemistry. Furthermore, the 2100 century, represented by the time-slices 1990s and 2090s, has been investigated with respect to the impacts of both climate change and

emissions changes on ozone, BC, total SO_4, total $PM_{2.5}$ and total nitrogen. In the following the results will be discussed specie by specie beginning with the results of ozone.

The impacts of climate change on the future ozone concentration have been investigated thoroughly in this thesis. The general conclusion is that the changes in the future ozone concentration due to climate change alone depend on two competitive effects; A decrease due to increased humidity where reactions between OH and CH_4 or CO acts as sink of ozone; or an increase in ozone due to increased biogenic emissions of VOC (isoprene) which together with high NO_x leads to increased ozone production. In general the ozone concentration is decreasing over the remote and semi-remote areas and in the urban areas with high NOx concentration the ozone contraction is estimated to increase in the future.

The Arctic marine areas differ from this overall conclusion by being a remote area experiencing a significant increase in ozone concentrations in the future. In section 6.2.5 several physical processes that can explain this result is given. However, whether it is a combination of decreased dry deposition, increased import from source areas cannot be determined by the simulations carried out here and it is the aim to study this further in the future. One possibility here is to use the tagging method described in paper IV [Brandt et al., 2011] and V included in this thesis.

Over Europe, East Asia and most of the U.S. (the south-eastern part) the ozone concentrations are estimated to increase due to impacts of climate change alone. This can be explained by the increased isoprene emission. The biogenic emission (in this case only isoprene) is calculated interactively in the model and is free to vary according to changes in the climate conditions. The fact that the future isoprene emissions are the controlling factor for impacts of climate change on the future ozone concentrations is confirmed in several earlier studies (see e.g. Hedegaard et al. [2008]; Lam et al. [2011]; Andersson & Engardt [2010]). However, Andersson & Engardt [2010] have recently carried out experiments showing that the dry deposition of ozone to vegetation might impact the future ozone concentrations even larger. Andersson & Engardt [2010] did some sensitivity studies where they changed the dry deposition to vegetation to be dependent on several meteorological parameters. When plants are exposed to climate change they change their ozone uptake and here soil moisture is one of the key parameters. When already dry areas, dries out even more the ozone uptake to vegetation stops and this decrease the dry-deposition to vegetation. Particularly Andersson & Engardt [2010] found that in Spain this process amounts for 80% of the total change in ozone.

In the current model setup the EMEP [Simpson et al., 2003] parameterisation has been used and the dry deposition to vegetation does depend on changes in meteorology, however the soil moisture dependence in the depo-

sition velocity for vegetation is set to one (as in the EMEP model) [Simpson et al., 2003]. This means, that the results presented in this thesis do not account for the soil moisture effect described by [Andersson & Engardt, 2010], which are a aim for the future work with the DEHM model.

Since isoprene is the single most important nmVOC for ozone production [Fowler et al., 2008] and several future studies have proven that the isoprene emissions are extremely sensitive to climate change and a governing parameter with respect to future ozone concentrations, a correct description of the isoprene emissions are important. Nevertheless to fully describe the emission of isoprene is a complicated task. Since isoprene emissions originates from vegetation it is depend on temperature and sunlight. However, investigations have shown that the emission rate of isoprene also depend on the ambient CO_2 and O_3 concentration, biomass, plant specie, leaf age, soil moisture, wind damage etc [Fowler et al., 2008], but there are large uncertainties connected to each of these variables. For example some studies argues that enhanced ambient CO_2 levels lead to increased isoprene emission due to the resulting increase in biomass and controversially other studies have shown that increased CO_2 levels impact the isoprene synthesis rate for some plant species and hence decrease the isoprene emissions [Fowler et al., 2008].

In this thesis the the IGAC-GEIA biogenic emission model [Guenther et al., 1995] has been used to calculate the isoprene emission dynamically in the DEHM model. Recently the more comprehensive Model of Emissions of Gases and Aerosols from Nature (MEGAN) has been implemented in the DEHM model. Comparison of the two model setups have shown that the domain-total annual isoprene emissions increase from 488 Tg/year in the IGAC-GEIA setup to 732 Tg/year applying MEGAN, which both are within the range 460-770 Tg/year found in previous studies by Guenther et al. [2006]; Arneth et al. [2008]; Ashworth et al. [2010]. Further, a comparison against the European measurements from the EMEP measuring network has shown that the ozone concentrations resulting from the MEGAN emissions are more consistent than the IGAC-GEIA setup in the Mediterranean area. The MEGAN model is much more sensitive to temperature rise than the IGAC-GEIA. [These results are carried out by A.Zare[1]] and are not yet published]. Applying the MEGAN model in the DEHM-climate setup inherently will affect the results of impacts from climate change on the future emissions levels and a comparison of this will be some of the aims in the future. Nevertheless in the study described in chapter 7 the total impact is expected to be less pronounced since most of the results to a large extent are dominated by the impact from chances in the future anthropogenic emission.

[1]Geophysics Institute, Tehran University, Iran and Department of Environmental Science, Aarhus University, Denmark

Future land use and land cover change are currently some of the main sources of uncertainties related to projection of the future the biogenic emissions. Climate change implies changes in vegetation type and distributions. However, there are several possibilities on how vegetation can respond to climate change. If the temperature rises, vegetation from low latitudes will possibly migrate to higher latitudes or the physiological properties of the vegetation will adapt to the new conditions, which are likely to change their emissions of isoprene. Secondly new vegetation types will appear and other will eradicate due to climate change. Finally population growth increase the need for crops and natural environments are likely to be changed into farm land resulting in e.g. deforestation and changes in crop species.

Currently the model setup used in this thesis only includes a static land use and land cover data set, which therefore is independent of climate change. In paper III [Skjøth et al., 2008] included in this thesis, we present a grided treespecie inventory over Europe, which is ready to use as input to a dynamic vegetation model. Such model can describe the evolution of vegetation due to changes the meteorological parameters and hence provide the current model setup with data on the future vegetation due to climate change.

Ganzeveld et al. [2010] have recently presented a study where they have compared responses in the atmospheric composition due to 2000 and 2050 land use and land cover. They used the chemistry-climate model EMAC which is based on the ECHAM5 climate model [Roeckner et al., 2003] and the Modular Earth Submodel System MESSy [Jöckel et al., 2005]. They found that the overall impact of land cover and land use changes on reactive gases (e.g. O_3) is small due to compensating effects of the involved process like e.g. foliage uptake, turbulent exchange and deforestation. However, they state that the results depend strongly on the applied parameterizations and the semi-empirical model used. Further several sub-grid scale processes are found which indicate that higher resolution is also important in the future. Further investigation of the individual processes related future land use and land cover changes and implementation of these processes in models would definitely be beneficial for the research in future atmospheric composition and climate change.

When including both the impacts of climate change and changes in anthropogenic emissions, the ozone concentration in the Arctic region were projected to remain nearly unchanged in the future despite the major reductions of the ozone precursor that led to a significant decrease in most of the source areas. Moreover it was found that impact of climate change was the absolutely dominating factor over the Arctic, which means that the signal from climate change and the signal from changes in anthropogenic emissions are opposing each other in this area. Since there are only a few sources of ozone precursors regionally within the Arctic the decrease due to emission change is most likely to be due to decreased import from the source

areas wherein precursor emissions are reduced in the future.

11 Conclusion and future perspectives

The aim of this thesis has been to investigate the impacts of climate change and changes in anthropogenic emissions on the future air pollution levels. A 340-year long climate simulated from the ECHAM5/MPI-OM model forced with the SRES A1B emission scenario has been used to drive the chemical transport model DEHM. Several DEHM simulations have been carried out with different combination of past, present and future meteorology and different emission data in order to investigate the individual impacts from climate change and emission change on the future air pollution levels in the northern hemisphere. Special emphasis has been put on the analysis of ozone and the related photochemistry with respect to the individual processes leading to the projected changes in ozone. The impacts of climate change on ozone and related precursors have been investigated over four decades (1890s, 1990s, 2090s and 2190s) representing 20th, 21st and 22nd century conditions. For the 21st century also the fate of BC, SO_4, total N and $PM_{2.5}$ have been analysed and besides a brief analysis of the processes leading to the projected chances the impact from climate change and emission change have been quantified for these species.

Furthermore, the climate simulation has been analysed with respect to decadal and inter-annual variability in order to verify the use of ten-year time-slices in the chemical transport model experiments. Several statistical methods have been applied on the Z500 geopotential height (gph) field in order to identity the internal variability of the large scale circulation in the ECHAM5/MPI-OM climate simulation. EOF analysis has been performed on the z500 gph field over the full period and over the four specific decades used as input to the CTM DEHM. In order to determine if ten-year long time-slices of the current simulation was sufficient in order to capture the inter-annual and decadal variability, surrogate data were created. It was found that the four decades (1890s, 1990s, 2090s and 2190s) did capture the internal variability of the full period within a significance level of 10%. Shortening of the length of these time-slices to 5 years decreased the number of time-slices that were able to capture the variability satisfactorily from

88% in the case of ten-year long time-slices to 75% in the case of five-year long time-slices.

Further it was shown that the Z500 gph field reasonably well could represent the variability in the surface ozone concentration. This was necessary to assume in order to perform the variability analysis since the ozone projection only were available in the four time-slices (1890s, 1990s and 2090s and 2190s) and not for the full period. However shown to be a reasonably assumption with a chance of 4 out 34 to have been choosing a abnormal decade to be part of the four time slices.

From literature it was found that minor attention have been put into analysis of the climate simulations when used to drive CTMs. The results based on the climate simulation in this thesis only relates to the specific climate simulation and similar analysis should be carried out in other studies before drawing any conclusions on impacts of climate change. The method described can be considered as an example of a recipe on how to analyse a climate simulation before using it as input to atmospheric models or other impact studies in general.

Turning the attention to the experiments carried out by the chemical transport model (DEHM). One DEHM simulation was carried out with constant year 2000 anthropogenic emissions and future 2090s meteorology projected by the ECHAM5/MPI-OM climate model. This was compared to a basis simulation of the 1990s with 2000 emissions and 1990s meteorology in order to identify the impacts of climate change alone on the future air pollution levels. Ozone and the related precursors was analysed thoroughly and it was found that the general surface ozone concentration will decrease in the future, but in the populated areas where sufficient NO_x is present, increased amount of BVOCs combined with increased humidity lead to increased ozone concentrations in the future.

Over the Arctic Ocean the ozone concentration was also found to increase which most likely is due to increased import from the source areas (where the O_3 increases) combined with a decrease in the dry deposition. Increases vertical transport of ozone could also contribute to the future ozone concentrations levels found at surface level. By the simulations carried out in this thesis, it is not possible to determine the individual contribution from these three processes and this will one of the aims of the future research possibly by application of the tagging method described in paper IV.

Next the RCP4.5 emission scenario was applied to project changes in O_3, BC, total SO_4, total $PM_{2.5}$ due to impacts from changed anthropogenic emissions. The impacts from changes in the anthropogenic emissions were further quantified relative to the impacts from climate change. The changes in anthropogenic emissions dominate in general over the signal from climate change. However in some cases the signal from climate change are opposing

the signal from the prescribed emission reductions, which implies that to obtain a certain reduction target in the future, additional reductions must be made in order to compensate from the opposing signal from climate change. This feature is known as "the climate penalty".

Specifically, the ozone concentration over the Arctic area is found to decrease a little in the future due to impact from both climate change and changes in the emission. Prescribed reduction of the ozone precursors in the source areas implies a significant decrease in the Arctic in the future. Oppositely do the impacts from climate result in a significant increase which is a little weaker than the decrease due to emissions reductions which minimize the overall effect to a minor decrease in the Arctic future ozone concentration.

In Western Europe it was found that future NO_x reductions results in a rise in the ozone concentration, due to the dominating urban chemical regime in this area. This means that that future air pollution control policies have to account for the opposing impact from climate change in order reach a specific reduction target. This implies that emissions of VOCs also needs to be considered as well in order to reduce both ozone and NO_x levels in the future in Europe.

With respect to the impact of climate change on ozone levels it was found that the effect from biogenic VOCs (isoprene), to a large extent is the controlling factor in the densely populated areas. Since the emissions of VOCs have such high impact, it is important to describe these correctly. The DEHM model have recently been setup with more comprehensive emission model MEGAN and so far analysis have shown that the estimated ozone levels in specifically the Mediterranean area have been improved significantly (A. Zare, AU, Personal communication). It is already known that the MEGAN model is much more sensitive to temperature change and therefore is likely to alter the results of impacts from climate change shown in this thesis. In the near future simulations will be carried out in order to determine this impact.

Another future aim is to include the effect from soil moisture in the dry deposition module by letting it be dependent on the applied meteorology. Furthermore, the land cover and land use data also play an important role with respect to the future emissions and by time it is the aim to included changes in land cover and land use possibly based on simulations provided by the LPJ-Guess vegetation model which is currently being developed.

The current resolution of the climate model data is relatively coarse ($1.5° \times 1.5°$). The DEHM model has the possibility of running in nested mode with a resolution of 50 km $\times$ 50 km over Europe, 16.7 km $\times$ 16.7 km over North-western Europe and finally a resolution of 5.6 km $\times$ 5.6 km over Denmark. It does not make sense to run DEHM in nested mode driven with the coarse resolution climate data from ECHAM5 and hence one of the aims

in the future is to use climate data from a regional climate model to drive DEHM including the nested domains as listed above. This will provide a better possibility to explore the impacts of climate and emission change over especially Europe and the Arctic and more sub-grid scale processes will be resolved.

Moreover, a study of climate change impacts on source-receptor relationships in the climate change model framework used in this thesis is planed, carried out using the tagging method, which accounts for the non-linear effects of chemistry. The tagging method is described in details in paper IV [Brandt et al., 2011] where a source-receptor study with present day (year 2006) climate and emission between North America and Europe is presented. The aim in the future is to investigate source-receptor relationship between the continents under changed climate conditions and with future anthropogenic emissions scenarios. This could e.g. provide information on the background ozone contribution from the other continents e.g. to Arctic and give an idea of the size of intercontinental transport of particles. This would provide all information that are needed to be accounted when specific air pollution targets are translated into emission legislations.

From a broader perspective there is no doubt that online models and Earth system models is the way forward. Since these can cover the two-way interaction between climate change and atmospheric composition. The different air pollutants known as the short-lived climate forcers (like e.g. ozone and black carbon) have impacts on the radiative forcings important for the climate system. Furthermore, the climate system has impacts on chemical, biological or physical changes changing the atmospheric composition. The feedback processes can only be captured in an online systems because of the dynamic nature of the forcing and responses. Nevertheless to build up a dynamic online systems covering several spheres in the climate system, off-line models are still an important and necessary tool. Off-line models are e.g. useful to identify, study and evaluate the individual processes involved. Studies like the one presented in this thesis can provide the knowledge needed for selecting suitable and validated parameterizations can be selected for application in the more comprehensive online models.

12 Acknowledgement

This PhD project has been a multi-institutional research project with fruitful cooperating between Department of Environmental Science, Faculty of Science Aarhus University (formerly known as the National Environmental Research Institute (NERI)) and Danish Climate Centre, Danish Meteorological Institute(DMI) and the Niels Bohr Institute, faculty of Science, University of Copenhagen. The majority of the work has been carried out in Department of Environmental Science, Aarhus University under supervision of Jørgen Brandt and and co-supervision of Jesper H. Christensen (AU). The analysis of the climate simulation has been carried out in the Danish Climate Centre with Jens Hesselbjerg Christensen as main supervisor in close cooperation with Peter Tjell (DMI) and Wilhelm May (DMI). At the Niels Bohr Institute, University of Copenhagen Aksel Walløe Hansen has been the formal supervisor of the project.

I would like to thank especially the PhD School of Science, Faculty of Science, University Of Copenhagen for financing 2/3 of third project[1] , The Danish Climate Centre, Danish Meteorological institute for financing 1/6 and Department of atmospheric Environment, Faculty of Science, Aarhus University for financing 1/6, my maternity leave etc. Further the PhD project has been part of the research of the Centre for Energy, Environment and Health, financed by The Danish Strategic Research Program on Sustainable Energy under contract no 2104-06-0027 and this is acknowledged as well.

This project has a long learning process scientifically as well as personally. Many people has been involved in the project and contributed with their knowledge and practical advice and I am grateful for your help during the last four years.

First I like to pay a special thanks to my supervisor at AU (Jørgen) for the the scientific guidance that he has giving through the last four years. However today I am even more grateful for his endless insistent on me completing this project despite the personal obstacles I have run into during the

[1] 1/3 from the former COGCI PhD-school (University of Copenhagen) and 1/3 from Faculty of Science, University of Copenhagen

last four years. Also I like to thank Jesper H. Christensen (AU) who always has been ready to answer any questions that I had.

I would like to thank my formal supervisor at the Niels Bohr Institute Aksel Walløe Hansen for guiding me through this work and supporting when things got difficult. Further I am especially grateful to Jens Hesselbjerg Christensen who has been an invaluable support within the last half year. I have learned a lot from his scientific experience and is grateful for the support on keeping me on the track in the final months of this project.

Moreover a special thank is paid to Willy May who have provided me the climate data used in the project and have supported me when I needed it through out the last four years and Peter Thejll who has been patient with me and taught me on statistics and programming. Further my colleagues in the DEHM group are acknowledged for their involvement in my project. A special thanks to Jeremy D. Silver, Camilla Geels, Allan Gross and Majbritt Ulrich for the professional and personal support you have given me.

Finally I would like to thank my Father, Inger, Hanne, Michael, Annette and Marianne for helping me and my family in all sorts of way. The three persons that supported me the most and suffer the most under this work is my son Magne (born 2008), my daughter Filippa (born 2005) and my Husband Morten. I am glad we did this together and finally it is over!

Bibliography

Andersson, C. & Engardt, M. (2010). European ozone in a future climate: Importance of changes in dry deposition and isoprene emissions. *J. Geophys. Res.*, page D02303.

Arneth, A., Monson, R. K., Schurgers, G., Niinemets, U., & Palmer, P. I. (2008). Why are estimates of global terrestrial isoprene emissions so similar (and why is this not so for monoterpenes)? *Atmos. Chem. Phys.*, **8**, 15 pp.

Ashworth, K., Wild, O., & Hewitt, C. N. (2010). Sensitivity of isoprene emissions estimated using megan to the time resolution of input climate data. *Atmos Phys Chem*, **10**, 1193–1201.

Asman, W. A. H., Sørensen, L. L., Berkowicz, R., Granby, K., Nielsen, H., Jensen, B., Runge, E., Lykkelund, C., Gryning, S. E., & Sempreviva, A. M. (1994). Dry deposition processes. Marine Research 35, Danish Environmental Protection Agency, Copenhagen,Denmark.

Baddour, O. & Kontongomde, H. (2007). The role of climatological normals in a changing climate. WCDMP 61, World Meteorological Organisation, Geneva. WMO-TD No. 1377.

Barnston, A. G. & Livezey, R. E. (1987). Classification, seasonality and persistence of low-frequency atmospheric circulation patterns. *Mon. Wea. Rev.*, **115**(1083-1126).

Brandt, J., Silver, J. D., Christensen, J. H., Frohn, L. M., Geels, C., Gross, A., Hansen, A. B., Hansen, K. M., Hedegaard, G. B., Skjøth, C. A., Villadsen, H., & Zare, A. (2011). An integrated model study for europe and north america using the danish eulerian hemispheric model with focus on intercontinental transport of air pollution. *Atmospheric Environment*, page pp.31. submitted to Atmos. Environ. May 2011.

Brasseur, G. P., Schulz, M., Granier, C., Schlesinger, M., Botzet, M., Roeckner, E., & Walters, S. (2005). Impacts of climate change on the future chemical composition of the global troposphere. *Journal of Climate*, **19**, 3932–3951.

Carmichael, G. & Dentener, F. (2007). Global and regional modelling -

future changes in source-receptor relationships. In:hemispheric transport of pollution, LRTAP Assessment report.

Christensen, J. H. (1997). The Danish Eulerian Hemispheric Model - A three-dimensional air pollution model used for the Arctic. *Atmospheric Environment*, **31**(24), 4169–4191.

Christensen, J. H., Hewitt, C., Busuioc, A., Chen, A., Gao, X., Held, I., Jones, R., Kolli, R. K., Kwon, W.-T., Laprise, R., Magaña Rueda, V., Mearns, L., Menendez, C. G., Räisänen, J., Rinke, A., Sarr, A., & Whetton, P. (2007). *Climate Change 2007: The Physical Science Basis*, contribution of working group i to the fourth assessment report of the intergovernmental panel on climate change Regional Climate Projections, pages 847–940. Cambridge University Press.

Clarke, L., Edmonds, J., Jacoby, H., Pitcher, H., Reilly, J., & Richels, R. (2007). Synthesis and assessment product 2.1 by the u.s. climate change science program and the subcommittee on global change research. subreport 2.1A, Department of Energy, Office of Biological and Environmental Research, Washington DC, USA. 154 pp.

Collins, W. J., Stevenson, D. S., Johnson, C., & Derwent, R. (1997). Tropospheric ozone in a global-scale 3-d lagragrian model and its response to NO_x emission controls. *´Journal of Atmopheric Chemistry*, **26**, 223–274.

Collins, W. J., Stevenson, D. S., Johnson, C., & Derwent, R. (1999). Role of convection in determining the budget of odd hydrogen in the upper troposphere. *Journal of geophysical research*, **104**, 26927–26941.

Cuvelier, C., Thunis, P., Vautard, R., Amann, M., Bessagnet, B., Bedogni, M., Berkowicz, R., Brandt, J., Brocheton, F., Builtjes, P., Denby, B., Douros, G., Graf, A., Hellmuth, O., Honore, C., Jonson, J., Kerschbaumer, A., de Leeuw, F., Moussiopoulos, N., Philippe, C., Pirovano, G., Rouil, L., Schaap, M., Stern, R., Tarrason, L., Vignati, E., Volta, L., White, L., Wind, P., & Zuber, A. (2007). Citydelta: A model intercomparison study to explore the impact of emission reductions in european cities in 2010. *Atmospheric Environment*, **41**(1), 189–207.

Dabdub, D. & Seinfeld, J. H. (1994). Numerical advective schemes used in air quality models–sequential and parallel implementation. *Atmospheric Environment*, **28**, 3369–3385.

Dawson, J. P., Racherla, P. N., Lynn, B. H., Adams, P. J., & Pandis, S. N. (2008). Simulating present-day and future air quality as climate changes: Model evaluation. *Atmospheric Environment*, **42**, 4551–4566.

Emberson, L., Simpson, D., Tuovinen, J.-P., Ashmore, M. R., & Cambridge, H. M. (2000). Towards a model of ozone deposition and stomatal uptake over europe, emep msc-w note 6/2000. MSC-W Note 6, EMEP.

Engardt, M., Bergström, R., & Andersson (2009). Climate and emission changes contributing to changes in near-surface ozone in europe over the coming decades - results from model studies. *Ambio*, **38**(8), 452–458.

Fall, R. (1999). *Reactive Hydrocarbons in the Atmosphere*, chapter Biogenic Emissions of Volatile Organic Compounds from Higher Plants, pages 41–96. Academic Press, San Diego, California.

Forkel, R. & Knoche, R. (2006). Regional climate change and its impact on photooxidant concentrations in southern germany: Simulations with a coupled regional climate-chemistry model. *Journal of Geophysical Research*, **111**, D12302. doi:10.1029/2005JD006748.

Fowler, D., Amann, M., Anderson, R., Ashmore, M., Cox, P., M, M. D., Derwent, D., Grennfelt, P., Hewitt, N., Hov, Ø., Jenkin, M., Kelly, F., Liss, P., Pilling, M., Pyle, J., Slingo, J., & Stefenson, D. (2008). Ground-level ozone in the 21st century: future trends, impacts and policy implications. Science Policy Report 15/08, The Royal Society. pp. 148.

Frohn, L. M. (2004). *A study of long-term high-resolution air pollution modelling*. Ph.D. thesis, University of Copenhagen and National Environmental Research Institute.

Frohn, L. M., Christensen, J. H., Brandt, J., & Hertel, O. (2001). Development of a high resolution integrated nested model for studying air pollution in denmark. *Physics and Chemistry of the Earth*, **26**(PART B), 769–774.

Frohn, L. M., Christensen, J. H., & Brandt, J. (2002a). Development and testing of numerical methods for two-way nested air pollution modelling. *Physics and Chemistry of the Earth*, **27**, 1487–1494.

Frohn, L. M., Christensen, J. H., & Brandt, J. (2002b). Development of a high-resolution nested air pollution model. the numerical approach. *Journal of Computational Physics*, **179**(1).

Ganzeveld, L., Bouwman, L., Stehfest, E., van Vuuren, D. P., Eickhout, B., & Lelieveld, J. (2010). Impact of future land use and land cover changes on atmospheric chemistry-climate interactions. *J Geophys Res*, **115**, D23301.

Geels, C., Brandt, J., Christensen, J., Frohn, L., & Hansen, K. (2005). Long-term calculations with a comprehensive nested hemispheric air pollution transport model. *Advances in Air Pollution Modeling for Environmental Security*, **54**, 185–196.

Giorgi, F. & Meleux, F. (2007). Modelling the regional effects of climate change on air quality. *C. R. Geosci*, **339**, 721–733.

Goldstein, A. H. & Galbally, I. E. (2007). Known and unexplored organic constituents in the earths atmosphere. *Environ. Sci. Technol.*, **41**(5), 1514–1521.

Goosse, H., Barriat, P. Y., Lefebvre, W., Loutre, M. F., , & Zunz, V. (2009). Introduction to climate dynamics and climate modelling. online.

Graedel, T., Bates, T., Bouwman, A., Cunnold, D., Dignon, J., Fung, I., Jacob, D., Lamb, B., Logan, J., Marland, G., Middleton, P., Pacyna, J., Placet, M., & Veldt, C. (1993). A compilation of inventories of emissions to the atmosphere. *Global Biogeochem. Cycl.*, **7**, 1–26.

Guenther, A., Hewitt, C., Erickson, D., Fall, R., Geron, C., Graedel, T., Harley, P., Klinger, L., Lerdau, M., McKay, W., Pierce, T., Scholes, B., Steinbrecher, R., Tallamraju, R., Taylor, J., & Zimmerman, P. (1995). A global-model of natural volatile organic-compound emissions. *Journal of Geophysical Research*, **100**, 8873–8892.

Guenther, A., Karl, T., Harley, P., Wiedinmyer, C., Palmer, P. I., & Geron, C. (2006). Estimates of global terrestrial isoprene emissions using megan (model of emissions of gases and aerosols from nature. *Atmos. Chem. Phys.*, **6**, 3181–3210.

Hansen, K. M., Christensen, J. H., Brandt, J., Frohn, L. M., Villadsen, H., Geels, C., Skjøth, C. A., Gross, A., Hedegaard, G. B., Sørensen, A.-L., Silver, J. D., Hansen, A. B., & Zare, A. (2011). Two decades of european air quality. *to be submitted to Atmospheric Chemistry and Physics autum 2011.* In preparation.

Hedegaard, G. B. (2007). Impacts of climate change on air pollution levels in the northern hemisphere. Technical report 240, National Environmental Research Institute, Aarhus University, Frederiksborgvej 399, P.O. Box 358, 4000 Roskilde, Denmark.

Hedegaard, G. B. (2009). *Air Pollution - from a local to a global perspective*, chapter Natural Sources, pages 163–174. Polyteknisk Forlag, Danmark, Anker Engelunds Vej 1, Dk-2800 Lyngby, 1 edition.

Hedegaard, G. B., Brandt, J., Christensen, J. H., Frohn, L. M., Geels, C., Hansen, K. M., & Stendel, M. (2008). Impacts of climate change on air pollution levels in the northern hemisphere with special focus on europe and the arctic. *Atmospheric Chemistry and Physics*, **8**, 3337–3367.

Hedegaard, G. B., Gross, A., Christensen, J. H., May, W., Skov, H., Geels, C., Hansen, K. M., & Brandt, J. (2011). Modelling the impacts of climate change on tropospheric ozone over three centuries. *Atmospheric Chemistry and Physics Discussions*, **11**, 6805–6843.

Hertel, O., Christensen, J., Runge, E. H., Asman, W. A. H., Berkowicz, R., Hovmand, M. F., & Hov, ø. (1995). Development and testing of a new variable scale pollution model - acdep. *Atmos. Environ.*, **29**(11), 1267–1290.

Hjorth, J. & Raes, F. (2009). Answers to the gothenburg questions. Accent second policy-driven synthesis, ACCENT secretariat, Universita di Urbino,Urbino, Italy.

Hogrefe, C., Lynn, B., Civerolo, K., Ku, J.-Y., Rosenthal, J., Rosenzweig, C., Goldberg, R., Gaffin, S., Knowlton, K., & Kinney, P. (2004). Simulating changes in regional air pollution over the eastern United States due to changes in global and regional climate and emissions. *Journal of Geophysical Research*, **109**, D22301, doi 10.1029/2004JD004690.

Hurrel, J. W., Kushnir, Y., Ottesen, G., & Visbeck, M., editors (2003). *The North Atlantic Oscillation: Climatic significance and environmental impact*. Number 134 in Geophysical Monograph. AGU, 2000 Florida Avenue, N.W. Washington, DC 20009.

Jacob, D. J. & Winner, D. A. (2009). Effects of climate change on air quality. *Atmos. Environ.*, **43**, 51–63.

Jöckel, P., Sander, R., Kerkweg, A., Tost, H., & Lelieveld, J. (2005). The modular earth submodel system (messy) - a new approach towards earth system modeling. *Atmos Chem Phys*, **5**, 433–444.

Johnson, C., Stevenson, D., Collins, W., & Derwent, R. (2001). Role of climate feedback on methane and ozone studied with a coupled ocean-atmosphere-chemistry model. *Geophysical Research Letter*, **28**(9), 1723–1726.

Jungclaus, J. H., Keenlyside, N., Botzet, M., Haak, H., Luo, J. J., Latif, M., Marotzke, J., Mikolajewicz, U., & Roeckner, E. (2006). Ocean circulation and tropical variability in the coupled model echam5/mpi-om. *Journal of Climate*, **19**, 3952–3972.

Katragkou, E., Zanis, P., Tegoulias, I., Melas, D., Kioutsioukis, I., Krüger, B. C., Huszar, P., Halenka, T., & Rauscher, S. (2010). Decadal regional air quality simulations over europe in present climate: near surface ozone sensitivity to external meteorological forcing. *Atmos. Chem. Phys.*, **10**, 11805–11821.

Lam, Y. F., Fu, J. S., & Mickley, L. J. (2011). Impacts of future climate change and effects of biogenic emissions on surface ozone and particulate matter concentartions in the united states. *Atmos. Chem. Phys.*, **11**, 4789–4806. doi:10.5194/acp-11-4789-2011.

Lambert, J. D. (1991). *Numerical methods for ordinary differential systems: the initial value problem*. John Wiley & Sons Ltd., 1 edition.

Langner, J., Bergstrøm, R., & Foltescu, V. (2005). Impact of climate change on surface ozone and deposition of sulphur and nitrogen in europe. *Atmospheric Environment*, **39**, 1129–1141.

Liao, H., Zhang, Y., Chen, W.-T., Raes, F., & Seinfeld, J. H. (2009). Effect of chemistry-aerosol-climate coupling on predictions of future climate and future levels of tropospheric ozone and aerosols. *J. Geophys. res.*, **114**, D10306.

Liao, K., Tagaris, E., Manomaiphiboon, K., Napelenok, S. L., Woo, J., He, S., Amar, P., & Russell, A. G. (2007). Sensitivities of ozone and fine particular matter formation to emissions under the impact of potential future climate change. *Environ. Sci. Technol.*, **41**, 8355–8361.

Liao, K., Tagaris, E., Russel, R. G., Amar, P., He, S., Manomaiphiboon, K., J., & Woo, J. (2010). Cost analysis of impacts of climate change on regional air quality. *J. Air and Waste Manage Association*, **60**, 195–2003.

Lollar, B. S., editor (2007). *Environmental Geochemistry, Treatise on geochemistry*, volume 9. Elsevir.

Lorenz, E. N. (1951). Seasonal and irregular variations of the northern hemisphere sea-level pressure profile. *J. Meteorol.*, **8**, p52–59.

Lorenz, E. N. (1956). Empirical orthogonal functions and statistical weather prediction. Technical report, Statistical Forecast Project Report 1, MIT, Dept. of Meteor. 49 pp.

Mareckova, K., Wankmueller, R., Anderl, M., Muik, B., Poupa, S., & Wieser, M. (2008). Inventory review 2008: Emission data reported under the lrtap convention and nec directive. status of gridded data. Technical report, EMEP Centre on Emission Inventories and Projections.

Marsland, S. J., Haak, H., Jungclaus, J. H., Latif, M., & Roske, F. (2003). The max-planck-institute global ocean/sea ice model with orthogonal curvilinear coordinates. *Ocean Modelling*, **5**, 91–127.

May, W. (2008). Climatic changes associated with a global 2 degrees c-stabilization scenario simulated by the echam5/mpi-om coupled climate model. *Climate Dynamics*, **31**, 283–313.

McRae, G., Goodin, W., & Seinfeld, J. (1982). Numerical solution of the atmospheric diffusion equations for chemical reacting flows. *Journal of Computational Physics*, **45**, 1–42.

Meehl, G. A., Stocker, T. F., Collins, W. D., Friedlingstein, P., Gaye, A. T., Gregory, J. M., Kitoh, A., Knutti, R., Murphy, J. M., Noda, A., Raper, S. C. B., Watterson, I. G., Weaver, A. J., & Zhao, Z.-C. (2007a). *Climate Change 2007: The Physical Science Basis*, contribution of working group i to the fourth assessment report of the intergovernmental panel on climate change Global Climate Projections, pages 747–846. Cambridge University Press, Cambridge, United Kingdom and New York, NY, USA.

Meehl, G. A., Covey, C., Delworth, T., Latif, M., McAvaney, B., Mitchell, J. F. B., Stouffer, R. J., & Taylor, K. E. (2007b). The wcrp cmip3 multimodel dataset: A new era in climate change research. *Bulletin of the American Meteorological Society*, **88**, 1383–1394.

Meleux, F., Solmon, F., & Giorgi, F. (2007). Increase in summer european ozone amounts due to climate change. *Atmos. Environ.*, **41**, 7577–7587.

Monastersky, R. (2009). A burden beyond bearing. *Nature*, **458**, 1091–1094.

Moss, R., Babiker, M., Brinkman, S., Calvo, E., Carter, T., Edmonds, J., Elgizouli, I., Emori, S., Erda, L., K. Hibbard, R. J., Kainuma, M., Kelleher, J., Lamarque, J. F., Manning, M., Matthews, B., Meehl, J., Meyer, L., Mitchell, J., Nakicenovic, N., ONeill, B., Pichs, R., Riahi, K., Rose, S., Runci, P., Stouffer, R., van Vuuren, D., Weyant, J., Wilbanks, T., van Ypersele, J. P., & Zurek, M. (2008). Towards new scenarios for analysis of emissions, climate chnage, impacts and response strategies. Technical summary, IPCC, Geneva. 132 pp.

Moss, R. H., Edmonds, J. A., Hibbard, K. A., Manning, M. R., Rose, S. K., van Vuuren, D. P., Carter, T. R., Emori, S., Kainuma, M., Kram, T., Meehl, G. A., Mitchell, J. F. B., Nakicenovic, N., Riahi, K., Smith, S. J., Stouffer, R. J., Thomson, A. M., Weyant, J. P., & Wilbanks, T. J. (2010). The next generation of scenarios for climate change research and assessment. *Naure*, **463**(11), 747–756. isbn:doi:10.10338/nature08823.

Murazaki, K. & Hess, P. (2006). How does climate change contribute to surface ozone change over the united states. *Journal of Geophysical Research*, **111**, D05301. 10.1029/2005JD005873.

Nakicenovic, N., Alcamo, J., Davis, G., de Vries, B., Fenhann, J., Gaffin, S., Gregory, K., Grübler, A., Jung, T., Kram, T., Rovere, E. L., Michaelis, L., Mori, S., Morita, T., Pepper, W., Pitcher, H., Price, L., Riahi, K., Roehrl, A., Rogner, H.-H., Sankovski, A., Schlesinger, M., Shukla, P., Smith, S., Swart, R., van Rooijen, S., Victor, N., & Dadi, Z. (2000). *Special Report on Emission Scenarios: a special report of Working Group III of the Intergovernmental Panel on Climate Change*. Cambridge University Press, New York, NY (US), United States.

Olivier, J., Bouwman, A., van der Maas, C., Berdowski, J., Veldt, C., Bloos, J., Visschedijk, A., Zandveld, P., & Haverlag, J. (1996). Description of EDGAR Version 2.0: A set of global emission inventories of greenhouse gases and ozone-depleting substances for all anthropogenic and most natural sources on a per country basis and on 1 degree x 1 degree grid. RIVM report, TNO MEP report R96/119, RIVM, Bilthoven.

Olivier, J. G. J. & Berdowski, J. J. M. (2001). *The Climate System*, chapter Global emissions sources and sinks, pages 33–78. A. A. Balkema Publishers, Lisse, The Netherlands.

Pachauri, R. K. & Reisinger (2007). Climate change 2007: Synthesis report. Contribution of working group i, ii and iii to the fourth assessment report of the intergovernmental panel on climate change, IPCC.

Paulot, F., Crounse, J. D., Kjaergaard, H. G., Kürten, A., St. Clair, J. M., Seinfeld, J. H., & Wennberg, P. O. (2009). Unexpected epoxide formation in the gas-phase photooxidation of isoprene. *Science*, **325**(5941), 730–733.

Pearson, K. (1902). On lines and planes of closetbfit to sytems of points in space. *Phil. Mag.*, **2**, 559–572.

Pepper, D., Kern, C., & Long, J. P. (1979). Modelling the dispersion of atmospheric pollution using cubic splines and chapeau functions. *Atmospheric Environment*, **13**, 223–237.

Pye, H. O. T., Liao, H., Mickley, L. J., Jacob, D. J., & Henze, D. K. (2009). Effects of changes in climate and emissions on future sulfate-nitrate-ammonium aerosol levels in the united states. *Journal of Geoph. Research*, **114**(D01205), 1–18. doi:10.1029/2008JD010701.

Racherla, P. N. & Adams, P. J. (2008). The respons of surface ozone to climate chnage over eastern united states. *Atmos. Chem. Phys.*, **8**, 871–885.

Racherla, P. N. & Adams, P. J. (2009). U.s. ozone air quality under changing climate and antropogenic emissions. *Environ Sci. Technol.*, **43**, 571–577.

Raes, F., Liao, H., Chen, W.-T., & Seinfeld, J. H. (2010). Atmopheric chemistry-climate feedbacks. *J Geophys. Res.*, **115**, D12121.

Rind, D., Lerner, J., Jonas, J., & McLinden, C. (2007). The effects of resolution and model physics on tracer transports in the nasa goddard institute for space studies general circulation models. *J. Geophys. Res.*, **112**.

Roeckner, E., Bauml, G., Bonaventura, L., Brokopf, R., Esch, M., Giorgetta, M., Hagemann, S., Kirchner, I., Kornblueh, L., Manzini, E., Rhodin, A., Schlese, U., Schulzweida, U., & Tompkins, A. (2003). The atmospheric general circulation model echam5, part i. Report 249, Max-Planck-Institute für Meteorologie, Hamburg, Germany.

Roeckner, E., Brokopf, R., Esch, M., Giorgetta, M., Hagemann, S., Kornblueh, L. Manzini, E., Schlese, U., & Schulzweida, U. (2006). Sensitivity of simulated climate to horizontal and vertical resolution in the echam5 atmosphere model. *Journal of Climate*, **19**, 3771–3791.

Rogerson, P. A. (2010). *Statistical methods for geography -A students guide.* SAGE Publications Inc., 1 Olivers Yard, 55 City Road, London ECIY 1SP, 3 edition.

Rollins, A. W., Kiendler-Scharr, A., Fry, J. L., Brauers, T., Brown, S. S., Dorn, H.-P., Dube, W. P., Fuchs, H., Mensah, A., Mentel, T. F., Rohrer, F., Tillmann, R., Wegener, R., Wooldridge, P. J., & Cohen, R. C. (2009). Isoprene oxidation by nitrate radical: alkyl nitrate and secondary organic aerosol yields. *Atmos. Chem. Phys.*, **9**, 6685–6703.

Seinfeld, J. H. & Pandis, S. P. (2006). *Atmospheric Chemistry and Physics: From Air Pollution to Climate Change.* John Wiley & Sons, Inc., Hoboken, New Jersey, US.

Simpson, D., Fagerli, H., Jonson, J., Tsyro, S., Wind, P., & Touvinen, J.-P. (2003). Transboundary acidification, eutrophication and ground level ozone in europe, part i. Unified emep model description emep msc-w, Norwegian Meteorological Institute.

Skjøth, C. A., Geels, C., Hvidberg, M., Hertel, O., Brandt, J., Frohn, L. M., Hansen, K. M., Hedegaard, G. B., Christensen, J. H., & Moseholm, L. (2008). An inventory of tree species in europe-an essential data input for air pollution modelling. *Ecological Modelling*, **217**(3-4), 292–304.

Skov, H., Hjorth, J., Lohse, C., Jensen, N. R., & Restelli, G. (1992). Products and mechanisms of the reactions of the nitrate radical (NO_3) with isoprene, 1,3-butadiene and 2,3-dimethyl-1,3-butadiene in air. *Atmos. Environ.*, **26**(15), 2771–2783.

Smith, S. & Wigley, T. (2006). Multi-gas forcing stabilization with the minicam. *Energy Journal*, **Special issue**(3), 373–391.

Spiegel, M. R. (1992). *Theory and problems of statistics*. Schaums Outline Series. McGraw-Hill, secound edition.

Stevenson, D., Hannachi, A., & ONeill, A. (2004). On the existence of multiple climate regimes. *Q.J.R. Meteorol Soc.*, **130**, 583–605. doi:1256/qj.02.146.

Stevenson, D., Doherty, R., Sanderson, M., Johnson, C., & Derwent, D. (2005). Impacts of climate change and variability on tropospheric ozone and its precursors. *Faraday Discuss.*, **130**, 41–57.

Storch, H. V. & Zwiers, F. W. (1999). *Statistical Analysis in climate Research*. Cambridge University Press. 484 pp.

Stott, P. A., Stone, D. A., & Allen, M. R. (2004). Human contribution to the european heatwawe of 2003. *Nature*, **432**, 610–614.

Strand, A. & Hov, Ø. (1994). A two diamentionalla global study of the tropospheric ozone production. *J. Geophys. res.*, **99**, 22877–22895.

Tagaris, E., Manomaiphiboon, K., Liao, K.-J., Leung, L. R., Woo, J.-H., He, S., p. Amar, & Russel, A. G. (2007). Impacts of global climate change and emissions on regional ozone and fine particulate matter concentrations over the united states. *Journal Geophys. Research*, **12**(D14312), 1–11. doi:10.1029/2006JD008262.

Tagaris, E., Liao, K.-J., Manomaiphiboon, K., He, S., Woo, J.-H., Amar, P., & Russell, A. G. (2008). The role of climate and emission changes in future air quality oversouthern canada and northern mexico. *Atmos. Chem. Phys.*, **8**, 3973–3983.

Tang, Y., Carmichael, G. R., Thongboonchoo, N., Chai, T., Horowitz, L. W., Pierce, R. B., Al-Saadi, J. A., Pfister, G., Vukovich, J. M., Avery, M. A., Sachse, G. W., Holloway, T. B. R. J. S., Atlas, E. L., Flocke, F. M., Weber, R. J., Huey, G., Dibb, J. E., Streets, D. G., & Brune, W. H. (2007). Influence of lateral boundary conditions on regional air quality prediction: A multiscale study coupling regional and global chemical transport models. *J. geophys res*, **112**, D10S18.

Taylor, K. E., Stouffer, R. J., & Meehl, G. A. (2009). A summary of the cmip5 experiment design. Technical report, Program for Climate Model Diagnosis and Intercomparison (PCMDI).

Unger, N., Menon, S., Koch, D. M., & Shindell, D. T. (2009). Impacts of aerosol-cloud interactions on past and future chages in tropospheric composition. *Atmos. Chem. Phys.*, **9**, 4115–4129.

Valcke, S., Caubel, A., Declat, D., & Terray, L. (2003). Oasis ocean atmosphere sea ice soil users guide. Tech. Rep. TR/CMGC/03/69, CERFACS, Toulouse, France.

Van Loon, M., Vautard, R., Schaap, M., Bergstrom, R., Bessagnet, B., Brandt, J., Builtjes, P. J. H., Christensen, J. H., Cuvelier, C., Graff, A., Jonson, J. E., Krol, M., Langner, J., Roberts, P., Rouil, L., Stern, R., Tarrason, L., Thunis, P., Vignati, E., White, L., & Wind, P. (2007). Evaluation of long-term ozone simulations from seven regional air quality models and their ensemble. *Atmospheric Environment*, **41**, 2083–2097.

Vautard, R. & Hauglustaine, D. (2007). Impact of global climate change on regional air quality: Introduction to the thematic issue. *C. R. Geosci.*, **339**, 703–708.

Vautard, R., Van Loon, M., Schaap, M., Bergstrom, R., Bessagnet, B., Brandt, J., Builtjes, P. J. H., Christensen, J. H., Cuvelier, C., Graff, A., Jonson, J. E., Krol, M., Langner, J., Roberts, P., Rouil, L., Stern, R., Tarrason, L., Thunis, P., Vignati, E., White, L., & Wind, P. (2006). Is regional air quality model diversity representative of uncertainty for ozone simulation? *Geophysical Research Letters*, **33**, p. L24818.

Vautard, R., Schaap, M., Bergstrom, R., Bessagnet, B., Brandt, J., Builtjes, P. J. H., Christensen, J. H., Cuvelier, C., Foltescu, V., Graff, A., Kerschbaumer, A., Krol, M., Roberts, P., Rouil, L., Stern, R., Tarrason, L., Thunis, P., Vignati, E., & Wind, P. (2009). Skill and uncertainty of a regional air quality model ensemble. *Atmospheric Environment*, **43**, 4822–4832.

Vestreng, V. (2001). Emission data reported to UNECE/EMEP: Evaluation of the spatial distribution of emission. EMEP/MSC-W Note 1/01, EMEP.

Walsch, J. E., Chapman, W. L., Romanovsky, V., Christensen, J. H., & Stendel, M. (2008). Global climate model performance over alaska and greenland. *Journal of Climate*, **21**, 6156–6174. doi:10.1175/2008JCLI2163.1.

Weaver, C. P., Liang, X.-Z., Zhu, J., Adams, P., Amar, P., Avise, J., Caughey, M., Chen, J., Cohen, R., Cooter, E., Dawson, J., Gilliam, R., Gilliland, A., Goldstein, A., Grambsch, A., D. Grano and, A. G., Gustafson, W., Harley, R., He, S., Hemming, B., Hogrefe, C., Hunt, H.-C. H. S., Jacob, D., Kinney, P., Kunkel, K., Lamarque, J.-F., Lamb, B., Larkin, N., Leung, L., Liao, K.-J., Lin, J.-T., Lynn, B., Manomaiphiboon,

K., Mass, C., McKenzie, D., Mickley, L., ONeill, S., Nolte, C., Pandis, S., Racherla, P., Rosenzweig, C., Russell, A., Salathé, E., Steiner, A., Tagaris, E., Tao, Z., Tonse, S., Wiedinmyer, C., Williams, A., Winner, D., Woo, J.-H., Wu, S., & Wuebbles, D. (2009). A preliminary synthesis of modeled climate change impacts on u.s. regional ozone concentrations. *Am. Meterol. Soc.*, **90**, 1843–1863.

Wise, M. A., Calvin, K. V., Thomson, A., Clarke, L. E., Bond-Lamberty, B., Sands, R. D., Smith, S. J., Janetos, A. C., & Edmonds, J. A. (2009). Implications of limiting co2 concentrations for land use and energy. *Science*, **324**, 1183–1186.

Wu, S., Mickley, L., Jacob, D., Logan, J., Yantosca, R., & Rind, D. (2007). Why are there large differences between models in global budgets of tropospheric ozone? *J. Geophys. Res.*, **112**.

Wu, S., Mickley, L. J., Jacob, D. J., Rind, D., & Streets, D. G. (2008a). Effects of 2000–2050 changes in climate and emissions on global tropospheric ozone and the policy-relevant background ozone in the united states. *J. Geophys.*, **113**.

Wu, S., Mickley, L. J., Leibensperger, E. M., Jacob, D. J., Rind, D., & Streets, D. G. (2008b). Effects of 2000–2050 global change on ozone air quality in the united states. *J. Geophys. Res.*, **113**.

Zhang, Y. (2008). Online-coupled meteorology and chemistry models: history, current status, and outlook. *Atmos Chem. Phys.*, **8**, 2895–2932.

Appendix

A: Extra Figures

12.0.1 The first EOF of 34 decades

Figure 12.1: 1st EOF

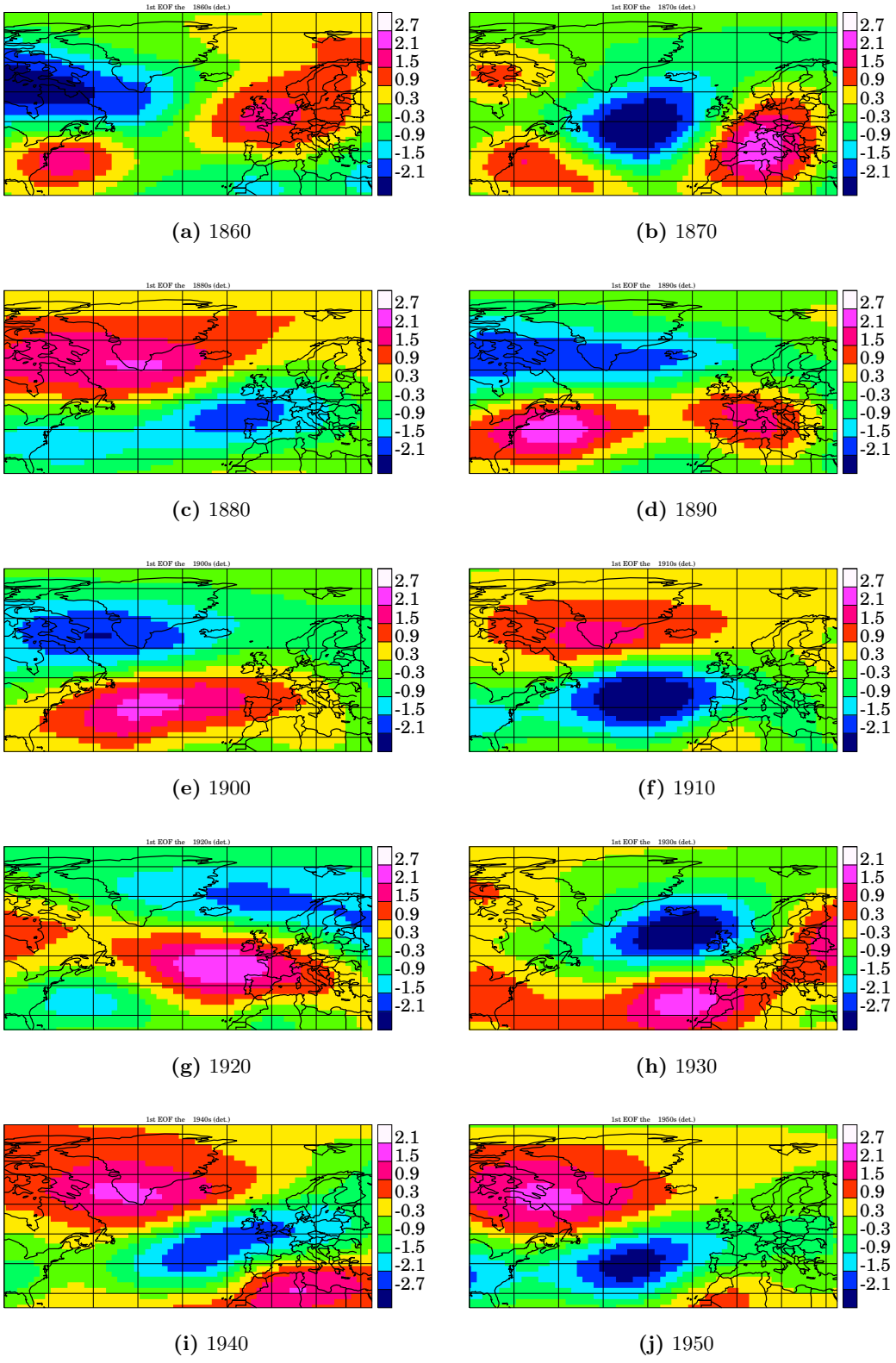

(a) 1860 **(b)** 1870

(c) 1880 **(d)** 1890

(e) 1900 **(f)** 1910

(g) 1920 **(h)** 1930

(i) 1940 **(j)** 1950

Figure 12.2: 1st EOF, continued....

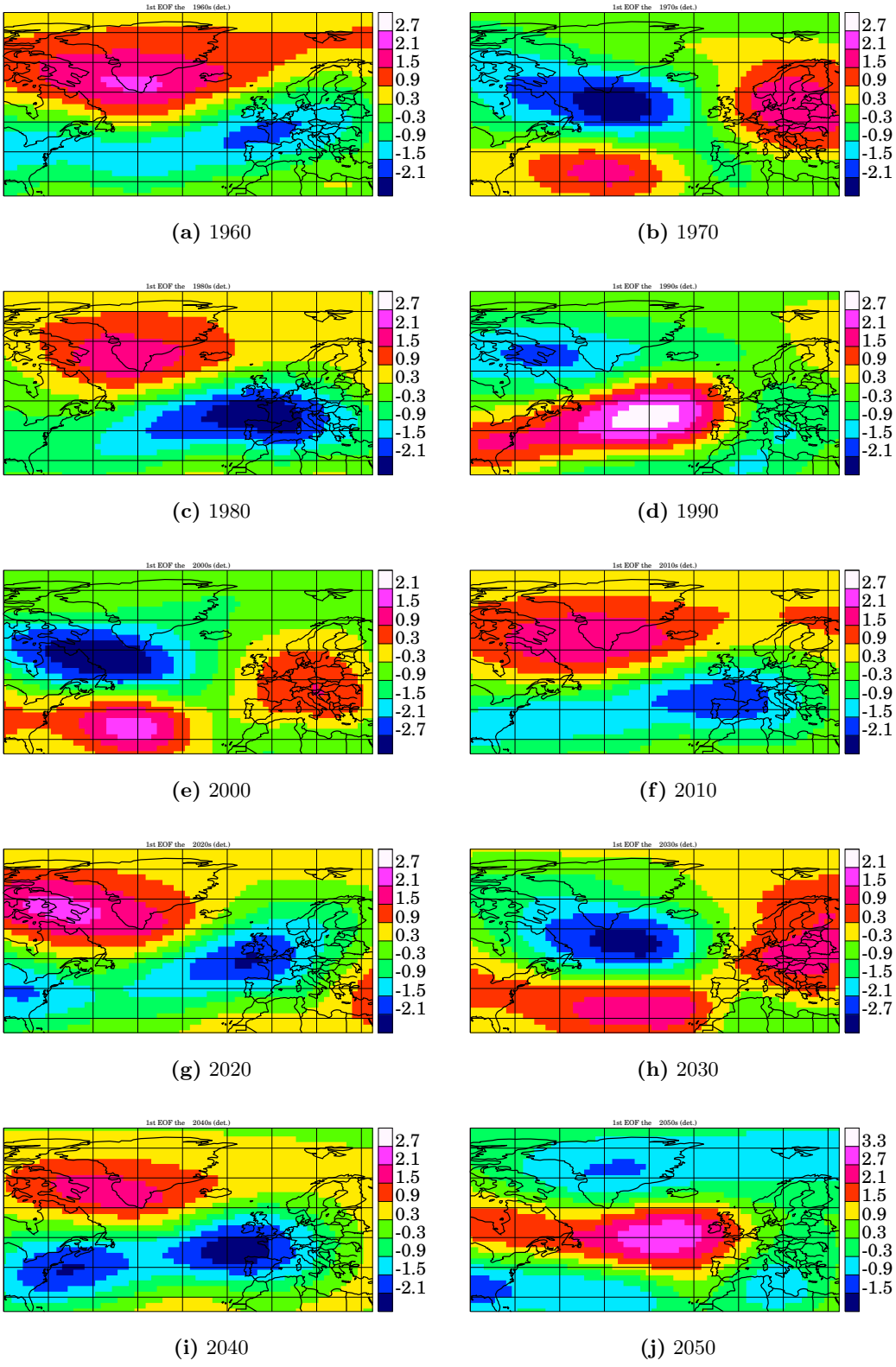

(a) 1960 **(b)** 1970

(c) 1980 **(d)** 1990

(e) 2000 **(f)** 2010

(g) 2020 **(h)** 2030

(i) 2040 **(j)** 2050

Figure 12.3: 1st EOF, continued....

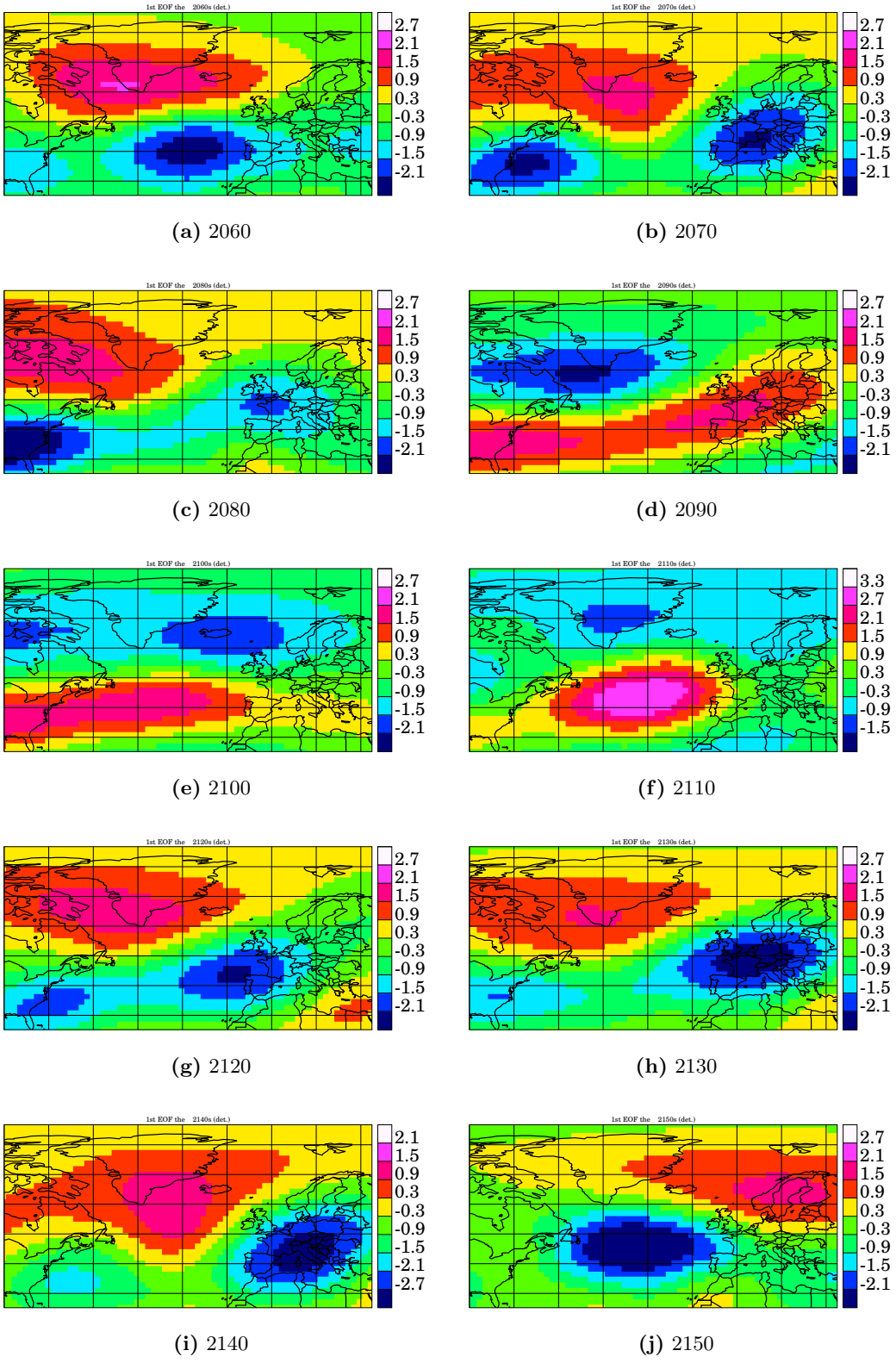

(a) 2060 **(b)** 2070

(c) 2080 **(d)** 2090

(e) 2100 **(f)** 2110

(g) 2120 **(h)** 2130

(i) 2140 **(j)** 2150

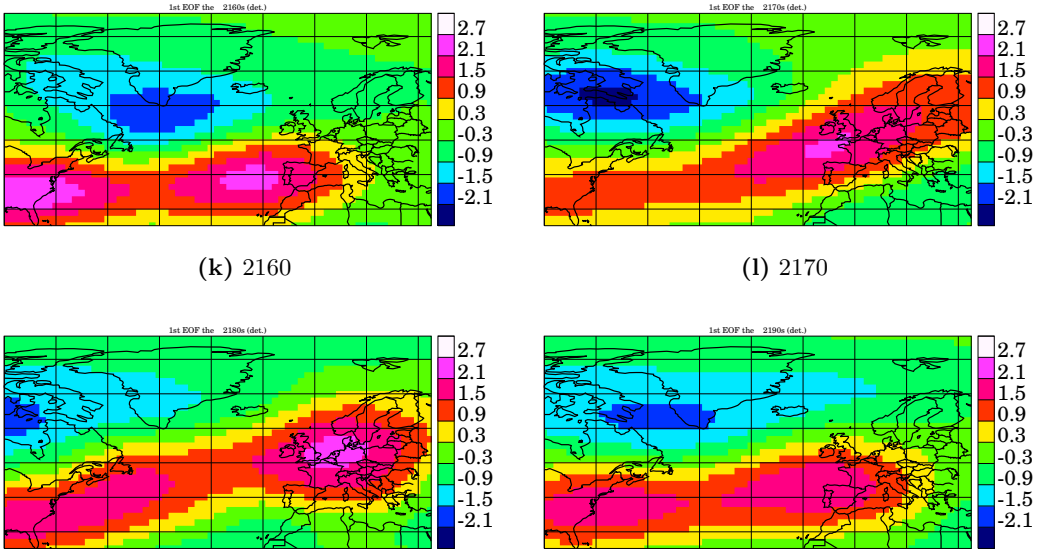

(k) 2160 **(l)** 2170

(m) 2180 **(n)** 2190

Figure 12.4: 1st EOF of the individual decades

12.0.2 Supplementary figures for chapter 9

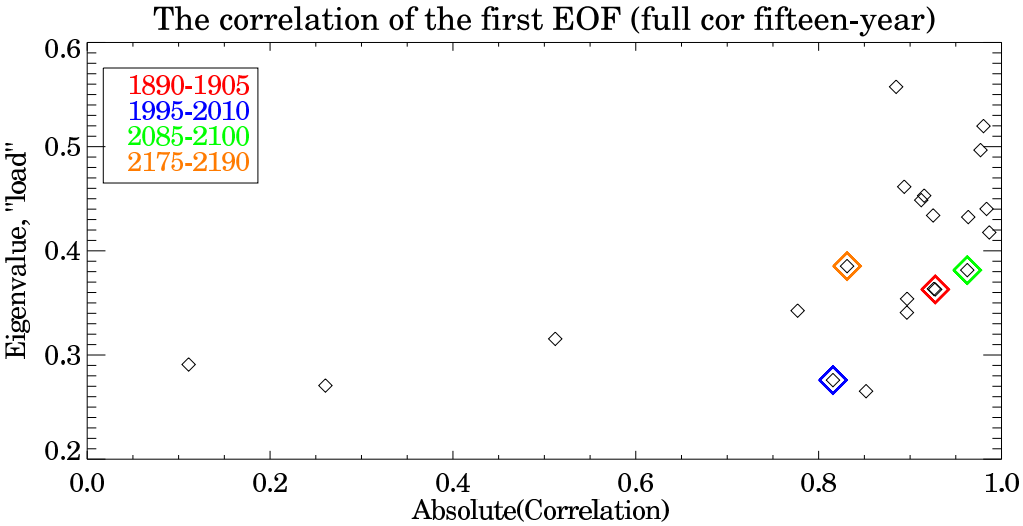

Figure 12.5: Fifteen-year periods correlation with the full period.

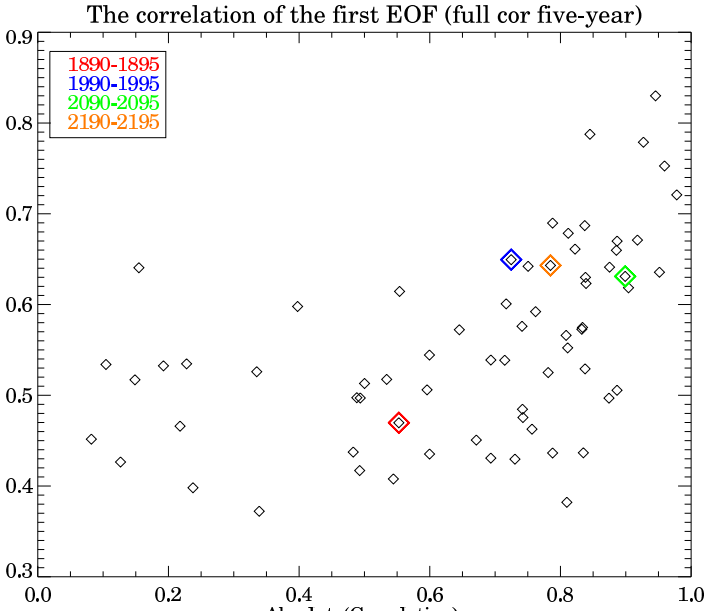

Figure 12.6: Five-year periods correlation with the full period.

12.0.3 Supplementary figures for chapter 7

In figure 12.7 the individual contributions to to the projected future sulfate concentration is shown. This figure is similar to figure 7.3 and in a) the impacts from climate change b) the impact of emission change c) the total impact and finally the relative contribution from climate change relative to emission change is shown. Like for BC the impact from emission dominates 12.7(a)

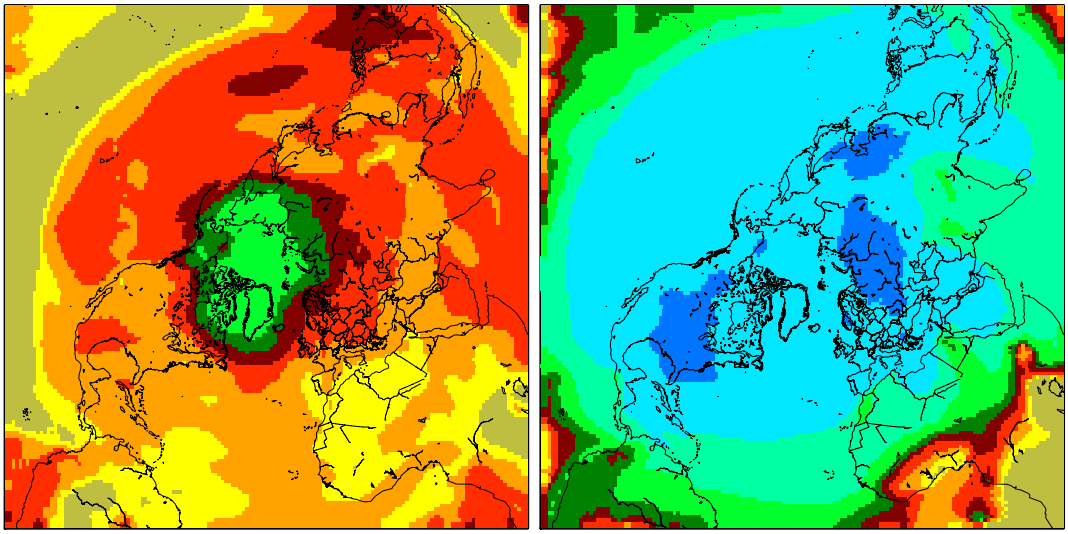

(a) SO_4: Climate signal (see eq. 7.1)

(b) SO_4: Emission signal (see eq. 7.2)

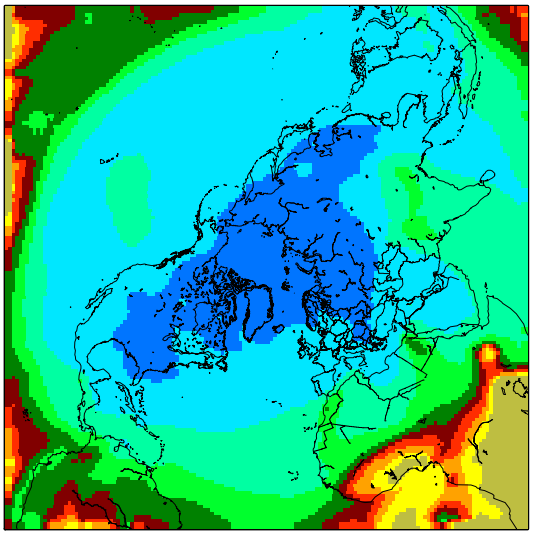

(c) SO_4: Total signal (see eq. 7.3)

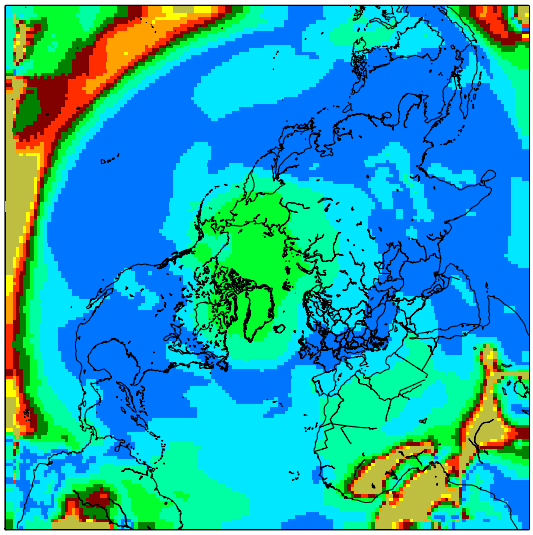

(d) Climate signal/Emission signal (see eq. 7.4)

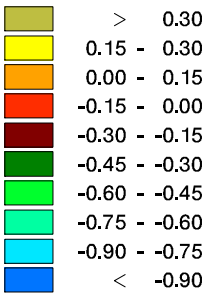

(e) Legend for a,b,c (fraction)

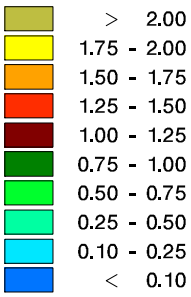

(f) Legend for d (fraction)

Figure 12.7: Total Sulfate (SO_4): The signal from a) climate change and b) emission change c) the total change on the surface total SO_4 concentration and d) the climate signal relative to the total signal. a) The climate signal, simulated with constant year-2000 emissions and projected ECHAM5 meteorology. b) The signal from changes in the anthropogenic emissions, simulated with projected RCP4.5 emissions and constant 1990s meteorology projected ECHAM5. c) The total signal from both changes in climate and emissions, simulated with projected emissions (RCP4.5) and projected meteorology by ECHAM5.

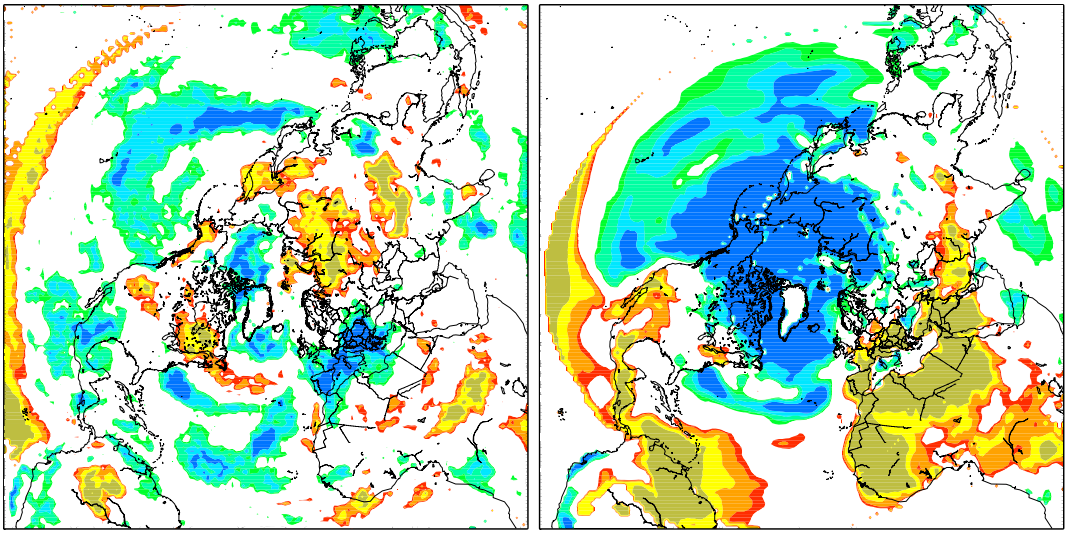

(a) SO_4:wet deposition $mg/m^{-2}/year$ **(b)** SO_4: Dry deposition $mg/m^{-2}/year$

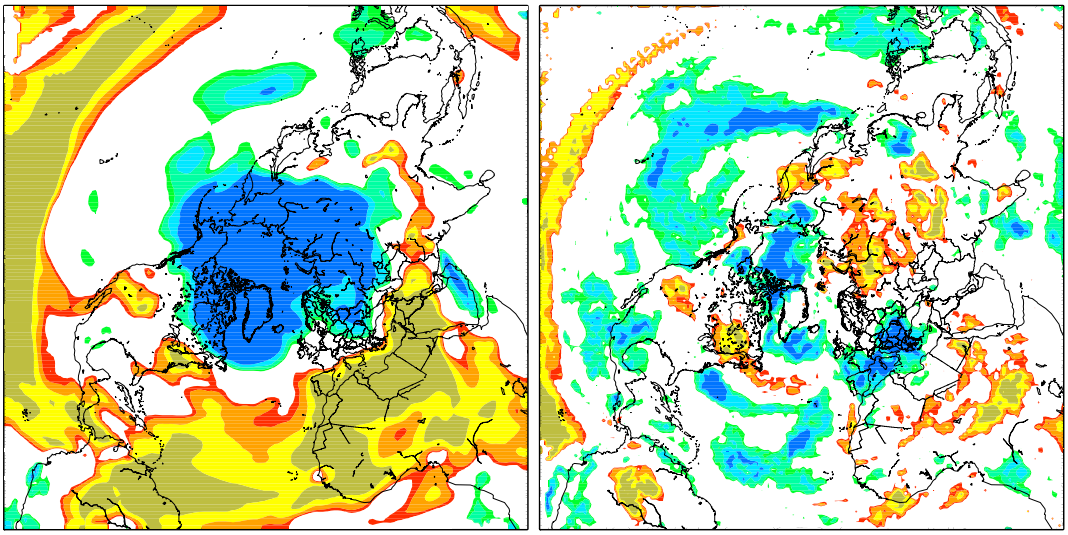

(c) SO_4: Concentration ppbV **(d)** SO_4: Total deposition $mg/m^{-2}/year$

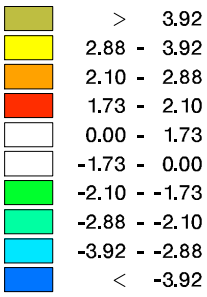

(e) Significance

Figure 12.8: Total Sulphate (SO_4): Changes due to impacts of climate change: The significance of change in a) wet deposition in $mg/m^{-2}/year$ and b) dry deposition in $mg/m^{-2}/year$ c) concentration in ppbV and d) total deposition in $mg/m^{-2}/year$. The significance according to the students t-test, the threshold for significance is set to 10%. White areas indicates no significant chance, yellow/red areas indicates significant increase and blue values indicate significant decrease.

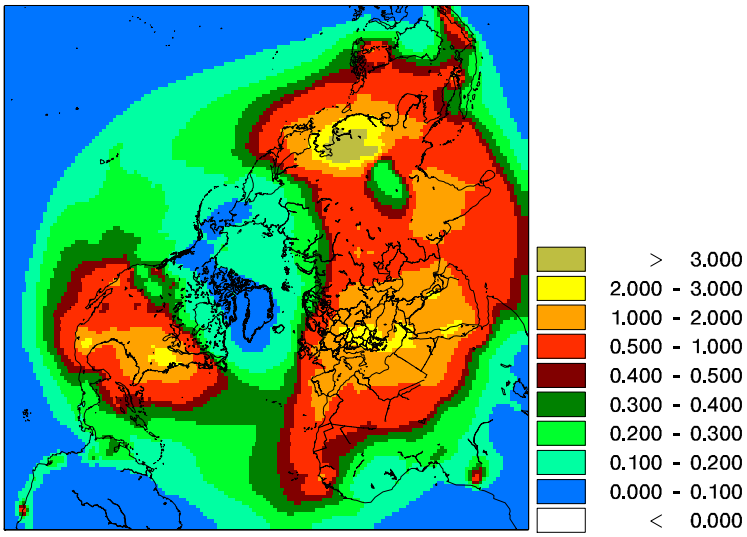

(a) tSO4 concentration mean concentration in the 1990s in ppbV

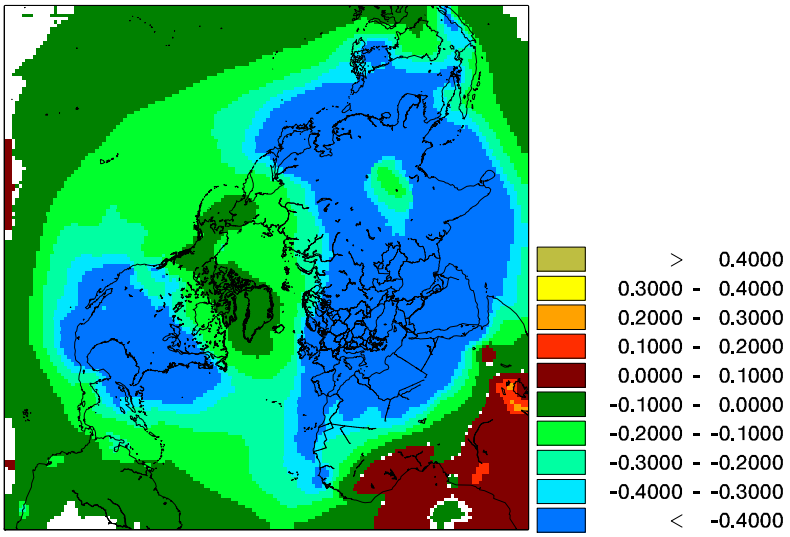

(b) tSO4 difference 2090s-1990s in ppbV

Figure 12.9: Total sulphate (tSO4): The signal from both climate change and emission change a) 1990s concentration b) difference (2090s-1990s) in ppbV.

Appendix B: Papers

The following papers were included in the PhD thesis:

B1: Paper I

Hedegaard, G. B., J. Brandt, J. H. Christensen, L. M. Frohn, C. Geels, K. M. Hansen and M. Stendel; Impacts of climate change on air pollution levels in the Northern Hemisphere with special focus on Europe and the Arctic, Atmospheric Chemistry and Physics, 8, 3337-3367, 2008.

B2: Paper II

Hedegaard, G. B.; Natural Sources, in: Air pollution - from a local to a global perspective, Polyteknisk Forlag, Eds.: Jes Fenger and Jens Christian Tjell., 163-174, 2008.

B3: Paper III

Skjøth, C. A., Geels, C., Hvidberg, M., Hertel, O., Brandt, J., Frohn, L. M., Hansen, K. M., Hedegaard, G. B., Christensen, J. H., Moseholm, L.; An inventory of tree species in Europe - An essential data input for air pollution modelling, Ecological Modelling, 217, 3-4, 292-304, 2008.

B4: Paper IV

J. Brandt, J. D. Silver, L. M. Frohn, C. Geels, A. Gross, A. B. Hansen, K. M. Hansen, G. B. Hedegaard, C. A. Skjøth, H. Villadsen, A. Zare and J. H. Christensen; An integrated model study for Europe and North America using the Danish Eulerian Hemispheric Model with focus on intercontinental transport of air pollution, submitted to Atmospheric Environment (Special issue), May 2011. (2011a), Accepted January 2012.

B5: Paper V

J. Brandt, J. D. Silver, J. H. Christensen, M. S. Andersen, J. H. Bønløkke, T. Sigsgaard, C. Geels, A. Gross, A. B. Hansen, K. M. Hansen, G. B.Hedegaard, E. Kaas and L. M. Frohn;Assessment of Health-Cost Externalities of Air Pollution in Denmark and Europe using the EVA Model System, draft. (2011b)

B6: Paper VI

Paper IX: Geels, C., Hansen, K. M., Christensen, J. H, Skjøth, C. A., Ellerman, T., Hedegaard, G. B, Hertel, O., Frohn, L. M., Gross, A., Hansen, A. B., Brandt, J.; Projected change in atmospheric nitrogen deposition to the Baltic Sea towards 2020, Atmospheric Chemistry and Physics Discussions, 11, 21533-21567, 2011.